

**BIRZEIT UNIVERSITY**  
Graduate Faculty  
Scientific Computing Masters Department

**Simulation, Analysis, and Advanced Control of  
Selected Nonlinear Dynamic Systems**

By  
**Jafar I. Titi**

Supervisor  
**Dr. Haithem Abu-Rub**

Submitted in partial fulfillment of the requirements for the Masters  
Degree in Scientific Computing from The Graduate Faculty at Birzeit  
University.

**December 2004**

## ACKNOWLEDGMENTS

بِسْمِ اللَّهِ الرَّحْمَنِ الرَّحِيمِ  
 " وَهُوَ الَّذِي جَعَلَكُمْ خَلَائِفَ الْأَرْضِ وَرَفَعَ بَعْضَكُمْ فَوْقَ بَعْضٍ دَرَجَاتٍ لِيُبْلِغَكُمْ فِي  
 مَا آتَاكُمْ إِنَّ رَبَّكَ سَرِيعُ الْعِقَابِ وَإِنَّهُ لَغَفُورٌ رَحِيمٌ " { الأنعام، 165 }

I would like to express my sincere thanks to my supervisor Dr. Haithem; for his continuous support, guidance, encouragement, and friendship.

To all who helped me to accomplish this thesis.

Last but definitely not least, to my family; for their support and patience in my hard times, as well as good times, without their contribution I would not have ever completed my study.

## ABSTRACT

Electrical motors and their control are considered time varying, nonlinear dynamic systems. This thesis work presents speed control of two types of these motors: speed control of a separately excited DC motor, and sensorless speed control of AC Induction motors.

The main aim of this thesis work is to model and simulate promising and inexpensive methods to develop and assess sensorless control schemes of induction motors. The proposed systems operate without a rotor speed sensor, and as a result getting rid of its disadvantages; the rotor angular speed is calculated in different ways using multiscalar state variables and power measurements. The methods are applied to field oriented control principle, which converts the control of the induction motor to the simpler control of the separately excited DC motor.

A Fuzzy logic controller is used for speed control of both types of motors. Simulation results are obtained and a comprehensive analysis and comparative study of several relationships of rotor angular speed is presented using fuzzy logic control and conventional proportional-integral control, based on a set of criteria to assign “figures of merit”.

## المستخلص

المحركات الكهربائية و التحكم بها، تعتبر من النظم الديناميكية غير الخطية و المتغيرة مع الزمن. هذه الرسالة تعالج التحكم بالسرعة لنوعين من هذه المحركات: التحكم بسرعة "محرك التيار الثابت ذو الإثارة المنفصلة"، وأيضاً التحكم بسرعة "المحرك الحثي ذو التيار المتناوب" بدون استخدام مجس للسرعة.

الهدف الرئيسي لهذا البحث، هو بناء نموذج حاسوبي محاكي للواقع لمجموعة من الطرق الواعدة و الاقتصادية للتحكم بسرعة "المحرك الحثي" بدون استخدام مجس للسرعة. الأنظمة المقترحة تعمل بدون الحاجة لاستخدام مجس لقياس سرعة دوار المحرك و بالتالي التخلص من المشاكل المصاحبة له، و يتم حساب سرعة الدوار بعدة طرق تقريبية باستخدام "كميات عددية واصفة للحالة" و "قياس القدرة". طرق التحكم هذه تعمل على أساس مبدأ "التحكم الموجه نحو المجال"، و الذي يحول التحكم بالمحرك الحثي إلى صيغة تبسيطية تشابه التحكم بمحرك التيار الثابت ذي الإثارة المنفصلة.

سيستخدم للتحكم بسرعة النوعين الأنفين الذكر من المحركات، ضابط سرعة يعمل على أساس " المنطق الضبابي". تم الحصول على نتائج مفصلة للمحاكاة. وتم القيام بتحليل شامل و مُقارنٌ لمختلف العلاقات الرياضية الحاسبة لسرعة دوار المحرك باستخدام "ضابط المنطق الضبابي"، و أيضاً باستخدام الطريقة التقليدية وهي "ضابط التحكم النسبي المتكامل". و تم الاعتماد في عملية المقارنة على منهجية "دلائل قياس الجدارة للنظام".

## TABLE OF CONTENTS

<b>ACKNOWLEDGMENTS</b>	<b>II</b>
<b>ABSTRACT</b>	<b>III</b>
المستخلص	<b>IV</b>
<b>TABLE OF CONTENTS</b>	<b>V</b>
<b>LIST OF TABLES</b>	<b>VIII</b>
<b>LIST OF FIGURES</b>	<b>IX</b>
<b>NOMENCLATURE</b>	<b>XI</b>
Abbreviations	<b>XI</b>
Symbols	<b>XI</b>
<b>INTRODUCTION</b>	<b>1</b>
Overview of the Chapters	<b>4</b>
<b>1 SEPARATELY EXCITED DC MOTOR SPEED CONTROL</b>	<b>6</b>
1.1 Introduction	<b>6</b>
1.2 Construction of DC motor	<b>7</b>
1.2.1 Types of DC motors	<b>10</b>
1.3 Separately Excited DC Motor	<b>10</b>
1.3.1 Equivalent circuit	<b>10</b>
1.3.2 Mathematical model	<b>11</b>
1.3.3 Modeling	<b>12</b>
1.4 Separately Excited DC Motor Speed Control	<b>13</b>
1.4.1 Control objectives	<b>13</b>
1.4.2 Cascade control structure	<b>14</b>
1.4.3 Speed control system model	<b>15</b>
<b>2 FIELD ORIENTED CONTROL OF 3-PHASE INDUCTION MOTOR</b>	<b>18</b>

<b>2.1</b>	<b>Introduction</b>	<b>18</b>
<b>2.2</b>	<b>Squirrel-Cage Induction Motor</b>	<b>20</b>
2.2.1	Construction	20
2.2.2	Equivalent circuit	22
2.2.3	Space vectors	22
2.2.4	Mathematical model	24
2.2.5	Modeling	25
<b>2.3</b>	<b>Field Oriented Control</b>	<b>26</b>
<b>2.4</b>	<b>Coordinate Transformations</b>	<b>27</b>
2.4.1	Clarke transformation $(A, B, C) \rightarrow (\alpha, \beta)$	28
2.4.2	Park transformation $(\alpha, \beta) \rightarrow (d, q)$	29
2.4.3	Inverse park transformation $(d, q) \rightarrow (\alpha, \beta)$	31
<b>2.5</b>	<b>Basic Scheme for FOC</b>	<b>32</b>
<b>3</b>	<b>SENSORLESS SPEED CONTROL OF INDUCTION MOTORS</b>	<b>34</b>
<b>3.1</b>	<b>Introduction</b>	<b>34</b>
<b>3.2</b>	<b>Sensorless Speed Control</b>	<b>36</b>
<b>3.3</b>	<b>Multiscalar State Variables of Induction Motor</b>	<b>38</b>
<b>3.4</b>	<b>State Variables Calculations</b>	<b>38</b>
3.4.1	Rotor flux magnitude and angle	38
3.4.2	The use of power measurements	40
<b>3.5</b>	<b>Rotor Angular Speed Calculations Using Power Measurements</b>	<b>40</b>
<b>3.6</b>	<b>MATLAB/SIMULINK System Model</b>	<b>43</b>
<b>4</b>	<b>FUZZY LOGIC CONTROL OF INDUCTION MOTOR</b>	<b>47</b>
<b>4.1</b>	<b>Basic Concepts of Fuzzy Logic</b>	<b>47</b>
4.1.1	Research history on fuzzy Logic	48
4.1.2	History of AC motor Fuzzy control	49
<b>4.2</b>	<b>Fuzzy Sets Fundamentals:</b>	<b>50</b>
4.2.1	Membership functions – fundamental definitions	51
4.2.2	Approximate reasoning	52
4.2.3	The role of linguistic variables	53
4.2.4	Fuzzy system structure	54
4.2.5	Fuzzy propositions	54
4.2.6	Logical operations	56
4.2.7	Methods of defuzzification	57
<b>4.3</b>	<b>Control Design and Stability</b>	<b>58</b>
4.3.1	Fixed fuzzy controller design	59
4.3.2	Used control design approach	61

<b>4.4</b>	<b>Speed Fuzzy Logic Controller</b>	<b>62</b>
4.4.1	Implementation	65
4.4.2	Fuzzy logic algorithm summary	65
<b>5</b>	<b>SIMULATION RESULTS AND FUZZY/PI COMPARISON</b>	<b>67</b>
<b>5.1</b>	<b>Introduction</b>	<b>67</b>
5.1.1	Why using MATLAB®/SIMULINK®	67
5.1.2	Computer setup and specifications	69
<b>5.2</b>	<b>Separately Excited DC Motor Simulation Results</b>	<b>69</b>
5.2.1	System specifications	69
5.2.2	Simulation results	70
<b>5.3</b>	<b>Speed Sensorless Induction Motor Simulation Results</b>	<b>73</b>
5.3.1	System specifications	73
5.3.2	Simulation results	74
5.3.3	Applied load torque effect	87
<b>5.4</b>	<b>Comparison between Fuzzy and PI Sensorless Speed Control of IM</b>	<b>90</b>
5.4.1	Steady-State Error (SSE)	90
5.4.2	Dynamic Behavior (DB)	90
5.4.3	Low Speed Operation (LSO)	90
<b>6</b>	<b>CONCLUSIONS AND FUTURE WORK</b>	<b>93</b>
<b>6.1</b>	<b>Conclusions</b>	<b>93</b>
<b>6.2</b>	<b>Future Work</b>	<b>94</b>
	<b>REFERENCES</b>	<b>96</b>
	<b>APPENDICES</b>	<b>100</b>
<b>A.</b>	<b><i>MATLAB Fuzzy Editor</i></b>	<b>101</b>
<b>B.</b>	<b><i>Conference Proceedings Paper</i></b>	<b>105</b>

## LIST OF TABLES

Table 4-1: Fuzzy Logic Controller Rules of Inference.....	64
Table 5-1: Separately Excited DC Motor Simulation Parameters.....	69
Table 5-2: IM Control System Simulation Parameters.....	73
Table 5-3: Used Low Pass Filters (LPF) Time Constants for Control of IM.....	74
Table 5-4: Comparison between Different Schemes .....	91



## LIST OF FIGURES

Figure 1-1: Schematic view of the DC motor with commutator and compensation winding.....	8
Figure 1-2: Rotor winding arrangement (a), Triangular mmf from rectangular winding distribution (b).....	9
Figure 1-3: Equivalent circuit of a Separately Excited DC motor.....	11
Figure 1-4: Separately Excited DC motor block.....	13
Figure 1-5: Separately Excited DC Motor Model.....	13
Figure 1-6: Simplified feedback control system.....	14
Figure 1-7: Cascade control of a motor drive.....	14
Figure 1-8: Speed control system of a Separately Excited DC motor.....	15
Figure 1-9: PI controller with anti-windup model.....	16
Figure 1-10 : Armature voltage signal.....	16
Figure 2-1: Typical stator, and rotor of induction motor.....	20
Figure 2-2: Three-phase stator winding axes of an induction motor.....	21
Figure 2-3: Construction of squirrel-cage induction motor rotor.....	21
Figure 2-4: Equivalent circuit of an induction motor.....	22
Figure 2-5: Stator current space vector and its component in $(A, B, C)$ .....	23
Figure 2-6: Induction motor block.....	25
Figure 2-7: Inside the induction motor block.....	26
Figure 2-8: Stator current space vector and its components in $(\alpha, \beta)$ .....	28
Figure 2-9: Block diagram of the Clarke transformation.....	29
Figure 2-10: Stator current space vector and its component in $(\alpha, \beta)$ and in the $(d, q)$ rotating reference frame.....	30
Figure 2-11: Park transformation block diagram.....	31
Figure 2-12: Inverse Park transformation block diagram.....	32
Figure 2-13: Basic scheme of FOC for induction motor.....	32
Figure 3-1: Block diagram of an adjustable-speed induction motor drives.....	34
Figure 3-2: Detailed Speed sensorless control system of induction motor, Based on FOC.....	37
Figure 3-3: Model of sensorless speed control system of IM in SIMULINK.....	44
Figure 3-4: State Variables Calc. block model.....	45
Figure 3-5: Rotor flux calculation block.....	46
Figure 4-1: Structure of a fuzzy system.....	55
Figure 4-2: Fuzzy logical operators.....	57
Figure 4-3: Fuzzy control and conventional control.....	60
Figure 4-4: Mamdani type FLC.....	62
Figure 4-5: Membership functions of $e$ , $\Delta e$ , and $\Delta u$ .....	63
Figure 4-6: Surface view of $e$ , $\Delta e$ , and $\Delta u$ .....	64
Figure 4-7: Fuzzy logic controller block.....	65
Figure 4-8: Fuzzy logic algorithm chart.....	66
Figure 5-1: Reference values for speed and torque.....	70
Figure 5-2: DC Simulation results (Case 1).....	71
Figure 5-3: DC Simulation results (Case 2).....	72
Figure 5-4: IM Reference command values.....	75

Figure 5-5: Simulation results for Sensored case .....	76
Figure 5-6: Simulation results for equation (3.16) .....	77
Figure 5-7: Simulation results for equation (3.17) .....	78
Figure 5-8: Simulation results for equation (3.18) .....	79
Figure 5-9: Simulation results for equation (3.19) .....	80
Figure 5-10: Simulation results for equation (3.20) .....	81
Figure 5-11: Simulation results for equation (3.21) .....	82
Figure 5-12: Simulation results for equation (3.22) .....	83
Figure 5-13: Simulation results for equation (3.23) .....	84
Figure 5-14: Simulation results for equation (3.24) .....	85
Figure 5-15: Simulation results for equation (3.25) .....	86
Figure 5-16: Zooming of Figure 5-8, around positive torque application point....	87
Figure 5-17: Negative load applied to the motor .....	88
Figure 5-18: Zooming of Figure 5-17, around negative torque application point.	88
Figure 5-19: A mixture of step and ramp input for rotor speed reference used ....	89
Figure 5-20: Graphical representation of Table 5-4 .....	92
Figure A- 1: FIS editor.....	101
Figure A- 2: Membership functions editor .....	102
Figure A- 3: Rule editor.....	103
Figure A- 4: Rule viewer .....	103
Figure A- 5: Surface viewer.....	104

## NOMENCLATURE

### ***Abbreviations***

---

<b>AC</b>	alternating current
<b>AM</b>	asynchronous motor
<b>DB</b>	dynamic behavior
<b>DC</b>	direct current
<b>DoS</b>	degree of support
<b>emf</b>	electromotive force
<b>FLC</b>	fuzzy logic controller
<b>FOC</b>	field oriented control
<b>IM</b>	induction motor
<b>LPF</b>	low pass filter
<b>LSO</b>	low speed operation
<b>mmf</b>	magneto-motive force
<b>PI</b>	proportional integral
<b><i>pu</i></b>	per unit system
<b>PWM</b>	pulse width modulation
<b>Ref.</b>	reference
<b>SM</b>	synchronous motor
<b>SSE</b>	steady-state error
<b>SVPWM</b>	space vector pulse width modulation
<b>VVVF</b>	variable voltage, variable frequency drives

### ***Symbols***

---

#### **DC Motor**

---

<b><math>R_a</math></b>	armature resistance
-------------------------	---------------------

$L_{aa}$	armature inductance
$ea$	back electromotive force
$I_a$	armature current
$u_a$	armature voltage
$R_f$	field resistance
$L_{ff}$	field inductance
$I_a$	field current
$u_f$	field voltage
$L_{af}$	electromechanical coupling inductance
$\omega_r$	angular speed of the rotor (armature) shaft
$J_m$	radius of rotor wheel
$B_m$	mass of wheel
$T_L$	load torque
$T_{ind}$	induced torque
$\psi(I_f)$	field flux
$\omega_r^*, T_L^*, u_f^*$	reference values for rotor speed, applied torque, and field voltage
<b>Kp , Ki</b>	proportional, and integral gains of PI controller respectively

### **Induction Motor**

---

$R_r$	rotor resistance
$L_r$	rotor inductance
$L_m$	electromechanical mutual inductance
$J$	inertia
$m_0$ , or $T_l$	load torque
$(A, B, C)$	physical coordinate system
$(x, y)$ or $(\alpha, \beta)$	stationary two dimensional time variant orthogonal coordinate system
$(d, q)$	rotating frame time invariant orthogonal coordinate system
$u_s$	stator voltage
$I_s$	amplitude of the stator set value current

$i_s$	stator current
$i_r$	rotor current
$\psi_s$	stator flux
$\psi_r$	rotor flux
$\omega_s$	angular speed of coordinate system
$\omega_r$	angular speed of the rotor shaft
$\omega_i$	angular speed of the stator current vector frequency
$\omega_{si}$	angular speed of the slip frequency
$\overline{i_s}, \overline{u_s}, \overline{\psi_s}$	stator current, voltage, and flux vectors
$\overline{i_r}, \overline{u_r}, \overline{\psi_r}$	rotor current, voltage, and flux vectors
$\gamma_s$	rotor flux angle
$\omega_{rc}, \psi_{rc}, T_{lc}$	command values for rotor speed, rotor flux, and load torque
$z_1, z_2, z_3, z_4$	multiscalar state variables of induction motor
$p$	instantaneous active power
$P$	filtrated instantaneous active power
$q$	instantaneous reactive power
$Q$	filtrated instantaneous reactive power

### **Fuzzy logic Controller**

---

$X$	universal set
$A$	fuzzy set
$\mu_A(x)$	grade of membership in $A$
$L$	linguistic variable
$e$	control error
$\Delta e$	change of error
$\Delta u$	change of control signal

## INTRODUCTION

Electrical motors in general, are considered as highly nonlinear dynamic, time varying devices, with lack of accessibility to some states and outputs for measurements, and hence may be considered as a tricky engineering tight spot. The computations required for accurate modeling of the speed and torque of these machines requires fast processing devices.

Induction motors are comparatively rugged and inexpensive electrical motors. For that reason a great deal of concentration is given to their control for a variety of applications with diverse control requirements. An induction motor, especially squirrel-cage induction motor, has many advantages when compared with DC motors. First of all, it is very cheap. Next, it has a very compact structure and is insensitive to environment. In addition, it does not require periodic maintenance like DC motors. Even so, because of its highly nonlinear and coupled dynamic structure, an induction motor requires more complex control schemes than DC motors.

However, there are two key reasons to talk about DC motor drives [2]. Firstly, a number of such drives are currently in use and this number keeps increasing. Secondly, the control of AC motor drives emulates the operating principles of DC motor drives. Therefore, knowledge of DC motor drives is the first step in learning how to control AC drives.

DC motor control is considered simple compared to an AC induction motor, especially for the separately excited DC motor, since nonlinearities in the

description of the motor are virtually non-existent. Classical control theories are then easily used in designing the drive system.

Induction Motors with squirrel-cage rotors has been regarded for many years as the workhorse in industrial applications [2], [9]. Various market analyses showed that 90% of all industrial motor applications use induction type motors. The many reasons for this include high robustness, reliability, low price, and high efficiency (up to 80% higher) [10].

Multiphase AC Motors working without controlled rotor angular speed consume most of the electrical energy produced [12]. AC motors control drives are used increasingly due to their advantages like increased robustness, reliability, efficiency, and lowered price. Thanks to advances in technology and automation, controlled drives with AC motors are now employed increasingly frequently, and are considerably more economical in their use of energy [12].

For the past decade a lot of research effort had been done on the idea of sensorless speed control of induction motor, [14]-[24]. The rewards of speed sensorless induction motor drives are reduced hardware complexity, size, and cost. They also include elimination of the sensor cable, better noise immunity, and increased reliability and less maintenance requirements, making it suitable for hostile environments.

Field Orientated Control (FOC), as in [11], consists of controlling the stator currents represented by a vector. This control is based on projections which transform a three-phase time and speed dependent system into a two coordinate

time invariant rotating system. These projections lead to a structure similar to that of a separately excited DC motor control.

In this thesis work a power measurement for sensorless control of induction motors is used. A favorable solution is applied to FOC of induction motor without using a sensor of rotor angular speed. All state variables are calculated using only stator variables.

Fuzzy logic is a revolutionary technology that enhances system design with engineering knowledge. Using fuzzy logic, the need for hard mathematical modeling can be avoided. In fuzzy logic adjustments factors in control systems will be replaced by self-descriptive linguistics descriptions of the control strategy.

The control system of induction motor has difficult-to-describe analytical relationships caused by non-precise variable identification [33],[40]; in these situations, fixed Fuzzy Logic Controller (FLC) design using heuristic approach is best suited. This fuzzy approach is used here in this thesis context. Fuzzy logic controller is the main element in the speed control system of the induction motor, and also for Separately Excited DC Motor.

A comprehensive analysis and comparative study between several relationships for rotor angular speed is discussed. Fuzzy Logic Controller (**FLC**) will be used and the obtained results will be compared with these obtained when using conventional Proportional-Integral (**PI**) Controller one, based on a set of criteria to assign “figures of merit”.

Comparison of the system Behavior under FLC and PI control is performed by subjecting the control system of the motor to the same parameters, and with the



same command values. The control systems had been modeled in MATLAB/SIMULINK.

### ***Overview of the Chapters***

This thesis is organized as follows:

Separately Excited DC motor theory and control is presented in **Chapter 1**, and construction of DC motors in general will be presented. It also discusses the equivalent circuit, mathematical model, and MATLAB/SIMULINK model of separately excited DC motor. Moreover, this chapter focuses on the speed control of this Motor, with its modeling in MATLAB/SIMULINK.

**Chapter 2** presents the construction, equivalent circuit, mathematical model, and MATLAB/SIMULINK model of three-phase Squirrel-Cage Induction Motor. Furthermore, focus will be on the theory and basic schema of Field Oriented Control (FOC) of this motor.

Based on the Field Oriented Control basic schema, **Chapter 3** presents Speed sensorless Control of induction motor using power measurements. It discusses the advantages of sensorless speed control. Also the idea and calculation of Multiscalar State Variables of induction motor, and the theory of power measurements is shown. Moreover, it presents the calculation and estimation of the rotor angular speed using power measurements. Furthermore, it presents the MATLAB/ SIMULINK model of the sensorless speed control system.

**Chapter 4** discusses the theory and history of fuzzy logic control of Induction Motor. In addition, it presents control design approach used in this thesis. Moreover, it presents the implementation and specifications of speed fuzzy logic

(FLC) controller used for speed control of both the induction motor and separately excited DC motor.

**Chapter 5** shows the simulation results for speed control of separately excited DC motor, and sensorless speed control of squirrel-cage induction motor under FLC, and PI speed controllers. It also presents the computer setup and specifications used in the simulations, and the reason for choosing MATLAB/SIMULINK to model and simulate the systems. It also introduces a thorough analysis, and comparison between the performance of the FLC and PI sensorless speed control of Induction motors.

**Chapter 6** summarizes the thesis and presents the conclusions and contribution of this research thesis. In addition, it introduces suggestions to enhance and broaden this thesis in future research work.

# 1 SEPARATELY EXCITED DC MOTOR SPEED CONTROL

## 1.1 Introduction

Electric motors exist to convert electrical energy into mechanical energy. This is done by two interacting magnetic fields, one stationary, and another attached to a part that can move.

Direct Current (DC) motors have the potential for very high torque capabilities (even though this is generally a function of the physical size of the motor), are easy to miniaturize, and can be "throttled" via adjusting their supply voltage. DC motors are also not only the simplest, but the oldest electric motors.

The basic principles of electromagnetic induction were discovered in the early 19<sup>th</sup> century by Oersted, Gauss, and Faraday. In 1819, *Hans Christian Oersted* and *Andie Marie Ampere* discovered that an electric current produces a magnetic field. The next 15 years saw an outbreak of worldwide experimentation and innovation, leading finally to a simple DC rotary motor in 1832 by the work of *Joseph Henry* and *William Sturgeon* [1]. A number of scientists were involved in the work.

Historically, DC motor drives have been the most accepted drives for speed and position control applications. They have this popularity due to their low cost and ease of control. It has been predicted for many years that their use will come to an end, because they are losing their market share to AC drives, due to wear in their commutator and brushes, which require continuous maintenance.

Another factor in the decline of the market share of DC drives is cost. For power processing and control, AC drives require more complex electronics, making them at present more expensive than in DC motor drives. However, the cost of drive electronics continues to decrease. Therefore, AC drives are gaining market share over DC drives [2].

However, there are two key reasons to talk about DC drives. Firstly, a number of such drives are currently in use and this number keeps increasing. Secondly, the control of AC motor drives emulates the operating principles of DC motor drives. Therefore, knowledge of DC motor drives is the first step in learning how to control AC drives.

Direct current motors are extensively used in variable speed drives and position control systems where good dynamic response and steady-state performance are required. e.g. robotics, printers, machine tools, rolling mills for steel, paper and textile industries, etc.

DC motor control is simple compared to AC motor, especially for the separately excited DC motor, since nonlinearities in the description of the motor are virtually non-existent. This is due to the commutator-brush assembly. Classical control theories are then easily used in designing the drive system.

## **1.2 Construction of DC motor**

The mechanical construction of the DC motor contains a rotor and stator. The stator contains the magnets, or an electric field winding and the rotor contains the armature winding, see Figure 1-1 [3] (conductor dimensions are enlarged).

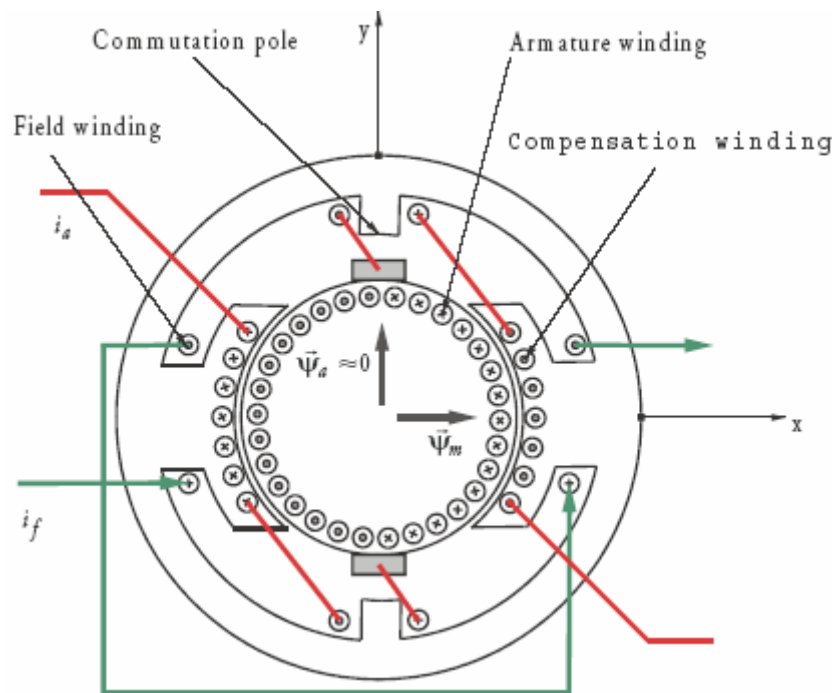


**Figure 1-1: Schematic view of the DC motor with commutator and compensation winding.**

With a field winding the stator is usually arranged with salient poles. Since eddy currents considerably deteriorate the dynamic properties of the machine its stator is usually manufactured of laminated metallic sheets.

The armature winding is a single continuous winding with a limited number of nodes connected to a segment of a commutator; see Figure 1-2 a). The current distribution is not sinusoidal, but triangular. This exception from the requirement of sinusoidal windings is compensated by the commutator that causes the rotor magneto-motive force (mmf) distribution to be triangular, independent of the rotor position, see Figure 1-2 b). Since the requirement of sinusoidal winding distribution partly was made to allow superposition of several windings, and this is overcome by the commutator function, the vector theory can still be applied, keeping in mind that the mmf from the rotor is triangular, not sinusoidal. Two

sliding contacts are connected to two of the commutator segments and thus allowing electrical connection to the armature winding. The commutator segments with their insulation are pressed on the rotor axis.

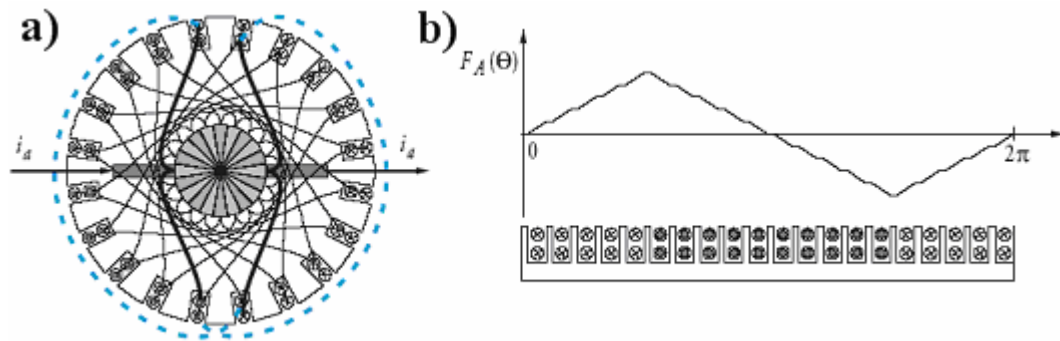


**Figure 1-2: Rotor winding arrangement (a), Triangular mmf from rectangular winding distribution (b)**

Besides the armature winding placed on the rotor the construction also contains two windings that also carry armature current. One of these additional windings is the so-called commutation winding and is arranged in such a manner that the armature current generates a local mmf interacting with the conductor closest to the sliding contacts. This additional winding does not influence the generated torque but helps to avoid sparking at the sliding contacts when current is switched from one segment to the other. The other additional winding is placed on the poles of the field winding and reduces the quadrature armature mmf to obtain only a direct fundamental of the resulting air gap flux. In other words, the inductance in the y-axis is negligible. In Figure 1-1 all conductors having the current direction indicated are carrying the same armature current.

Due to the commutator, the field and the armature circuits are fully decoupled. Top speed and maximum current are limited, maximum current and rate of change of current through the motor are also limited by the commutator[3].

### 1.2.1 Types of DC motors

There are five major types of DC motors in general use [4]:

1. Separately excited DC motor.
2. Shunt DC motor.
3. Permanent-magnet DC motor.
4. Series DC motor.
5. Compounded DC motor.

These types differentiate from each other in the way the armature winding and field winding are connected or disconnected from each other. For example, in separately excited DC motor the armature and field windings are separated from each other, while in shunt motor they are connected in parallel, and so on.

In this thesis context, emphasis will be on separately excited DC motor, since the control of induction motor drives *emulates* the operating principles of separately excited DC motor drives, i.e. to give the induction motor the behavior of separately excited DC motor using the methods of Field Oriented Control (FOC).

## 1.3 Separately Excited DC Motor

### 1.3.1 Equivalent circuit

For this motor, the field circuit is supplied separately from the armature, as indicated in Figure 1-3. The armature circuit is represented by the series circuit consisting of the armature resistance  $R_a$ , inductance  $L_{aa}$  and the back

Electromotive Force (emf)  $e_a$  which is due to the rotation of the armature. The armature current  $I_a$ , supplied from the armature voltage supply  $u_a$ .

The field circuit, consist of field resistance  $R_f$  and inductance  $L_{ff}$ , is supplied from the voltage source  $u_f$ . Note that the separately excited DC motor has field coils made of large number of turns of thin wire, so that the field circuit has a large resistance and carries a small current so that the power loss in field circuit is as small as practicable. Note that field circuit is not affected by any back emf.  $L_{af}$  is the Electromechanical Coupling inductance.

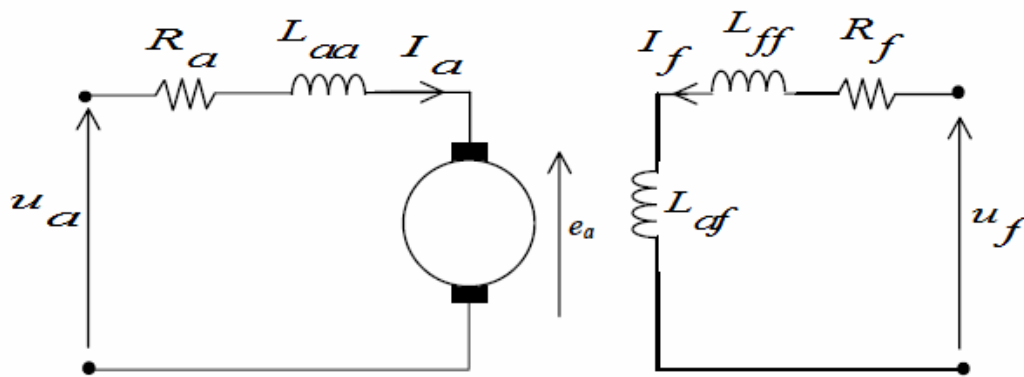


Figure 1-3: Equivalent circuit of a Separately Excited DC motor

### 1.3.2 Mathematical model

The non-linear dynamic equations of a simple separately excited DC motor are given by the following equations [4]:

$$\frac{dI_f}{dt} = \frac{-R_f}{L_{ff}} * I_f + \frac{1}{L_{ff}} * u_f \quad (1.1)$$

$$\frac{dI_a}{dt} = \frac{-R_a}{L_{aa}} * I_a - \frac{L_{af}}{L_{aa}} * I_f * \omega_r + \frac{1}{L_{aa}} * u_a \quad (1.2)$$



$$\frac{d \omega_r}{dt} = \frac{-B_m}{J_m} * \omega_r + \frac{L_{af}}{J_m} * I_f * I_a - \frac{1}{J_m} * T_L \quad (1.3)$$

Where:

$I_a, u_a, I_f, u_f$  are the armature and field current and voltage, respectively.  $\omega_r$  is the angular speed of the rotor (armature) shaft.  $R_f, R_a, L_{ff}, L_{aa}$  are field and armature resistance and inductances, respectively,  $L_{af}$  is the Electromechanical Coupling inductance,  $J_m$  is the Radius of rotor wheel,  $B_m$  is the Mass of wheel, and  $T_L$  is the load torque.

In a separately excited DC Motor, the axes of the armature and field currents are orthogonal to each other. This means that the magneto motive forces established by the currents in these windings are also orthogonal. If iron saturation is ignored the induced torque ( $T_{ind}$ ) is equal to [8]:

$$T_{ind} = K \psi(I_f) I_a \quad (1.4)$$

Where  $\psi(I_f)$  is the field flux, and depend solely on the field winding current and  $K$  is constant depending on the construction of the motor. If the flux is fixed then the torque is varied directly by the armature current. It is for this reason that DC machines are said to have decoupled or independent control over torque and flux.

### 1.3.3 Modeling

The model of the Separately Excited DC Motor is implemented by MATLAB/SIMULINK ([6], [7]). The block of motor is shown in Figure 1-4. As it

can be seen there are 3 inputs which are  $u_f$  ( $u_f$ ),  $u_a$  ( $u_a$ ), and  $T_L$  ( $T_L$ ). There are also 3 outputs which are  $I_f$  ( $I_f$ ),  $I_a$  ( $I_a$ ),  $\omega_r$  ( $\omega_r$ ).

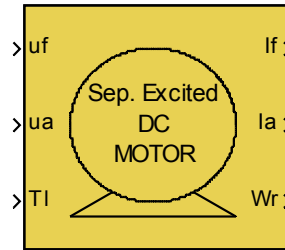


Figure 1-4: Separately Excited DC motor block

Inside this block, the model of the motor is implemented, based on equations from (1.1) to (1.3), as shown in Figure 1-5:

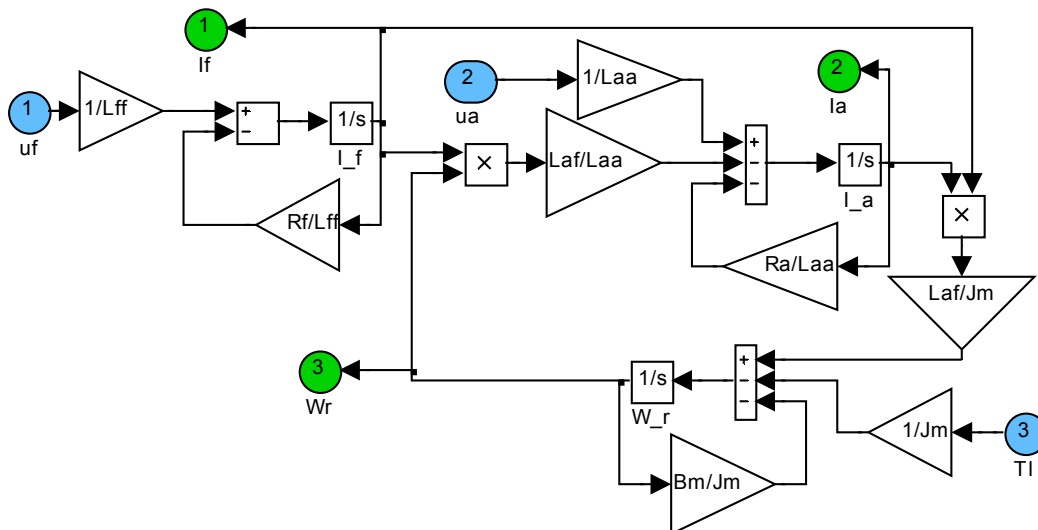


Figure 1-5: Separately Excited DC Motor Model

## 1.4 Separately Excited DC Motor Speed Control

### 1.4.1 Control objectives

The feedback control system, shown in Figure 1-6 [2], is a simplified version containing the basic parts of any control system. In terms of motor drive, the

**plant** block consists of the power-processing unit, the motor, and the mechanical load. The system must follow the desired (reference) input  $X^*$ , the output of the system is  $X$ .

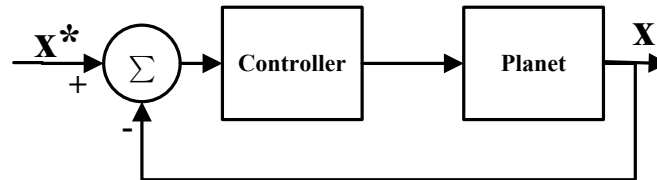


Figure 1-6: Simplified feedback control system

The controller block objectives are:

- A zero steady state error.
- A good dynamic response (which implies both a fast transient response, for example to a step-change, and a small settling time with very little overshoot).

### 1.4.2 Cascade control structure

The cascade control structure is commonly used for motor drives because of its flexibility [2]. It consists of distinct control loops as shown in Figure 1-7; the innermost current (torque) loop is followed by the speed loop. If position needs to be controlled accurately, the outermost position loop is superimposed on the speed loop. Cascade control requires that the bandwidth (speed of response) increase towards the inner loop, with the torque loop being the fastest and the position loop being the slowest. The cascade control structure is widely used in industry [2].

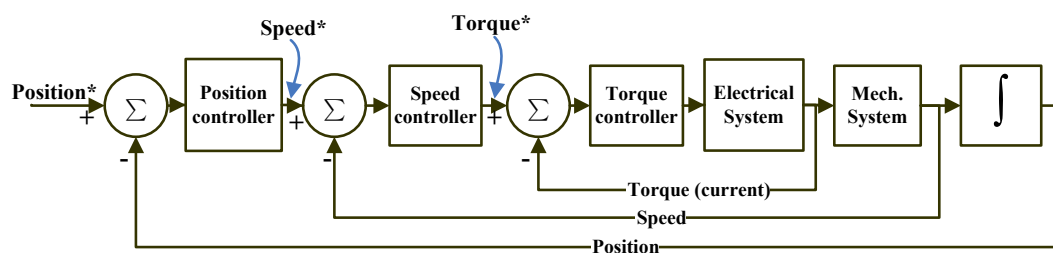


Figure 1-7: Cascade control of a motor drive

### 1.4.3 Speed control system model

Based on the idea of cascade control structure discussed in the previous section, the speed control system of the separately excited DC motor is shown in Figure 1-8. A similar system is found in [5] for other types of DC motor. The system had been modeled in MATLAB/SIMULINK.

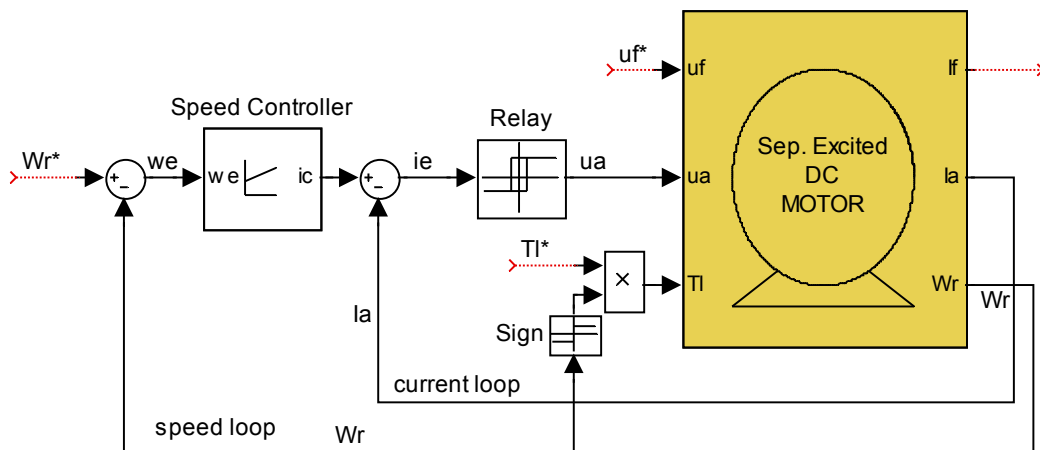


Figure 1-8: Speed control system of a Separately Excited DC motor

The following points must be noted about this model:

- The model contains 3 reference inputs:
  - $W_r^*(\omega_r^*)$ : speed reference.
  - $T_l^*(T_L^*)$ : applied load torque.
  - $u_f^*(u_f^*)$ : field voltage reference.
- The speed controller is of Proportional Integral (**PI**) type with anti-windup. The internal model of this controller block is shown in Figure 1-9. The system is very nonlinear due to the introduction of saturation needed to limit both the current delivered and the voltage applied to the

motor. The system is in the saturation mode when the errors are large; as a consequence, the controller functions as a constant current source, which is torque, resulting in the ramping of the speed. The inclusion of saturation limits on the PI integrator is therefore necessary to provide anti-windup action:

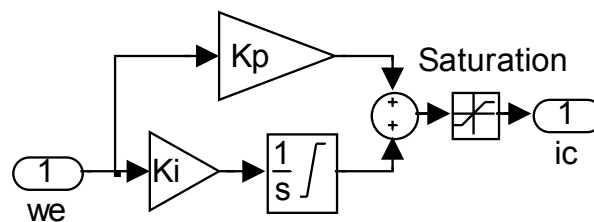


Figure 1-9: PI controller with anti-windup model

Where:

**Kp** is the proportional gain, **Ki** is the integral gain, and **saturation** is to provide anti-windup action.

- Fuzzy Logic Controller (FLC) can be used instead of the PI speed controller, and will be discussed in section 4.4, page 62; because it will make better response than the PI do, as will be shown in simulation results later.
- The relay works as a PWM, and makes a switch on the range  $-u_a$  to  $u_a$ , as the shown signal in Figure 1-10.

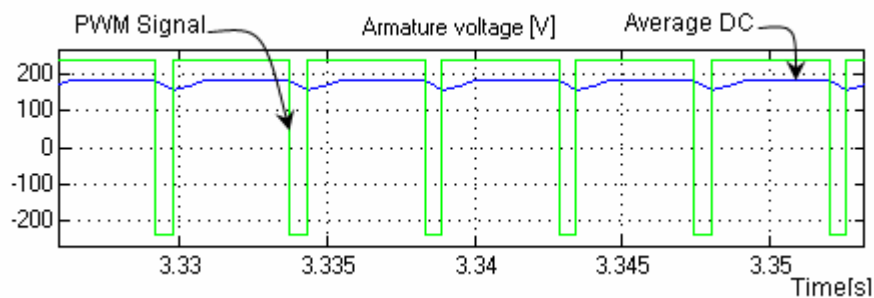


Figure 1-10 : Armature voltage signal

- The presence of the signum (**sign block**) function in the torque expression is required in order to assure that the load is passive whether the speed is positive or negative.

Full simulation results will be presented in section 5.2, page 69. Analysis and comparison between Fuzzy and PI approaches will be discussed in 5.4, page 90.

## **2 FIELD ORIENTED CONTROL OF 3-PHASE INDUCTION MOTOR**

### ***2.1 Introduction***

The most common type of electrical motor used in practice is the induction motor (IM), often called the Asynchronous Motor (AM) [3]. It is almost exclusively used as a motor in applications ranging from tape recorders up to railroad traction, electric vehicles, elevators etc. covering both low power and high power applications. The main reason why the induction motor is so widespread in practical use is its simple and cheap construction. Since the machine does not have brushes and slip rings it does not require any other maintenance than possibly lubrication of its bearings. For this reason, the IM is one of the most rugged electrical machine types.

Compared to the synchronous motor (SM) and the DC motor, the IM does not have a field winding connected to an external voltage source. The magnetic flux wave in the motor results from the superposition of the stator and rotor flux similar to all the other machine types. The rotor currents are driven by voltages induced in the rotor winding when the rotor flux rotates relative to the rotor. The flux wave rotates at synchronous rotational speed relative to the stator. In order to maintain the flux wave rotating relative to the rotor as well, the latter has to rotate at different speed (lower or higher) than the synchronous speed. The rotor speed is therefore "asynchronous" and this is where the name for the Asynchronous Motor

comes from. Since the rotor currents are induced in the rotor the Asynchronous Motor is called induction Motor.

The IM with squirrel-cage rotors has been regarded for many years as the workhorse in industrial applications ([2], [9]). Various market analyses show that 90% of all industrial motor applications use induction type motors. The many reasons for this include high robustness, reliability, low price, and high efficiency (up to 80% higher) [10].

In the last few decades, the induction motor has evolved from being a constant speed motor to a variable speed, variable torque machine. Its evolution was challenged by the easiness of controlling a DC motor at low power applications. When applications required large amounts of power and torque, the induction motor became more efficient to use. With the invention of variable voltage, variable frequency drives (VVVF); the use of an IM has increased. The formulation of Field Orientated Control (FOC) has lead to the induction motor replacing the DC motor as the main source of energy conversion in industrial applications.

Since an IM is a nonlinear, time varying device, the calculations required to accurately model the speed and torque of the machine require fast processing devices. With the invention of the Thyristor (the fast switching semiconductor), possibilities appeared to aid in controlling and modeling of the induction motor satisfactorily. The Thyristor was the first controlled semiconductor, and it has enabled the development of variable frequency converters to control the speed of the motor. Along with the ever increase in technology and computer processing



power, the IM is now a feasible option in applications where speed control is necessary.

The first methods of controlling an IM were by varying the stator voltage or frequency. Following this was the realization that the ratio of the voltage and frequency should be approximately constant. With the invention of Field Orientated Control, the complex IM can be modeled as a DC motor by performing simple transformations. These transformations are known as the *ABC- $\alpha\beta$ -dq* transformations, where the stator 3-phase currents are transformed into two dc currents. The two DC currents are then transformed into a rotating reference frame. Transforming the stator currents allows the motor to be modeled as a DC motor and not a complex three-phase motor [2].

## 2.2 Squirrel-Cage Induction Motor

### 2.2.1 Construction

The IM as any motor has a stator and rotor, Figure 2-1 shows a typical stator and rotor for an IM:

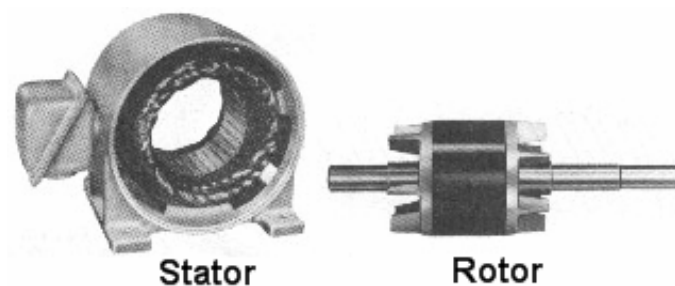


Figure 2-1: Typical stator, and rotor of induction motor

The stator of an IM consists of three-phase windings, sinusoidally-distributed in the stator slots. The three windings are displaced by  $120^\circ$  in space with respect to each other [2], as shown in Figure 2-2.

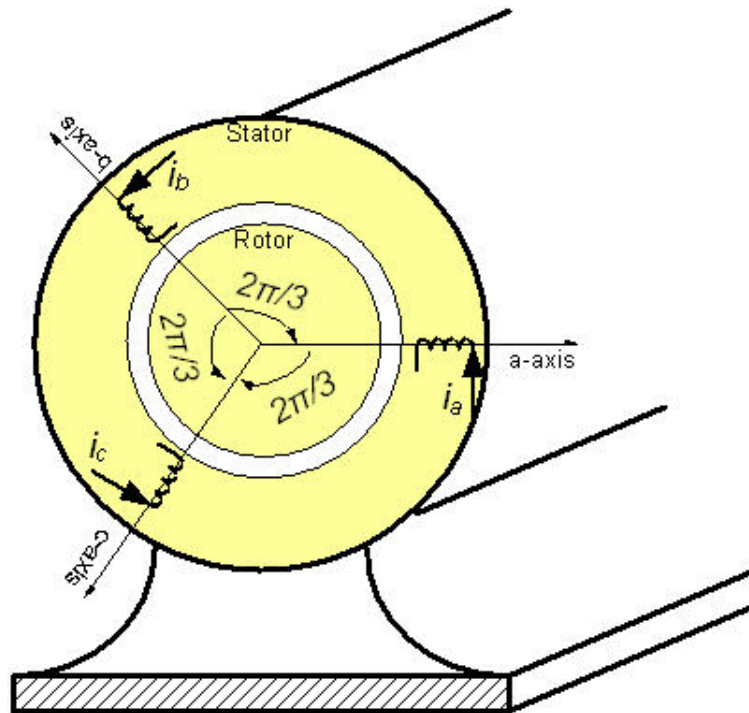


Figure 2-2: Three-phase stator winding axes of an induction motor

The squirrel-cage rotor winding is made of copper or aluminum bars which are layed into the rotor slots. On both ends the bars are short circuited by means of two conductor rings, as in Figure 2-3.

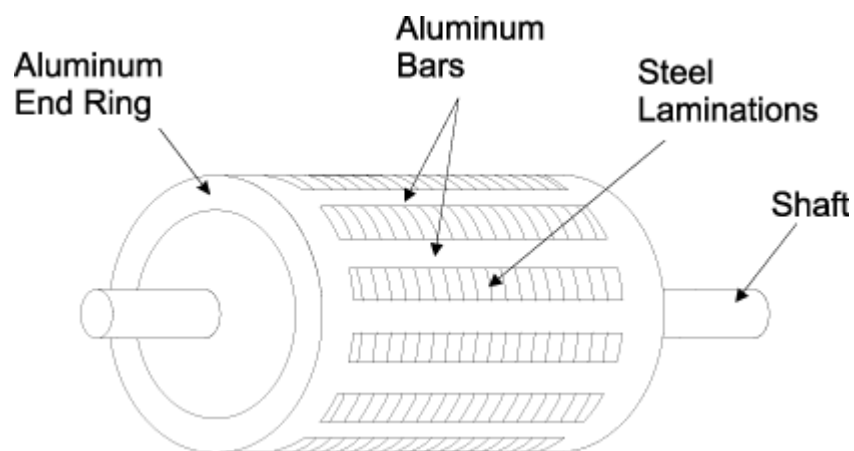


Figure 2-3: Construction of squirrel-cage induction motor rotor

### 2.2.2 Equivalent circuit

The equivalent circuit of an induction motor is shown in Figure 2-4. The stator is represented by stator resistance  $R_s$  and inductance  $L_s$ , and is supplied from the voltage source  $u_s$ . The rotor is represented by the rotor resistance  $R_r$ , inductance  $L_r$  and the induced rotor voltage  $u_r$  which is due to the rotation of the rotor, the induced rotor current  $i_r$ ,  $S$  represents the slip.  $L_m$  is the electromechanical mutual inductance.

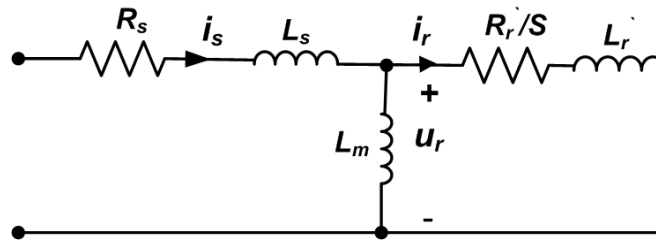


Figure 2-4: Equivalent circuit of an induction motor

### 2.2.3 Space vectors

Three phase induction motors are described in terms of the complex space vector method, by which the static and dynamic properties of induction motor will be described.

If  $K_A(t)$ ,  $K_B(t)$ , and  $K_C(t)$  denote arbitrary quantities of AC motor of physical coordinates ( $A, B, C$ ), and satisfying the condition:

$$K_A(t) + K_B(t) + K_C(t) = 0 \quad (2.1)$$

Then a space vector is defined as:

$$K = \frac{2}{3} [K_A(t) + \alpha K_B(t) + \alpha^2 K_C(t)] \quad (2.2)$$

Where  $\alpha = e^{j\frac{2}{3}\pi}$  and  $\alpha^2 = e^{j\frac{4}{3}\pi}$ , represent the spatial operators. Figure 2-5

shows the stator current complex space vector.

The space vector  $\mathbf{K}$  can represent the quantities of the IM such as the currents, voltages and flux linkages. The main idea of the space vector control is to deal with the AC Motor as a separately excited DC motor. The vector control method makes a transformation from the physical coordinate system  $(A, B, C)$  to a stationary frame  $(x, y)$  or  $(\alpha, \beta)$ <sup>1</sup>, or rotating frame  $(d, q)$ , as in [9] and [11].

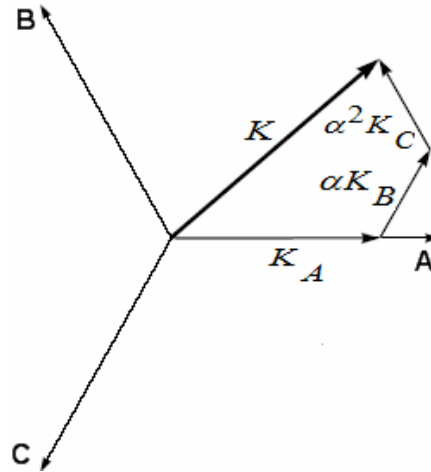


Figure 2-5: Stator current space vector and its component in  $(A, B, C)$

If we assume arbitrary frame  $\mathbf{K}$  rotating with arbitrary angular speed  $\omega_k$ , then the induction motor can be represented by 5 main per-unit ( $pu$ ) differential equations [11]:

$$u_{sk} = R_s i_{sk} = T_N \frac{d\psi_{sk}}{dt} + j\omega_k \psi_{sk} \quad (2.3)$$

$$u_{rk} = R_r i_{rk} + T_N \frac{d\psi_{rk}}{dt} + j(\omega_k - \omega_r)\psi_{rk} \quad (2.4)$$

$$\psi_{sk} = L_s i_{sk} + L_m i_{rk} \quad (2.5)$$

$$\psi_{rk} = L_r i_{rk} + L_m i_{sk} \quad (2.6)$$

<sup>1</sup>  $(x, y)$  and  $(\alpha, \beta)$  can be used interchangeably, and denote stationary two dimensional time variant orthogonal coordinate system.

$$\frac{d\omega_r}{dt} = \frac{1}{T_M} [\text{Im}(\psi_{sk} * i_{sk}) - T_l] \quad (2.7)$$

Where  $T_N$  is the nominal time, and  $T_M$  is the Mechanical time constants.

When resolving vector equations one may adopt an arbitrary coordinate's reference frame.

### 2.2.4 Mathematical model

The squirrel cage type of induction motor as differential equations for the stator current and rotor flux vector components presented in the  $x$ - $y$  stationary coordinate system with arbitrary angular speed in per-unit ( $pu$ ) system is described as follows[28]:

$$\frac{di_{sx}}{dt} = a_1 i_{sx} + a_2 \psi_{rx} + \omega_s i_{sy} + a_3 \omega_r \psi_{ry} + a_4 u_{sx} \quad (2.8)$$

$$\frac{di_{sy}}{dt} = a_1 i_{sy} + a_2 \psi_{ry} - \omega_s i_{sx} - a_3 \omega_r \psi_{rx} + a_4 u_{sy} \quad (2.9)$$

$$\frac{d\psi_{rx}}{dt} = a_5 \psi_{rx} + (\omega_s - \omega_r) \psi_{ry} + R_r \frac{L_m}{L_r} i_{sx} \quad (2.10)$$

$$\frac{d\psi_{ry}}{dt} = a_5 \psi_{ry} - (\omega_s - \omega_r) \psi_{rx} + R_r \frac{L_m}{L_r} i_{sy} \quad (2.11)$$

$$\frac{d\omega_r}{dt} = \frac{L_m}{L_r J} (\psi_{rx} i_{sy} - \psi_{ry} i_{sx}) - \frac{1}{J} T_l \quad (2.12)$$

Where  $\psi_{rx}$ ,  $\psi_{ry}$ , and  $i_{sx}$ ,  $i_{sy}$ ,  $u_{sx}$ ,  $u_{sy}$  are the rotor flux, and stator current and voltage vectors in coordinate system  $x$ - $y$  rotating with arbitrary angular speed  $\omega_s$ ,  $\omega_r$  is the angular speed of the rotor shaft,  $R_r$ ,  $R_s$ ,  $L_r$ ,  $L_s$  are rotor and stator

resistance and inductances respectively,  $L_m$  is a mutual inductance,  $J$  is the inertia,  $T_l$  is the load torque, and:

$$a_1 = -\frac{R_s L_r^2 + R_r L_m^2}{L_r w}; \quad a_2 = \frac{R_r L_m}{L_r w}; \quad a_3 = \frac{L_m}{w}; \quad a_4 = \frac{L_r}{w}; \quad a_5 = -\frac{R_r}{L_r};$$

$$w = \delta L_r L_s; \quad \delta = 1 - \frac{L_m^2}{L_r L_s}$$

Thus it is seen that an IM is a nonlinear multivariable system with coupling between direct and quadrature axes. It is very difficult to use the above model directly in the control process.

### 2.2.5 Modeling

The model of the IM is implemented by MATLAB/SIMULINK ([6], [7]). The block of motor is shown in Figure 2-6. As we can see there are 3 inputs which are,  $u_{sx}$  ( $u_{sx}$ ),  $u_{sy}$  ( $u_{sy}$ ), and  $T_l$  ( $T_l$ ) also there are 5 outputs which are  $i_{sx}$  ( $i_{sx}$ ),  $i_{sy}$  ( $i_{sy}$ ),  $\psi_{rx}$  ( $\psi_{rx}$ ),  $\psi_{ry}$  ( $\psi_{ry}$ ),  $\omega_r$  ( $\omega_r$ ).

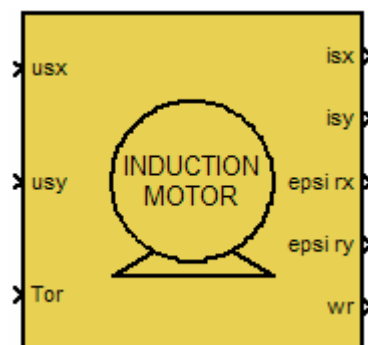


Figure 2-6: Induction motor block

Inside this block the model of the motor is implemented, based on equations from (2.8) to (2.12), as shown in Figure 2-7.

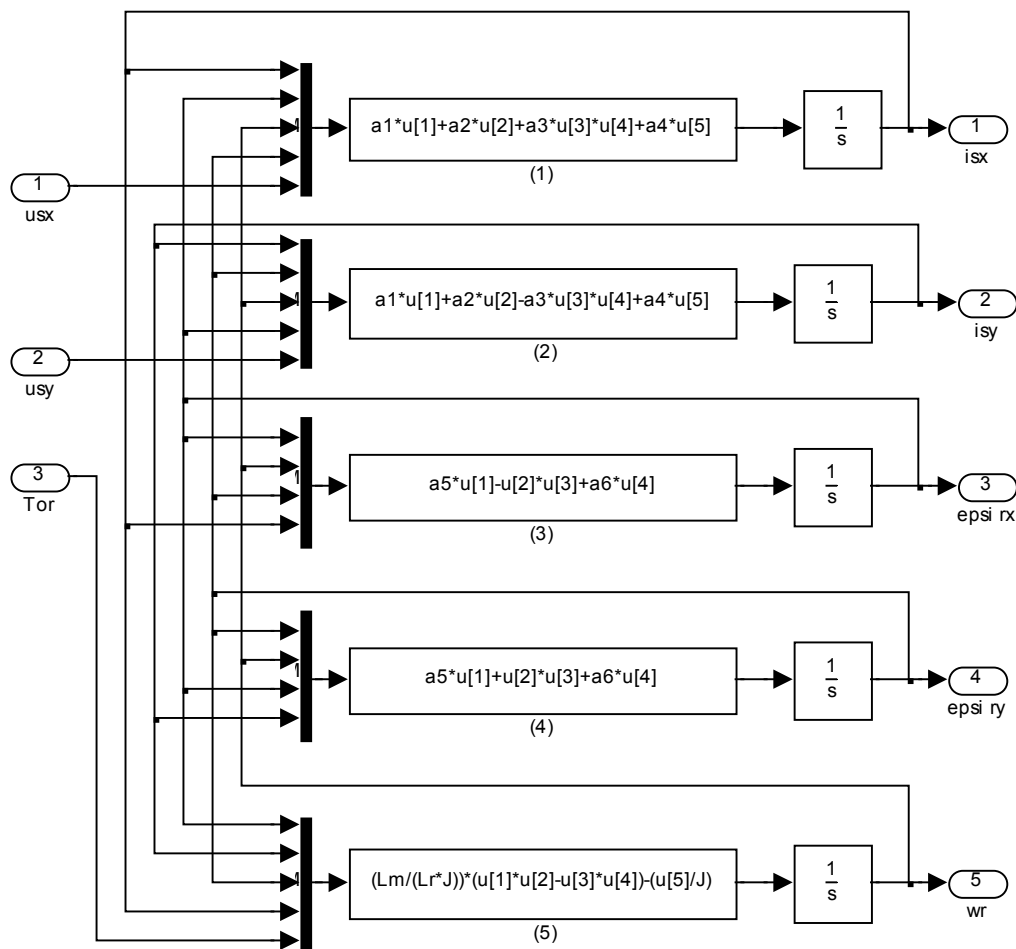


Figure 2-7: Inside the induction motor block

### 2.3 Field Oriented Control

The Field Oriented Control (FOC), as in [11], consists of controlling the stator currents represented by a vector. This control is based on projections which transform a three-phase time and speed dependent system into a two coordinate ( $d$  and  $q$  coordinates) time invariant system. These projections lead to a structure similar to that of a separately excited DC Motor control. Field oriented controlled motors need two constants as input references: the torque component (aligned with the  $q$  coordinate) and the flux component (aligned with  $d$

coordinate). As FOC is simply based on projections the control structure handles instantaneous electrical quantities. This makes the control accurate in every working operation (steady state and transient) and independent of the limited bandwidth mathematical model. The FOC thus solves the classic scheme problems, in the following ways:

- The ease of reaching constant reference (torque component and flux component of the stator current).
- The ease of applying direct torque control because in the  $(d, q)$  reference frame the expression of the torque is:

$$T_l \propto \psi_r i_{sq} \quad (2.13)$$

Note that equation (2.13) is similar to equation (1.4) for a separately excited DC motor. By maintaining the amplitude of the rotor flux ( $\psi_r$ ) at a fixed value we have a linear relationship between torque and torque component ( $i_{sq}$ ). Then torque can be controlled by controlling the torque component of stator current vector.

## 2.4 Coordinate Transformations

Assume  $(A, B, C)$  three phase system axes. the current space vector<sup>2</sup>  $\left[ i_{sA}, i_{sB}, i_{sC} \right]$  depicts the three phase sinusoidal system. It needs to be transformed into a two time invariant coordinate system. This transformation can be split into two steps, as in [9] and [11]:

---

<sup>2</sup> Discussed in section 2.2.3 Space vectors



- $(A, B, C) \rightarrow (\alpha, \beta)$  (The Clarke transformation) which outputs a two coordinate time variant system.
- $(\alpha, \beta) \rightarrow (d, q)$  (The Park transformation) which outputs a two coordinate time invariant system.

### 2.4.1 Clarke transformation $(A, B, C) \rightarrow (\alpha, \beta)$

The space vector can be reported in another reference frame with only two orthogonal axis called  $(\alpha, \beta)$ . Assuming that the axis  $A$  and the axis  $\alpha$  are in the same direction we have the vector diagram shown in Figure 2-8:

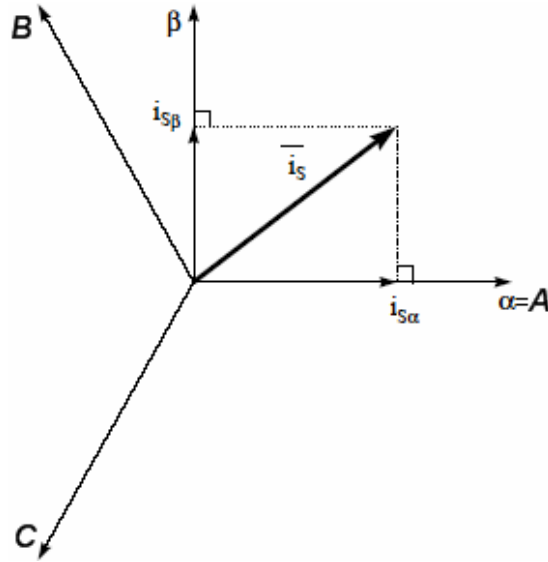


Figure 2-8: Stator current space vector and its components in  $(\alpha, \beta)$

We have:

$$\overline{i_s} = i_{s\alpha} + j i_{s\beta} \quad (2.14)$$

Then:

$$i_{s\alpha} = \text{Re} \left\{ \frac{2}{3} [i_{sA} + \alpha i_{sB} + \alpha^2 i_{sC}] \right\} \quad (2.15)$$

$$i_{s\beta} = \text{Im} \left\{ \frac{2}{3} [i_{sA} + \alpha i_{sB} + \alpha^2 i_{sC}] \right\} \quad (2.16)$$

So:

$$\begin{cases} i_{s\alpha} = i_{sA} \\ i_{s\beta} = \frac{1}{\sqrt{3}}(i_{sA} + 2i_{sB}) \end{cases} \quad (2.17)$$

In matrix form:

$$\begin{bmatrix} i_{s\alpha} \\ i_{s\beta} \end{bmatrix} = \begin{bmatrix} 1 & 0 & 0 \\ \frac{1}{\sqrt{3}} & \frac{2}{\sqrt{3}} & 0 \end{bmatrix} \begin{bmatrix} i_{sA} \\ i_{sB} \\ i_{sC} \end{bmatrix} \quad (2.18)$$

Inverse Clarke transformation  $(\alpha, \beta) \rightarrow (A, B, C)$  as follows:

$$\begin{bmatrix} i_{sA} \\ i_{sB} \\ i_{sC} \end{bmatrix} = \begin{bmatrix} 1 & 0 \\ -\frac{1}{2} & -\frac{\sqrt{3}}{2} \\ -\frac{1}{2} & \frac{\sqrt{3}}{2} \end{bmatrix} \begin{bmatrix} i_{s\alpha} \\ i_{s\beta} \end{bmatrix} \quad (2.19)$$

The block diagram and calculations of the Clarke transformation (modeled in MATLAB/SIMULINK) is shown in Figure 2-9:

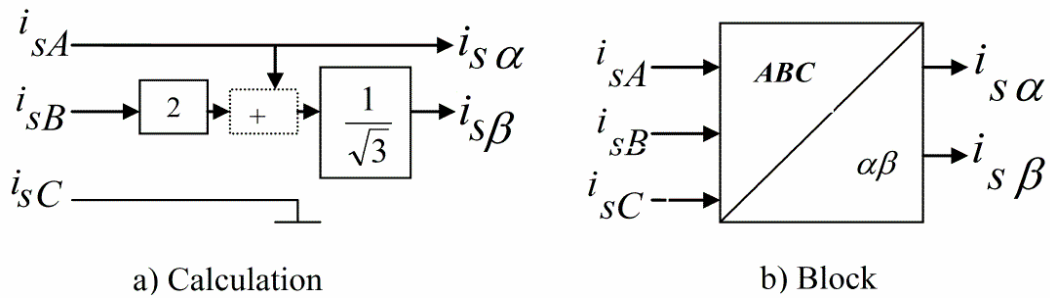


Figure 2-9: Block diagram of the Clarke transformation

### 2.4.2 Park transformation $(\alpha, \beta) \rightarrow (d, q)$

It's considered as the most important transformation in FOC. In fact, this projection modifies a two phase orthogonal system  $(\alpha, \beta)$  rotating with angular speed  $\omega_s$  into the  $(d, q)$  rotating reference frame. If we consider the  $d$  axis aligned

with the rotor flux, Figure 2-10 shows, for the current vector, the relationship from the two reference frame [11]:

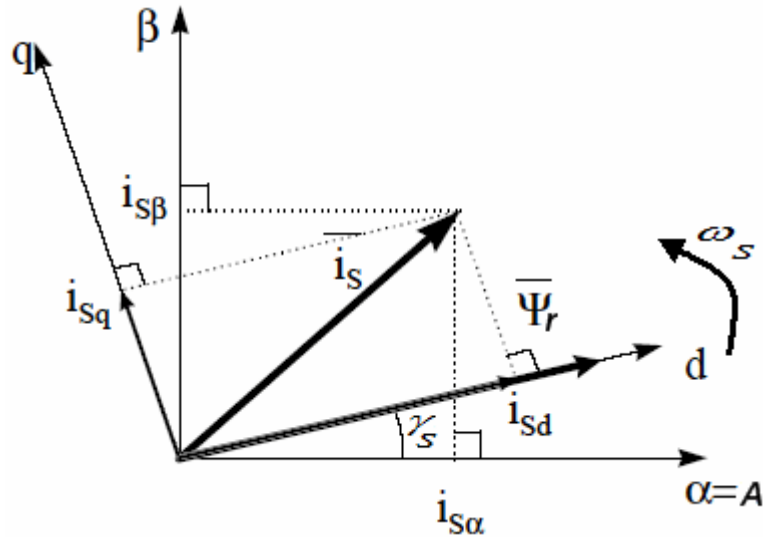


Figure 2-10: Stator current space vector and its component in  $(\alpha, \beta)$  and in the  $(d, q)$  rotating reference frame

Then:

$$\bar{i}_s = i_{sd} + j i_{sq} \quad (2.20)$$

And:

$$\bar{i}_s = \left( i_{s\alpha} \cos(\gamma_s) + i_{s\beta} \sin(\gamma_s) \right) + j \left( i_{s\beta} \cos(\gamma_s) - i_{s\alpha} \sin(\gamma_s) \right) \quad (2.21)$$

In matrix form:

$$\bar{i}_s = \begin{bmatrix} i_{sd} \\ i_{sq} \end{bmatrix} = \begin{bmatrix} \cos(\gamma_s) & \sin(\gamma_s) \\ -\sin(\gamma_s) & \cos(\gamma_s) \end{bmatrix} \begin{bmatrix} i_{s\alpha} \\ i_{s\beta} \end{bmatrix} \quad (2.22)$$

These components depend on the current vector  $(\alpha, \beta)$  components and on the rotor flux position; if we know the right rotor flux position then, by this projection, the  $d, q$  component becomes a constant, two coordinate system

$(i_{sd}, i_{sq})$  can be obtained with the following characteristics:

- Two coordinate time invariant system

- With  $i_{sd}$  (flux component) and  $i_{sq}$  (torque component) the direct torque control is possible and easy.

The block had been modeled in MATLAB/SIMULINK as shown in Figure 2-11:

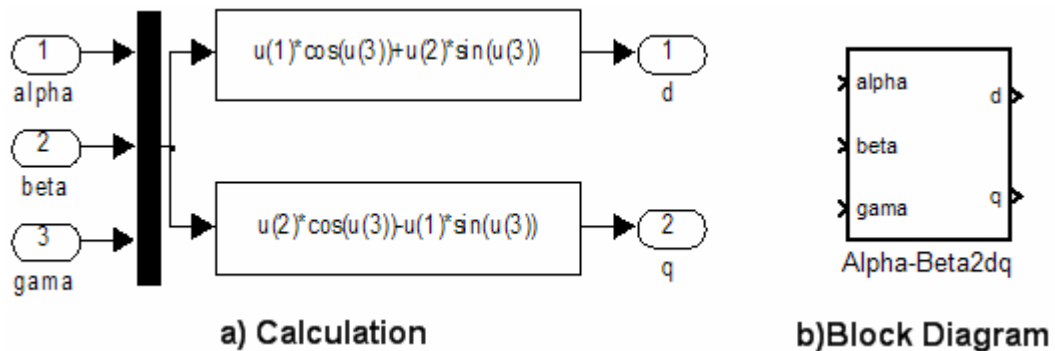


Figure 2-11: Park transformation block diagram

### 2.4.3 Inverse park transformation $(d, q) \rightarrow (\alpha, \beta)$

The inverse park transformation introduced from this voltage transformation only the equation that modifies the voltages in  $(d, q)$  rotating reference frame into a two phase orthogonal system  $(\alpha, \beta)$  as follows in matrix form:

$$\overline{u_s} = \begin{bmatrix} u_s \alpha_{ref} \\ u_s \beta_{ref} \end{bmatrix} = \begin{bmatrix} \cos(\gamma_s) & -\sin(\gamma_s) \\ \sin(\gamma_s) & \cos(\gamma_s) \end{bmatrix} \begin{bmatrix} u_{sdref} \\ u_{sqref} \end{bmatrix} \quad (2.23)$$

The outputs of this block are the components of the reference vector that we call  $\overline{u_s}$ . It is the voltage space vector to be applied to the motor phases. The block had

been modeled in MATLAB/SIMULINK as shown in Figure 2-12:

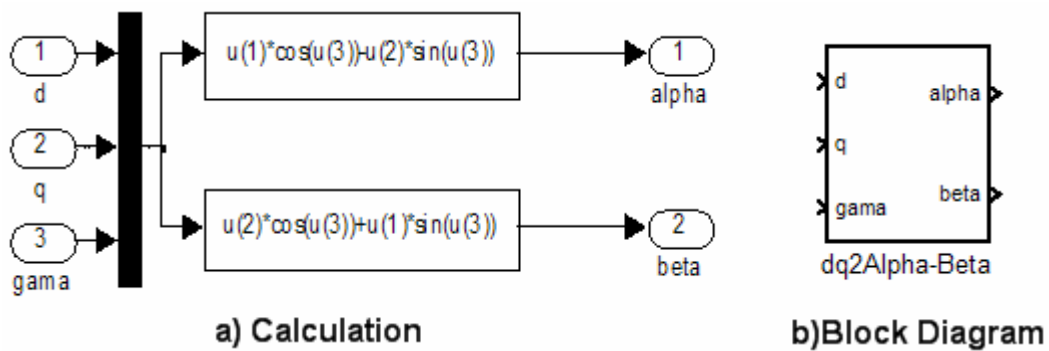


Figure 2-12: Inverse Park transformation block diagram

## 2.5 Basic Scheme for FOC

Figure 2-13 summarizes the basic scheme of torque control with FOC, as in [9] and [11]:

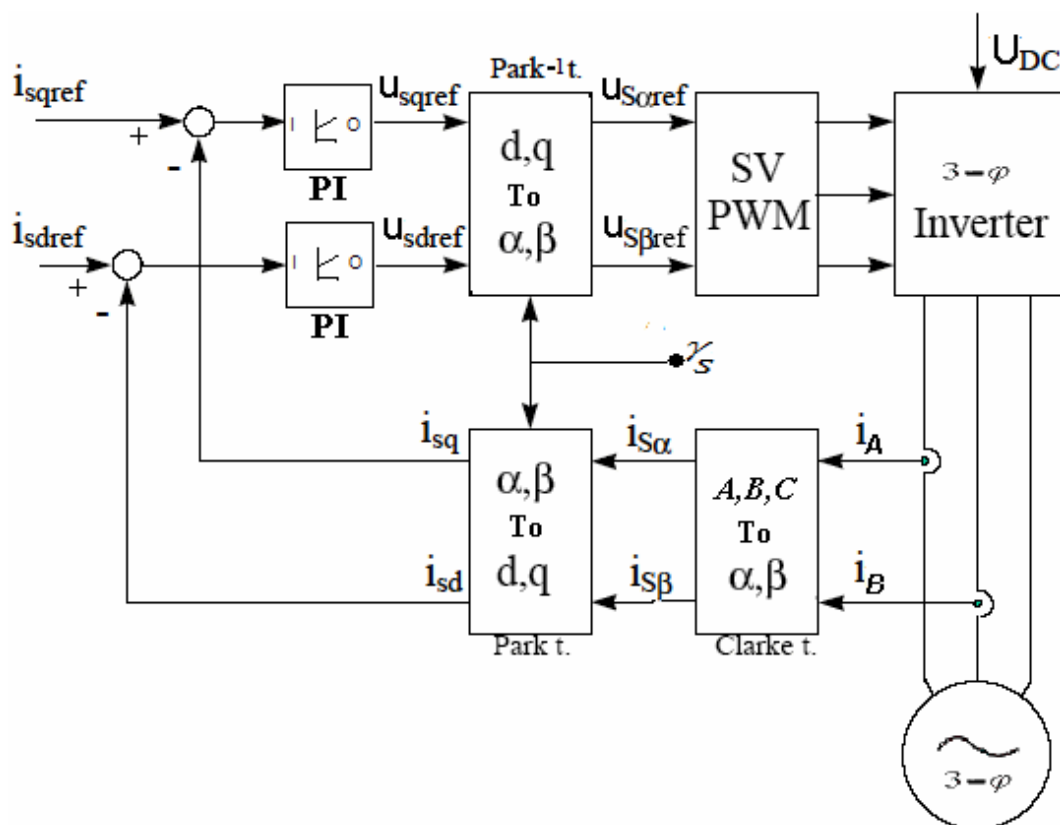


Figure 2-13: Basic scheme of FOC for induction motor

Two motor phase currents are measured. These measurements feed the Clarke transformation block. The outputs of this projection are designated  $i_{s\alpha}$  and  $i_{s\beta}$ .

These two components of the current are the inputs of the Park transformation that gives the current in the  $(d, q)$  rotating reference frame.

$i_{sd}$  and  $i_{sq}$  components are compared to the references  $i_{sdref}$  (the flux reference) and  $i_{sqref}$  (the torque reference). The torque command  $i_{sqref}$  could be the output of the speed regulator when we use a speed FOC.

The outputs of the current regulators are  $u_{sdref}$  and  $u_{sqref}$ ; they are applied to the inverse Park transformation. The outputs of this projection are  $u_{s\alpha ref}$  and  $u_{s\beta ref}$  which are the components of the stator vector voltage in the stationary orthogonal reference frame. These are the inputs of the Space Vector pulse width modulation (SVPWM). The outputs of this block are the signals that drive the inverter. Note that both Park and inverse Park transformations need the rotor flux position  $\gamma_s$ . Rotor flux angle  $\gamma_s$  calculation will be discussed in section 3.4.1, page 38.

## 3 SENSORLESS SPEED CONTROL OF INDUCTION MOTORS

### 3.1 Introduction

Induction motor (IM) speed control drives are used in the process-control industry to adjust the speeds of fans, compress pumps and the like [2]. In many applications, the capabilities to vary speed efficiently can lead to large savings in energy. Adjustable-speed IM drives are also used for electric traction, and for motion control of automatic factories.

IM control drives, typically working at an uncontrolled angular speed and usually as multiphase induction machines, use most of the electrical energy produced. Thanks to advances in technology and automation, controlled drives with IM are now employed increasingly frequently, and are considerably more economical in their use of energy [12].

The block diagram of an adjustable-speed IM drives is shown in Figure 3-1.

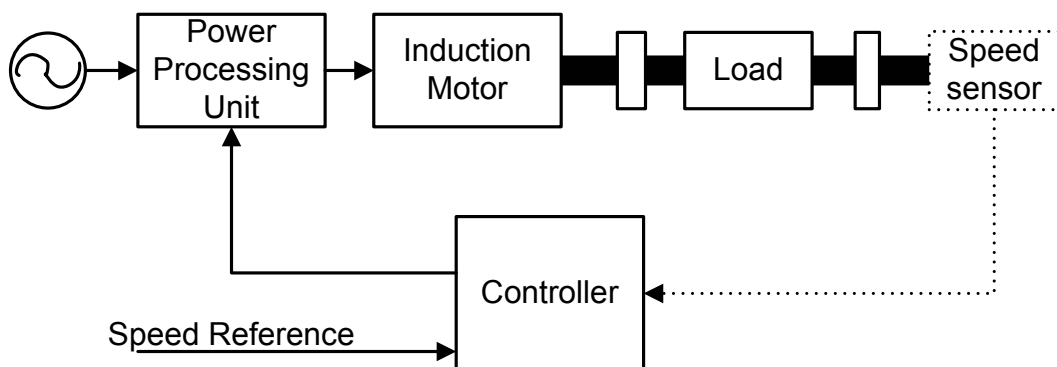


Figure 3-1: Block diagram of an adjustable-speed induction motor drives

The utility input can be either single-phase or three-phase. It is converted by the power processing into three-phase voltages of appropriate magnitude and

frequency, based on the controller input. In speed sensorless system the speed sensor and its input to controller are not used, so they are shown dotted.

There are two issues in speed control using a field-oriented controlled (**FOC**) induction motor, discussed in sections 2.3 to 2.5: One is to make the resulting control system and the controller robust against parameter deviations and disturbances. The other is to make the system intelligent, e.g. to adjust the control system itself to environment changes and task requirements. If the speed regulation loop fails to produce the command current correctly, then the desired torque response will not be produced by the induction motor. In addition, such a failure may cause the degradation of the slip command as well. As a result, a satisfactory speed regulation is extremely important not only to produce desired torque performance from the induction motor but also to guarantee the decoupling between control of torque and flux.

Conventionally, a Proportional Integral (**PI**) controller has been used for the speed regulation to generate a command current for the last two decades, and accepted by industry because of its simplicity. Even though, a well-tuned PI controller performs satisfactorily for a field-oriented induction motor during steady state. The speed response of the machine at transient, especially for the variable speed tracking, may sometimes be problematic. In the last two decades, alternative control algorithms for the speed regulation were investigated. Among these, fuzzy logic, sliding mode, and adaptive nonlinear control algorithms gained much attention [13]. Fuzzy logic control (**FLC**) will be used in this thesis context beside PI control, and a comparative study will be made between them.



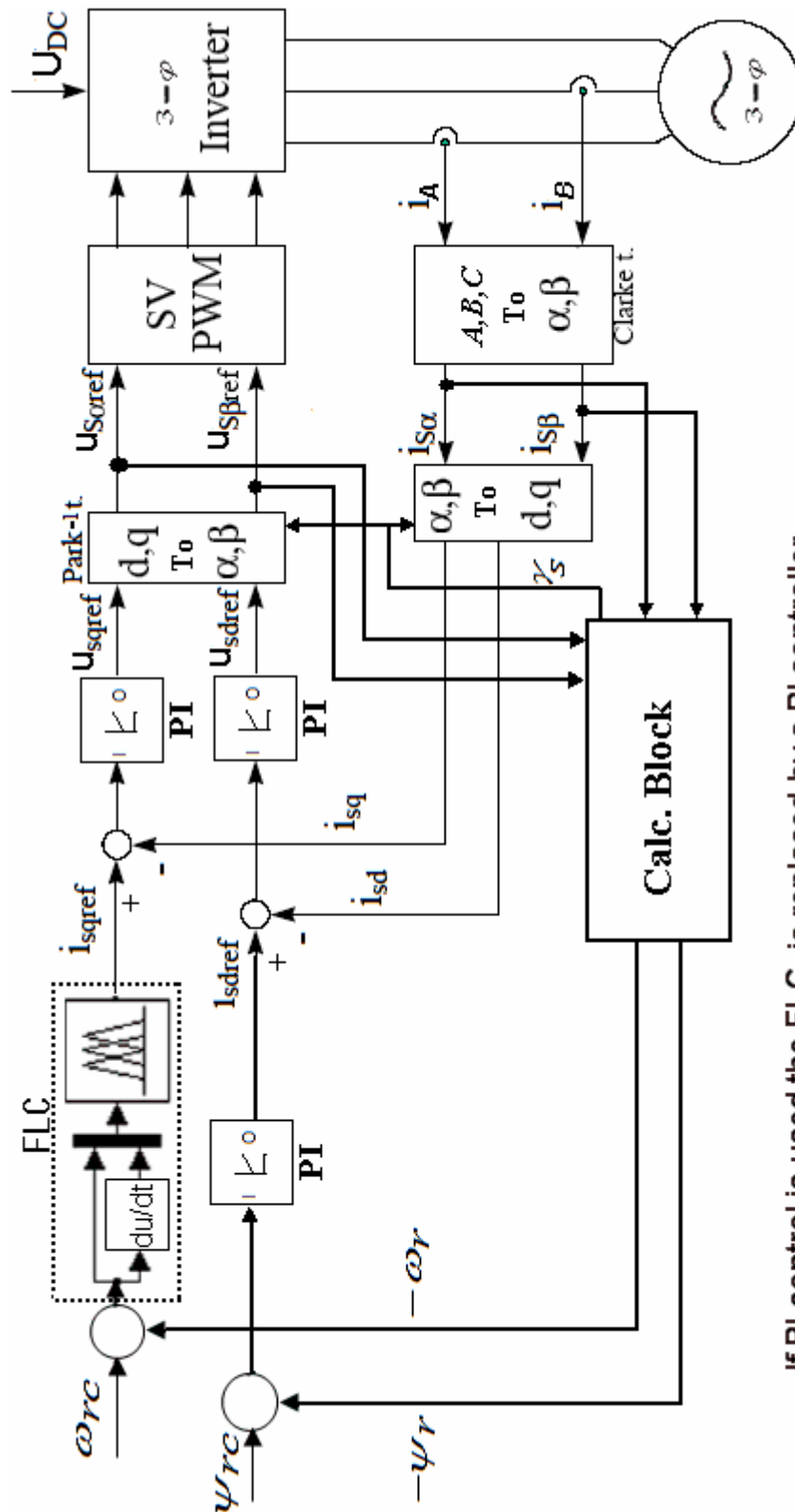
### 3.2 Sensorless Speed Control

From the beginning of the last decade there was a lot of research had been conducted throughout the world to use sensorless control of electrical machines, as in [14] to [24].

Speed sensor has many defects. Among the problems it presents are the spoiling of the ruggedness and the simplicity of AC motors. The encoder is a cost factor, since the provision of special motor-shaft extension encoder mounting surfaces leads to more expensive motors. The use of the delicate optical encoders lowers the system reliability, especially in hostile environments. Because of these problems, there are important requirements to eliminate the speed sensor from control systems.

Eliminating the speed sensor requires the system to provide a way to estimate the variables of the rotor such as the speed and flux from the stator variables. Multiscalar State Variables for sensorless control are used, as in [25], [26]. In this thesis it is presented as a favorable solution to FOC of induction motors without using a sensor of rotor angular speed to calculate the electromagnetic variables.

Based on the FOC basic schema, shown in Figure 2-13, and on the cascade control structure discussed in section 1.4.2 and shown in Figure 1-7, the detailed speed sensorless control system of induction motor is shown in Figure 3-2. The used speed controller is a FLC, and will be discussed in chapter 4. The *Calc. Block* is used to calculate and estimate the state variables:  $\omega_r$ ,  $\psi_r$ ,  $\gamma_s$ , which are rotor speed, rotor flux, and rotor flux angle respectively.  $\omega_{rc}$ ,  $\psi_{rc}$  are the reference values.



If PI control is used the FLC is replaced by a PI controller

Figure 3-2: Detailed Speed sensorless control system of induction motor, Based on FOC.

### 3.3 Multiscalar State Variables of Induction Motor

In section 2.2.4 it is seen that an IM is a nonlinear multivariable system with coupling between direct and quadrature axes. It is very difficult to use the differential equations model directly in the speed sensorless control process.

Four novel state variables have been used to calculate the rotor angular speed [25]. The new “multiscalar” variables may be interpreted as rotor angular speed, scalar and vector products of the stator current and rotor flux vectors, and the square of the rotor linkage flux, as follows:

$$z_1 = \omega_r \quad (3.1)$$

$$z_2 = \psi_{rx} i_{sy} - \psi_{ry} i_{sx} \quad (3.2)$$

$$z_3 = \psi_{rx} i_{sx} + \psi_{ry} i_{sy} \quad (3.3)$$

$$z_4 = \psi_{rx}^2 + \psi_{ry}^2 \quad (3.4)$$

When using these state variables it is possible to present a convenient sensorless solution of motor drives [26].

### 3.4 State Variables Calculations

#### 3.4.1 Rotor flux magnitude and angle

The definitions of stator and rotor flux vectors are as follows:

$$\overline{\psi}_s = \int (\overline{u}_s - R_s \overline{i}_s) dt \quad (3.5)$$

$$\overline{\psi}_s = L_s \overline{i}_s + L_m \overline{i}_r \quad (3.6)$$

$$\overline{\psi}_r = L_r \overline{i}_r + L_m \overline{i}_s \quad (3.7)$$

After some manipulation of equations (3.6) and (3.7) the expressions of rotor flux vector components in the stationary coordinate system  $(x, y)$  can be obtained:

$$\psi_{rx} = \frac{L_r}{L_m} (\psi_{sx} - \delta L_s i_{sx}) \quad (3.8)$$

$$\psi_{ry} = \frac{L_r}{L_m} (\psi_{sy} - \delta L_s i_{sy}) \quad (3.9)$$

And so the magnitude of the rotor flux  $\psi_r$  is as follows:

$$\psi_r = \sqrt{\left( \frac{L_r}{L_m} \left[ \int (u_{sx} - R_s i_{sx}) dt - \delta i_{sx} \right] \right)^2 + \left( \frac{L_r}{L_m} \left[ \int (u_{sy} - R_s i_{sy}) dt - \delta i_{sy} \right] \right)^2} \quad (3.10)$$

And the rotor flux angle  $\gamma_s$  is calculated as:

$$\gamma_s = \tan^{-1} \left( \frac{\psi_{ry}}{\psi_{rx}} \right) \quad (3.11)$$

Substituting equations (3.8) and (3.9) in equations (3.2) to (3.4) we get the entire state variables in terms of stator variables.

The disadvantage of this method is frequency limiting near zero, as in [28], because there will be problems with integrating small voltage signals with low frequency; the increase of operating range towards zero speed may be provided by using another model (current model) in this range. Basically it will fail at zero stator frequency as any other fundamental wave model of the induction motor. The control system using this method is sensitive to stator resistance, especially in the low frequency range, but is not sensitive to rotor resistance.

### 3.4.2 The use of power measurements

Estimation of rotor flux is possible in models or observers. The models are robust and insensitive to harmonics content in current and voltage signals but their error transients are slow. On the other hand, the error transients are fast in observers but their sensitivity to harmonics content in the voltage and current signals is high.

In sensorless speed control system it is essential to know the actual value of rotor flux. The availability of rotor flux vector affects the usability of the control system. The use of instantaneous reactive power and instantaneous active power provides a simplification of the control system.

Akagi and et al. in [27] provided new definitions of instantaneous powers in three-phase ( $p$  and  $q$ ) circuits based on the instantaneous voltages and currents. The new definitions are:

$$p = u_{sx} i_{sx} + u_{sy} i_{sy} \quad (3.12)$$

$$q = u_{sy} i_{sx} - u_{sx} i_{sy} \quad (3.13)$$

The used power  $P$  and  $Q$  are those obtained after filtration (using first order inertial element) of  $p$  and  $q$  calculated from (3.12) and (3.13).

### 3.5 Rotor Angular Speed Calculations Using Power Measurements

Rotor angular speed in the presented control system may be determined by using the differential equations of stator current and rotor flux vector components (motor model), equations (2.8) to (2.11).

The left-hand sides of equations (2.8) to (2.11) are equal to zero in steady state. Use of one or more equations from among the model of the squirrel cage induction motor, together with the definition of multiscalar state variables and power definitions, provides a large number of equations for rotor speed. The suggested coordinate system rotates with the stator current vector component in  $x$ -axis, therefore the current vector component in  $y$ -axis is equal to zero.

The angular frequency  $\omega_i$  of the stator current vector will be used in the rotor speed estimation equations. This value may be described as the sum of rotor angular speed and slip frequency  $\omega_{si}$  in steady state:

$$\omega_i = \omega_r + \omega_{si} \quad (3.14)$$

The slip frequency is described as follows:

$$\omega_{si} = \frac{R_r}{L_r} \frac{z_2}{z_3} \quad (3.15)$$

Multiplying equation (2.8) by stator current component  $\dot{\mathbf{i}}_{sx}$ , and taking into consideration Multiscalar State Variables and power definitions, the next relationship for rotor speed is obtained [28]:

$$\omega_r = \frac{a_1 I_s^2 + a_2 z_3 + a_4 P}{a_3 z_2} \quad (3.16)$$

Multiplying equation (2.9) with  $\dot{\mathbf{i}}_{sx}$ , the next relationship is easily obtained:

$$\omega_r = \frac{-a_2 z_2 - \omega_i I_s^2 + a_4 Q}{a_3 z_3} \quad (3.17)$$

Using equation (3.14) and after doing transformations, the following relationship for rotor speed may be obtained:

$$\omega_r = \frac{-a_2 z_2 - \omega_{si} I_s^2 + a_4 Q}{I_s^2 + a_3 z_3} \quad (3.18)$$

The same process for speed calculation may be used for rotor flux vector components. The rotor angular speed may be presented as the following:

$$\omega_r = \omega_i + \frac{R_r}{L_r} \left( \frac{z_3 - L_m I_s^2}{z_2} \right) \quad (3.19)$$

$$\omega_r = \omega_i - \frac{R_r}{L_r} \frac{z_2}{z_3} \quad (3.20)$$

Using the differential equations of both stator current vector components the rotor speed may be calculated. After some algebra, it is possible to get the following expression:

$$\omega_r = \frac{I_s^2 (a_1 - \omega_{si}) + a_2 (z_3 - z_2) + a_4 (P + Q)}{I_s^2 + a_3 z_3 + a_3 z_2} \quad (3.21)$$

Other relationships can be obtained by using a combination of all model equations as follows:

$$\omega_r = \frac{\frac{R_r}{L_r} z_3 - \frac{R_r L_m}{L_r} I_s^2}{z_2} + \omega_i \quad (3.22)$$

$$\omega_r = \frac{a_4 Q}{a_5 z_3 + I_s^2} - \frac{L_m R_r}{L_r} \frac{z_2}{z_4} \quad (3.23)$$

$$\omega_r = \frac{a_4 Q}{a_5 z_3 + I_s^2} - \omega_{si} \quad (3.24)$$

$$\omega_r = \frac{(L_m + \frac{a_1}{a_2}) I_s^2 + \frac{a_4}{a_2} P}{z_2 \frac{L_r}{R_r}} - \frac{R_r L_m z_2}{L_r z_4} \quad (3.25)$$

Estimating  $\omega_r$  using the equations (3.16) to (3.25) does not use a computationally expensive algorithm and is simple for practical implementation; because there is no matrix conversions or other complex transformations. In comparison with other methods, as in [14] to [21], the proposed systems are simple and may be practically realized with low cost [26].

Sensorless systems provide improved results by adding *low pass filters* (LPF) or delay elements in the speed command channel, feedback path, and on the output of the Speed controller in order to give small steady-state error. It is noticed that the best results are achieved using a time constant for the speed reference three times the time constant of the output of the speed controller. Furthermore, *limiters* must be used for various variables of the control systems.

The disadvantage of using these first order filters, and limiters is making the system response slower, see the simulation results in section 5.3, page 73.

### 3.6 MATLAB/SIMULINK System Model

The control system had been modeled in MATLAB/SIMULINK and is shown in Figure 3-3. The system is modeled in per unit (*pu*) values.



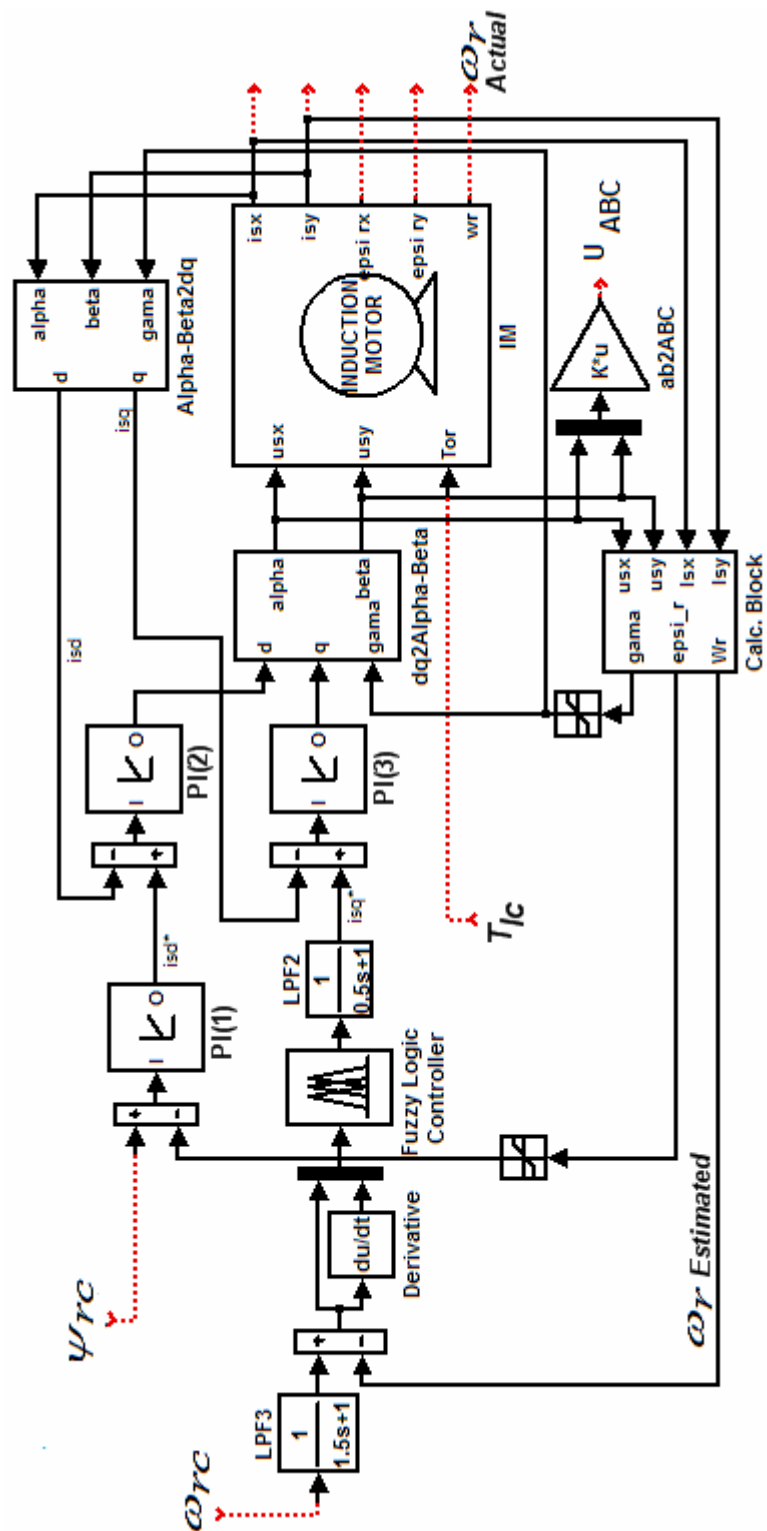


Figure 3-3: Model of sensorless speed control system of IM in SIMULINK.

The following points must be noted about this model:

- The model contains 3 reference inputs:
  - $\omega_{rc}$  : Speed reference.
  - $T_{lc}$  : Load Torque reference.
  - $\psi_{rc}$  : Rotor Flux reference.
- The IM Block is the induction motor block shown and discussed earlier in section 2.2.5, page 25.
- The controllers **PI**, **PI1**, and **PI2** are of Proportional Integral (**PI**) type with anti-windup. The internal model of this controller block had been described before in Figure 1-9, page 16. The system is in the saturation mode when the errors are large; the inclusion of saturation limits on the PI integrator is therefore necessary to provide anti-windup action.
- The Calculation (**Calc.**) block internal model is shown in Figure 3-4:

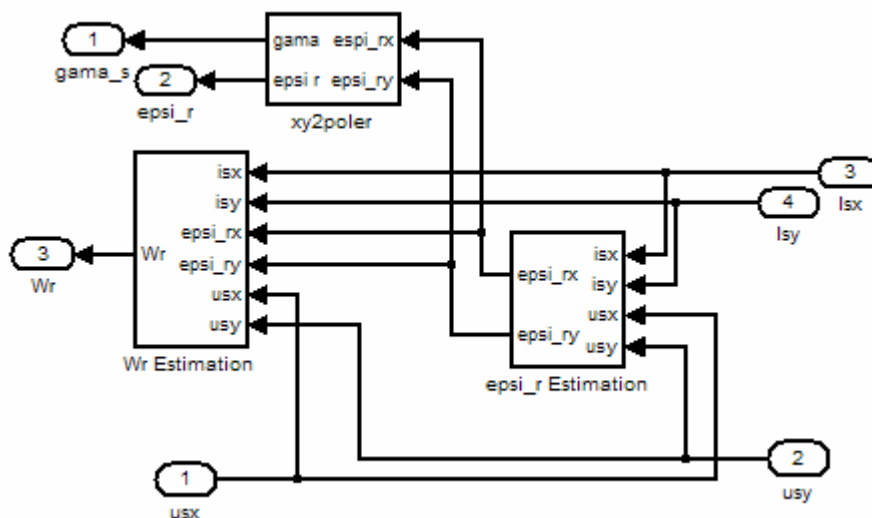


Figure 3-4: State Variables Calc. block model

Where:

- **epsi\_r Estimation** block is built using equations (3.8) and (3.9) to calculate  $\psi_{rx}$  and  $\psi_{ry}$ . The internal structure of this block is shown in Figure 3-5.

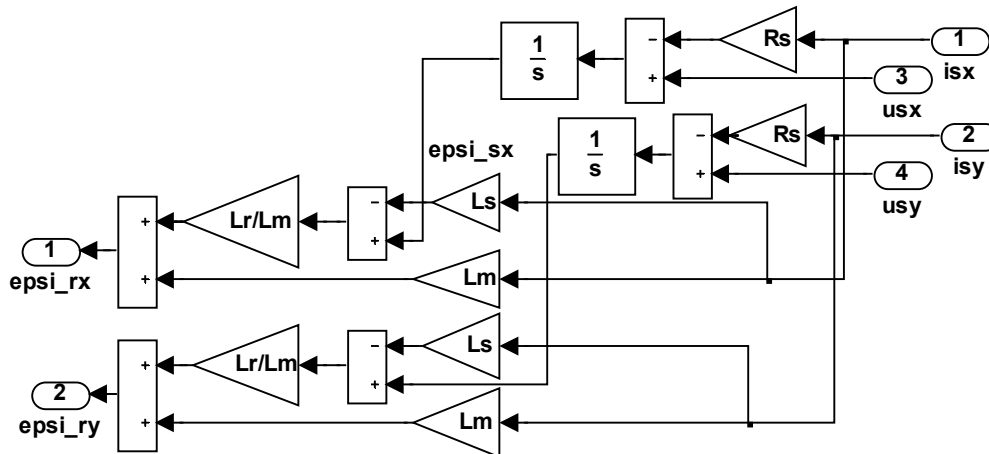


Figure 3-5: Rotor flux calculation block

- **xy2polar** block based on equations (3.10) and (3.11), where **gama** is rotor flux angle ( $\gamma_s$ ).
- **Wr estimation** block is built based on  $\omega_r$  estimation relationships presented in equations (3.16) to (3.25), and is built separately for each equation. The FLC speed controller will be discussed in details later in section 4.4, page 62.
- Sensored speed measurements could be investigated by removing the **Calc. Block** and using the feedback variables directly from the motor model.

Full simulation results with analysis and comparison between Fuzzy and PI approaches will be discussed in chapter 5, especially in section 5.3, page 73.

## 4 FUZZY LOGIC CONTROL OF INDUCTION MOTOR

### 4.1 *Basic Concepts of Fuzzy Logic*

Fuzzy logic is a revolutionary technology that enhances system design with engineering knowledge. Using fuzzy logic, the need for hard mathematical modeling can be avoided. Adjustment factors in control systems will be replaced by self-descriptive linguistics descriptions of the control strategy.

Fuzzy logic is the future technology that will enhance conventional system design, such as linear based Proportional Integral Derivative (**PID**) control and model based control to that of the human expert [29].

The use of fuzzy logic provides a definite way to avoid precise mathematical modeling in order to make exact the solution to the given system application. Adjustments factors in the system implementation and testing stages can be replaced by additional self-descriptive linguistics process description within the knowledge base of the already designed system. Hence once the basic fundamental design stage is complete, the fine-tuning stage will enable the knowledge base to support all varying operating conditions of the plant.

Theoretically, a fuzzy logic system can be designed using other conventional design methods such as linear based PID or Model Based Control [27]. In some cases, conventional methods are easier to design, allowing faster design time.

### 4.1.1 Research history on fuzzy Logic

In 1965, L.A. Zadeh laid the foundations of fuzzy set theory [34] as a method to deal with the imprecision of practical systems. Bellman and Zadeh wrote: "*Much of the decision-making in the real world takes place in an environment in which the goals, the constraints and the consequences of possible actions are not known precisely*" [35]. This "imprecision" or fuzziness is the core of fuzzy sets or fuzzy logic applications. Fuzzy sets were proposed as a generalization of conventional set theory. Partially as a result of this fact, fuzzy logic remained the purview of highly specialized and mathematical technical journals for many years. This changed abruptly with the highly visible success of several control applications in the late 1980s.

Many researchers and practitioners of fuzzy logic systems believe that fuzzy control design theory departs significantly from conventional control design theory, which is essentially based on mathematical modeling of the controlled Process [30]. Instead of modeling the control system mathematically, fuzzy logic utilizes the expert/operators knowledge. This means gathering all control actions that the expert/operator performs on a plant.

Human operator control behavior becomes the stored knowledge base of the fuzzy logic system. Conditional IF-THEN statements are utilized to account for the conditions and actions that the expert operator performs for the complete cycle of the process. Fuzzy set theory that relates back to fuzzy logic has stayed in the academic section of engineering for more than 30 years [31]. However, in the 1980s, Japan was the first in developing the first practical applications, which helped trigger further practical developments in Germany and America. These

soon followed suit in the race for furthering the applications of fuzzy logic technology [31].

Basically, the problem firstly arose from the industrial sector wanting a more diverse and flexible control system that would allow for “easy integration” of equipment. Easy integration in the sense that a system such as an automatic gearbox transmission for a family car can be tuned according to the specified countries regulations for their vehicle makes, rather than completely redesigning the electronics of the gearbox uniquely for each standard. With fuzzy logic this can be easily achieved by adding more modules or blocks within the fuzzy logic system to cater for the number of physical inputs/outputs, then modifying the degree of support (**DoS**) of the IF-THEN knowledge base in the fine-tuning stage. Fuzzy control was first introduced by E. Mamdani and S. Assilian in 1975 [38].

#### **4.1.2 History of AC motor Fuzzy control**

Many of today’s fuzzy methods of motor speed control have requirements such as performing tasks demanding a high level of accuracy, involving rapid speed acceleration/deceleration and end-effector’s positioning. Some of the work achieved by previous researchers in this area is summarized here, along with the results of their realizations.

Probably the first work successfully achieved in the fuzzy control of AC motor drive systems was that of Amin Suyitno and et al. in [32], their work and research papers started in 1986. These researches have looked at fuzzy logic based on a linear controller structure (**PI**) such that the controller makes the system respond quickly if the error  $e$  is large, and vice versa in order to obtain a robust controller

which is insensitive to both the plant noise equivalent disturbance, and the observation noise [32]. The next step taken by these researchers was to develop a variable structure PI controller by Fuzzy logic, for the AC motor drive system. It was the belief of these researchers that fuzzy control systems should be low cost and closely simulate human skill. It was also emphasized that fuzzy logic systems are nonlinear by nature and that linear control design procedures have almost been accomplished in many key areas. It was concluded that fuzzy logic systems are suited to nonlinear applications, hence yielding the most successful results when compared to linear controllers.

M. A. Denai and S. A. Attia in [33] stated that *“Induction motors are characterized by complex, highly nonlinear, and time-varying dynamics and inaccessibility of some states and outputs for measurements, and hence may be considered as a challenging engineering problem. The advent of vector control techniques has partially solved induction motor control because they are sensitive to drive parameter variations and performance may deteriorate if fixed parameter controllers are used. Fuzzy logic-based controllers are considered as potential candidates for such application”*.

## **4.2 Fuzzy Sets Fundamentals:**

Zadeh makes a case that humans reason not in terms of discrete symbols and numbers, but in terms of fuzzy sets [34]. These fuzzy terms define general categories, but not rigid, fixed collections. The transition from one category, concept, idea, or problem state to the next is gradual with some states having

greater or less membership in the one set and then another. From this idea of elastic sets, Zadeh proposed the idea of a fuzzy set. Fuzzy sets are functions that map a value that might be a member of the set to a number between zero and one indicating its actual degree of membership. A degree of *zero* means that the value is not in the set and a degree of *one* means that the value is completely representative of the set. This produces a curve across the members of the set. There are many books that have been written on the subject of fuzzy sets since Zadeh introduced the fuzzy set concept in 1965.

#### 4.2.1 Membership functions – fundamental definitions

Let  $X$  be a set of objects, called the universe, whose elements are denoted  $x$ . Membership in a subset  $A$  of  $X$  is the membership function [34],  $A$  from  $X$  to the real interval  $[0, 1]$ . The universe is all the possible elements of concern in the particular context.  $A$  is called a fuzzy set and is a subset of  $X$  that has no sharp boundary.  $A$  is the grade of membership  $x$  in  $A$ . The closer the value of  $A$  is to 1, the more  $x$  belongs to  $A$ . The total allowable universe of values is called the domain of the fuzzy set. The domain is a set of real numbers, increasing monotonically from left to right where the values can be both positive and negative.  $A$  is completely characterized by the set of pairs:

$$A = \{(x, \mu_A(x)), x \in X\} \quad (4.1)$$

Support of a fuzzy set  $A$  in the universal set  $X$  is the crisp set that contains all the elements of  $X$  that have a nonzero membership grade in  $A$ . That is:

$$\text{supp } A = \{x \in X \mid \mu_A(x) > 0\} \quad (4.2)$$



With a finite support, let  $x_i$  be an element of the support of fuzzy set  $A$  and that  $\mu_A(x)$  a grade of membership in  $A$ . Then  $A$  is written by convention as:

$$A = \frac{\mu_1}{x_1} + \dots + \frac{\mu_n}{x_n} = \sum_{i=1}^n \frac{\mu_i}{x_i} \quad (4.3)$$

When  $X$  is an interval of real numbers, a fuzzy set  $A$  is expressed as:

$$A = \int_x \frac{\mu_A(x)}{x} \quad (4.4)$$

An empty fuzzy set has an empty support which implies that the membership function assigns 0 to all elements of the universal set.

The degree of membership is known as the membership or truth function since it establishes a one-to-one correspondence between an element in the domain and a truth value indicating its degree of membership in the set. It takes the form:

$$\mu_A(x) \leftarrow f(x \in A) \quad (4.5)$$

The triangular membership function is the most frequently used function and the most practical, but other shapes are also used. One is the trapezoid which contains more information than the triangle. A fuzzy set can also be represented by a quadratic equation (involving squares,  $n^2$ , or numbers to the second power) to produce a continuous curve. Three additional shapes which are named for their appearance are: the **S**-function, the  **$\pi$** -function, and the **Z**-function.

#### 4.2.2 Approximate reasoning

The root mechanism in a fuzzy model is the proposition [41]. These are statements of relationships between mode variables and one or more fuzzy regions. A series of conditional and unconditional fuzzy associations or

propositions are evaluated for its degree of truth and all those that have some truth contribute to the final output state of the solution variable set. The functional tie between the degrees of truth in related fuzzy regions is called the method of implication. The functional tie between fuzzy regions and the expected value of a set point is called the method of *defuzzification*. Taken together these constitute the backbone of approximate reasoning. Hence an approximate reasoning system combines the attributes of conditional and unconditional fuzzy propositions, correlation methods, implication (truth transfer) techniques, proposition, aggregation, and defuzzification [36]. Unlike conventional expert systems where statements are executed serially, the principal reasoning protocol behind fuzzy logic is a *parallel paradigm*. In conventional knowledge-based systems pruning algorithms and heuristics are applied to reduce the number of rules examined, but in a fuzzy system all the rules are fired.

### 4.2.3 The role of linguistic variables

Fuzzy models manipulate linguistic variables. A linguistic variable is the representation of a fuzzy space which is essentially a fuzzy set derived from the evaluation of the linguistic variable. A linguistic variable encapsulates the properties of approximate or imprecise concepts in a systematic and computationally useful way. The organization of a linguistic variable  $L$  is:

$$L \text{ var} \leftarrow \{q_1 \dots q_n\} \{h_1 \dots h_n\} f_s \quad (4.6)$$

Where predicate  $q$  represents frequency qualifiers,  $h$  represents a hedge, and  $f_s$  is the core fuzzy set. The presence of qualifier(s) and hedge(s) are optional. Hedges change the shape of fuzzy sets in predictable ways and function in the

same fashion as adverbs and adjectives in the English language. Frequency and usuality qualifiers reduce the derived fuzzy set by restricting the truth membership function to a range consistent with the intentional meaning of the qualifier. Although a linguistic variable may consist of many separate terms, it is considered a single entity in the fuzzy proposition.

#### 4.2.3.1 Linguistic modifiers

A linguistic modifier is an operation that modifies the meaning of a term. For example, in the sentence “very close to 0”, the word Very modifies “close to 0” which is a fuzzy set. A modifier is thus an operation on a fuzzy set. Examples of other modifiers are a *little*, *more*, *less*, *big*, *large*, *possibly*, and *definitely*.

#### 4.2.4 Fuzzy system structure

In the context of feedback system control, control input and feedback error are given as real "crisp" numbers. In order to apply fuzzy concepts the feedback error  $e$  has to be presented by a fuzzy set. This set is modified according to the fuzzy rules into a fuzzy set of controls  $C$  which are translated back into a crisp control input  $u$ . This task is performed by a fuzzy system defined according to [37] and illustrated in Figure 4-1.

#### 4.2.5 Fuzzy propositions

A fuzzy model consists of a series of conditional and unconditional fuzzy propositions [41]. A proposition or statement establishes a relationship between a value in the underlying domain and a fuzzy space. A conditional fuzzy proposition is one that is qualified as an *if* statement. The proposition following the *if* term is the *antecedent* or *predicate* and is an arbitrary fuzzy proposition.

The proposition following the *then* term is the consequent and is also any arbitrary fuzzy proposition.

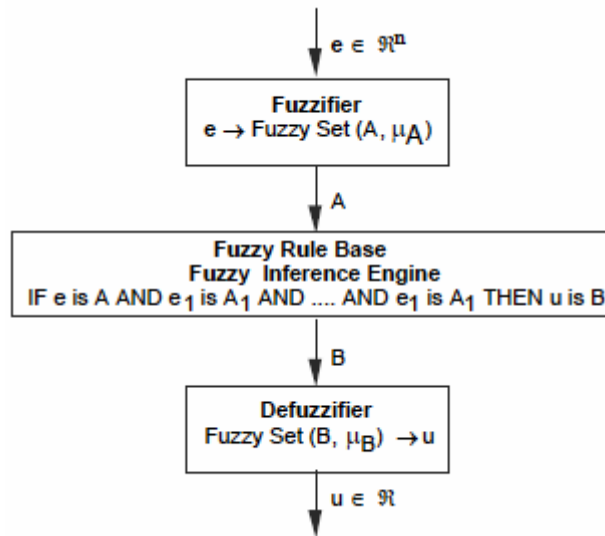


Figure 4-1: Structure of a fuzzy system

e.x. IF-THEN statement: *if w is Z then x is Y*

Where  $Z$  and  $Y$  are linguistic values defined by fuzzy sets. The *if-part* of the rule “ $w$  is  $Z$ ” is called the *antecedent* & the *then-part* of the rule “ $x$  is  $Y$ ” is called the *consequent*, Interpreted as:

**$x$  is a member of  $Y$  to the degree that  $w$  is a member of  $Z$**

An unconditional fuzzy proposition is one that is not qualified by an *if* statement.

**$x$  is  $Y$**

Where  $x$  is a scalar from the domain and  $Y$  is a linguistic variable. Unconditional statements are always applied within the model and depending on how they are applied, serve either to restrict the output space or to define a default solution space. We interpret an unconditional fuzzy proposition as:

### ***X is the minimum subset of Y***

If a model contains a mixture of conditional or unconditional propositions, then the order of execution becomes important. Unconditional propositions are generally used to establish the default support set for a model. If none of the conditional rules executes, then a value for the solution variable is determined from the space bounded by the unconditionals. For this reason, they must be executed before any of the conditionals.

The effect of evaluating a fuzzy proposition is a degree or grade of membership derived from the transfer function:

$$\mu \leftarrow (x \in Y) \quad (4.7)$$

Where  $x$  is a scalar from the domain and  $Y$  is a linguistic variable. This is the essence of an approximate statement. The derived truth membership value establishes compatibility between  $x$  and the generated fuzzy space  $Y$ . This truth value is used in the correlation and implication transfer functions to create or update fuzzy solution space. The final solution fuzzy space is created by aggregating the collection of correlated fuzzy propositions.

#### **4.2.6 Logical operations**

We now know what's fuzzy about fuzzy logic, but what about the logic?

The most important thing to realize about fuzzy logical reasoning is the fact that it is a superset of the standard Boolean logic. In other words, if we keep the fuzzy values at their extremes of 1 (completely true), and 0 (completely false), standard logical operations will hold. Fuzzy logic deals with following operators:

1. **AND** function can be implemented by **min (minimum)**, or **prod (product)** functions.
2. **OR** function can be implemented by **max (maximum)**, or **probor (probabilistic)** function. The **probabilistic** can be calculated as:

$$probor(A,B) = A + B - AB \quad (4.8)$$

3. **NOT** function can be replaced by **(1-A)**.

So fuzzy logical can be considered a Multi-Valued Logic, as shown in Figure 4-2:

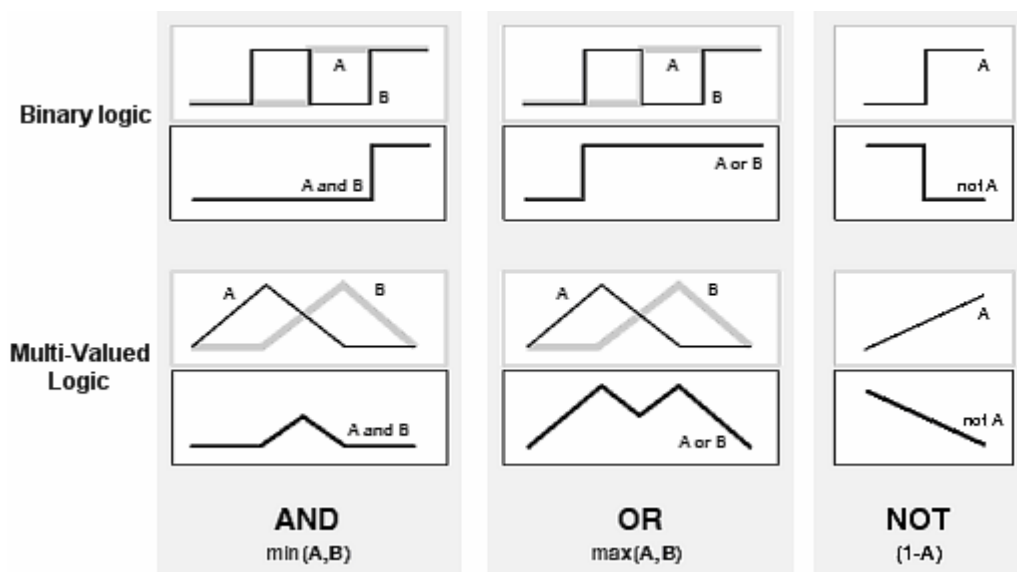


Figure 4-2: Fuzzy logical operators

#### 4.2.7 Methods of defuzzification

Using the general rules of fuzzy inference, the evaluation of a proposition produces one fuzzy set associated with each model solution variable. Defuzzification or decomposition involves finding a value that best represents the information contained in the fuzzy set. The defuzzification process yields the expected value of the variable for a particular execution of a fuzzy model. In fuzzy models, there are several methods of defuzzification that describe the ways we can derive an expected value for the final fuzzy state space.

Defuzzification means dropping a “plumb line” to some point on the underlying domain. At the point where this line crosses the domain axis, the expected value of the fuzzy set is read. Underlying all the defuzzification functions is the process of finding the best place along the surface of the fuzzy set to drop this line. This generally means that defuzzification algorithms are a compromise with or a trade-off between the need to find a single point result and the loss of information such a process entails.

The two most frequently used defuzzification methods are composite moments (*centroid*) and composite maximum. The *centroid* or center of gravity technique finds the balance point of the solution fuzzy region by calculating the weighted mean of the fuzzy region. Arithmetically, for fuzzy solution region  $\mathcal{A}$ , this is formulated as:

$$\mathfrak{R} \leftarrow \frac{\sum_{i=0}^n d_i \mu_A(d_i)}{\sum_{i=0}^n \mu_A(d_i)} \quad (4.9)$$

Where  $d$  is the  $i^{\text{th}}$  domain value and  $\mu(d)$  is the truth membership value for that domain point. A *centroid* or composite moment’s defuzzification finds a point representing the fuzzy set’s center of gravity.

### 4.3 Control Design and Stability

When fuzzy systems are used as controllers, they are called *fuzzy logic controllers (FLC)*. If fuzzy systems are used to model the process and controllers are designed based on the model, then resulting controllers also are called fuzzy

controllers. Therefore, fuzzy controllers are nonlinear controllers with a special structure. Fuzzy control has represented the most successful applications of fuzzy theory to practical problems.

Fuzzy control can be classified into *static fuzzy control* and *adaptive fuzzy control* [41]. In static fuzzy control, the structure and parameters of the fuzzy controller are fixed and do not change during real-time operation. On the other hand in adaptive fuzzy control, the structure and/or parameters of the fuzzy controller change during real-time operation, one method to do this is using artificial neural networks [33]. Fixed fuzzy control is simpler than adaptive fuzzy control, but requires more knowledge of the process model or heuristic rules. Adaptive fuzzy control, on the other hand, is more expensive to implement, but requires less information and may perform better. *In this thesis we are interested in fixed fuzzy controller design.*

#### **4.3.1 Fixed fuzzy controller design**

Fuzzy control and conventional control have similarities and differences. They are similar in the sense that they must address the same issues that are common to any control problem, such as stability and performance. However, there is a fundamental difference between fuzzy control and conventional control. Conventional control starts with a mathematical model of the process and controllers are designed based on the model. Fuzzy control, on the other hand, starts with heuristics and human expertise (in terms of fuzzy IF-THEN rules) and controllers are designed by synthesizing these rules. That is, the information used to construct the two types of controllers is different; see Figure 4-3. Advanced



fuzzy controllers, however, can make use of both heuristics and mathematical models.

The design techniques for fuzzy controllers can be classified into the *trial-and-error approach* and the *theoretical approach* [39]. In the trial-and-error approach, a set of fuzzy IF-THEN rules are collected from human experts or documented knowledge base, and the fuzzy controllers are constructed from these fuzzy IF-THEN rules. The fuzzy controllers are tested in the real system and if the performance is not satisfactory, the rules are fine-tuned or redesigned in a number of trial-and-error cycles until the performance is satisfactory. In theoretical approach, the structure and parameters of the fuzzy controller are designed in such away that certain performance criteria are guaranteed. Both approaches, of course, can be combined to give the best fuzzy controllers.

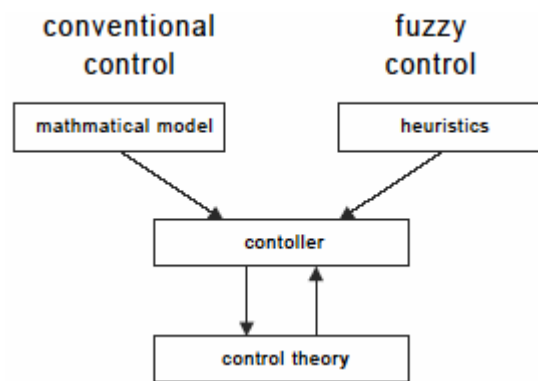


Figure 4-3: Fuzzy control and conventional control.

#### 4.3.1.1 Trial-and-error (heuristic) approach:

The trial-and-error approach to fuzzy controller design can be summarized in the following steps:

1. Select state and control variables. The state variables should characterize the key features of the system and the control variables should be able to

influence the states of the system. The state variables are the inputs to the fuzzy controller and the control variables are the output of the fuzzy controller.

2. Construct IF-THEN rules between the state and control variables. The formulation of these rules can be achieved in two different heuristic approaches. The most common approach is the linguistic verbalization of human experts. Another approach is to interrogate experienced experts or operators using a carefully organized questionnaire.
3. Test the fuzzy IF-THEN rules in the system. The closed-loop system with the fuzzy controller is run and if the performance is not satisfactory, fine tune or redesign the fuzzy controller and repeat the procedure until the performance is satisfactory.

#### **4.3.1.2 Theoretical approach:**

Knowing the mathematical model of a system is not a necessary condition for designing fuzzy controllers. However, in order to analyze the performance of the closed-loop fuzzy control system theoretically, we need to have some knowledge on the model of the system. This approach assumes a mathematical model for the system, so that mathematical analysis can be performed to establish the properties of the designed system.

#### **4.3.2 Used control design approach**

The control system of induction motor shown in Figure 3-2 has difficult to describe analytical relationships caused by non-precise variable identification as in [33] and [40]; in these situations, *Fixed Fuzzy logic controller (FLC) design using heuristic approach* is best suited. This fuzzy approach is used here in this thesis context.

#### 4.4 Speed Fuzzy Logic Controller

Fuzzy logic controller is the main element in the speed control system of the induction motor explained in section 3.2, page 36, and for separately excited DC Motor explained in section 1.4.3, page 15. Here is introduced how to use FLC in the speed control system, and how to build the fuzzy inference system (FIS).

In this section we deal only with induction motor only, and as it will be seen in the simulation results of the separately excited DC motor section 5.2, page 69, the same controller will be used but with small changes of the ranges for the membership functions.

So the idea is to develop a fuzzy control system that controls the rotor speed of a squirrel-cage induction machine, depending on the “Error” and “Change of Error”, between Reference speed and the estimated rotor speed from the sensorless calculation block.

Mamdani<sup>1</sup> type of FLC, presented in Figure 4-4, is used for speed control. The input signals for the controller are: control error ( $e$ ) and the change of error ( $\Delta e$ ) and the output is the change of control signal ( $\Delta u$ ). The controller consists of three elements: fuzzification block, block of rules (rules of inference) and defuzzification, which are related by proper relationships.

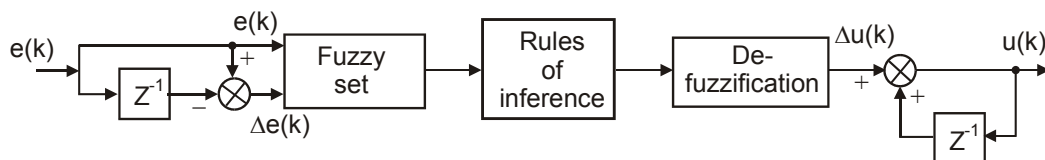
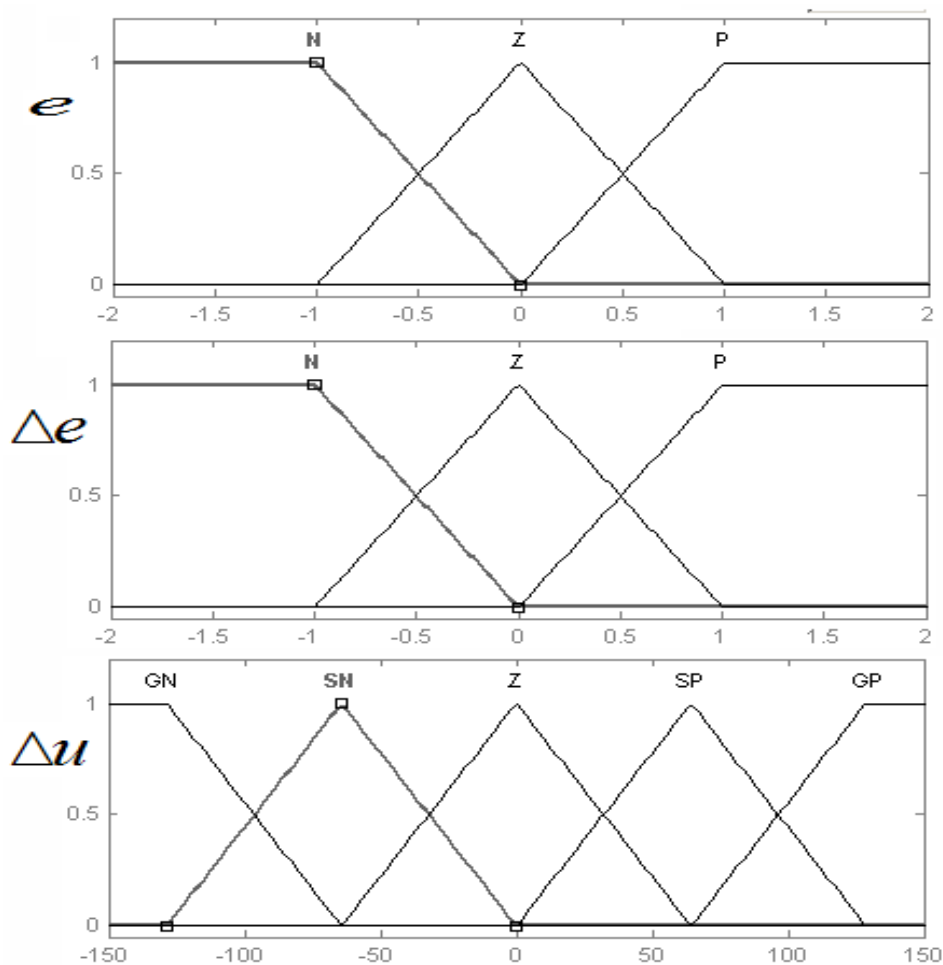


Figure 4-4: Mamdani type FLC

<sup>1</sup> Named after E. Mamdani [38].

On the basis of the values,  $e$  and  $\Delta e$ , the fuzzy numbers are calculated in the fuzzification block using the membership functions shown in Figure 4-5.

Simple membership functions for the three linguistic variables: Negative (**N**), Zero (**Z**), and Positive (**P**) are used. Symbol **G** means great and symbol **S** means small.



**Figure 4-5: Membership functions of  $e$ ,  $\Delta e$ , and  $\Delta u$**

The resulting block consists of logic table like ‘IF-THEN’ rules, which are described in Table 4-1. These form the rule base for inference, contains 9 rules, which is reduced form of the 49 rules FLC. These 9 rules give results similar to the 49 rules FLC, while reducing the complexity of the controller.

Table 4-1: Fuzzy Logic Controller Rules of Inference

		e		
		N	Z	P
$\Delta e$	N	GN	SN	SP
	Z	GN	Z	GP
	P	SN	SP	GP

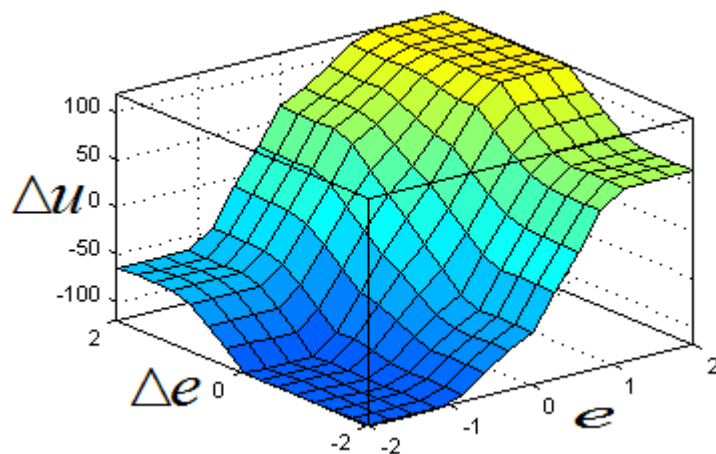
$\Delta u$

Surface view of the rules is shown in Figure 4-6. Sample rules extracted from the rule base:

- *If e is N AND  $\Delta e$  is P then  $\Delta u$  is SN.*
- *If e is P AND  $\Delta e$  is N then  $\Delta u$  is SP.*
- *If e is Z AND  $\Delta e$  is Z then  $\Delta u$  is Z.*

The operations that were used are:

- **Implication** by AND operators represented by (*prod*) function.
- **Aggregation** by OR operators represented by (*probor*) function.
- **Defuzzification** by *Centroid* method.

Figure 4-6: Surface view of e,  $\Delta e$ , and  $\Delta u$

#### 4.4.1 Implementation

The FLC controller is built using the graphical user interface(GUI) Fuzzy inference system editor (FIS Editor) provided by the Fuzzy logic Toolbox under MATLAB/SIMULINK ([6], [7]). Screen shots of the system are shown in Appendix A. The block of fuzzy controller in MATLAB/SIMULINK is shown in Figure 4-7.

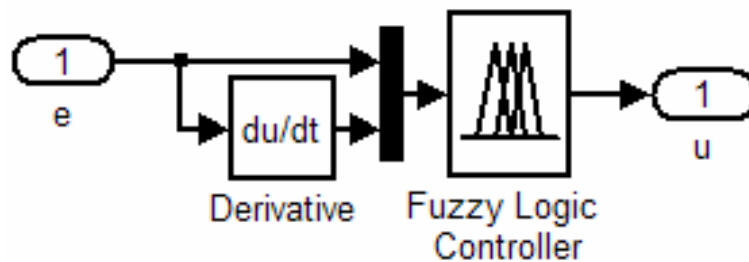


Figure 4-7: Fuzzy logic controller block

#### 4.4.2 Fuzzy logic algorithm summary

The definitions of Fuzzy logic terminology used in the Fuzzy Logic Controller (FLC) are explained with reference to the thesis work. The algorithm flow chart is shown in Figure 4-8.

The algorithm flowchart consisted of three steps [36]:

1. Fuzzification.
2. Inference.
3. DeFuzzification.

The inputs and outputs are shown for each step.

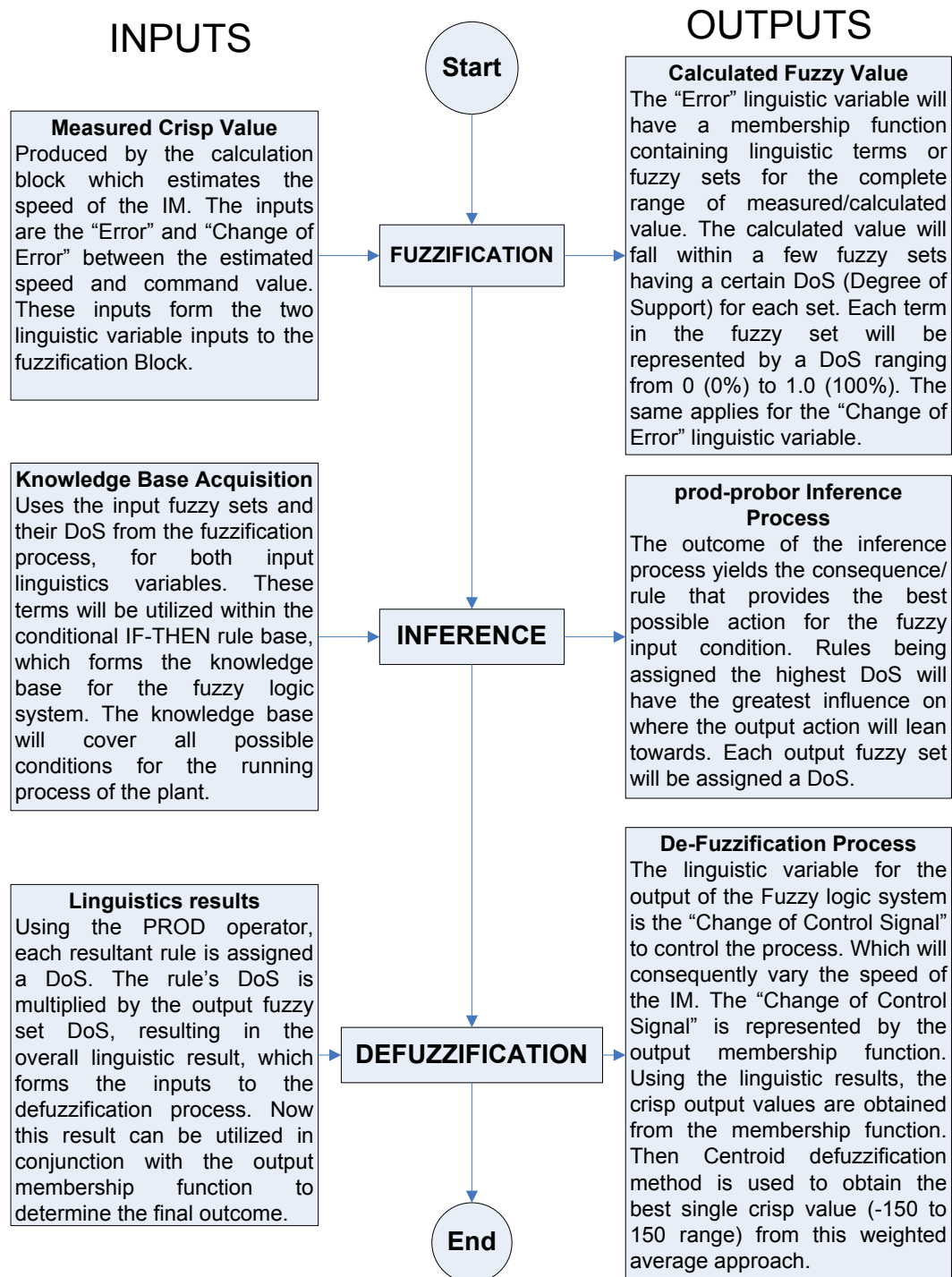


Figure 4-8: Fuzzy logic algorithm chart

## 5 SIMULATION RESULTS AND FUZZY/PI COMPARISON

### 5.1 Introduction

Comparison of the system behavior under Fuzzy Logic Controller (FLC) and Proportional Integral (PI) control is performed by subjecting the control system of the motor to the same parameters, and with the same command values.

#### 5.1.1 Why using MATLAB<sup>®</sup>/SIMULINK<sup>®</sup>

According to MATLAB documentation [6], MATLAB<sup>®</sup> is a high-performance language for technical computing. It integrates computation, visualization, and programming in an easy-to-use environment where problems and solutions are expressed in familiar mathematical notation. Typical uses include:

- Math and computation.
- Algorithm development.
- Data acquisition.
- Modeling, simulation, and prototyping.
- Data analysis, exploration, and visualization Scientific and engineering graphics.
- Application development, including graphical user interface building.

The name MATLAB stands for matrix laboratory. MATLAB was originally written to provide easy access to matrix software developed by the LINPACK and EISPACK projects. Today, MATLAB engines incorporate the LAPACK and BLAS libraries, embedding the state of the art in software for matrix computation.

MATLAB has evolved over a period of years with input from many users. In university environments, it is the standard instructional tool for introductory and



advanced courses in mathematics, engineering, and science. In industry, MATLAB is the tool of choice for high-productivity research, development, and analysis.

MATLAB features a family of add-on application-specific solutions called toolboxes. Very important to most users of MATLAB, toolboxes allow learning and applying specialized technology. Toolboxes are comprehensive collections of MATLAB functions (M-files) that extend the MATLAB environment to solve particular classes of problems. Areas in which toolboxes are available include signal processing, *control systems*, neural networks, *fuzzy logic*, wavelets, simulation, and many others.

Also, according to SIMULINK<sup>®</sup> documentation [7], SIMULINK has become the most widely used software package in academia and industry for modeling and simulating dynamic systems.

In SIMULINK simulations are interactive, parameters can be changed on the fly and immediately see what happens. Instant access to all the analysis tools in MATLAB are also provided, results can be taken and analyzed and visualized. A goal of SIMULINK is to give a sense of the fun of modeling and simulation, through an environment that encourages posing a question, modeling it, and seeing what happens.

With SIMULINK, PC computer can be converted into a lab for modeling and analyzing systems that simply wouldn't be possible or practical otherwise, whether the behavior of an automotive clutch system, the flutter of an airplane wing, the dynamics of a predator-prey model, or the effect of the monetary supply

on the economy. SIMULINK is also practical, with thousands of engineers around the world using it to model and solve real problems.

Due to what was mentioned above, MATALAB/SIMULINK had been chosen to realize the models throughout the thesis models.

### 5.1.2 Computer setup and specifications

- Workstation Type: PC.
- Processor: Type Pentium III, speed 866 MHz.
- Operating system: Windows XP.
- MATLAB: Version 6.5.0 Release 13.
- SIMULINK: Version 5.0, ode23tb Variable-step continuous solver [7].

## 5.2 Separately Excited DC Motor Simulation Results

### 5.2.1 System specifications

The simulation parameters used for the system control of separately excited DC motor, are presented in Table 5-1.

Table 5-1: Separately Excited DC Motor Simulation Parameters

Block	System Parameter	Value
Motor Block	$R_f$	240.0 $\Omega$
	$L_{ff}$	120.0 H
	$R_a$	0.60 $\Omega$
	$L_{aa}$	0.06 H
	$L_{af}$	1.80 H
	$J_m$	0.2 m
	$B_m$	$1 \times 10^{-5}$ Kg
Speed PI controller (if used)	$K_p$	1.5
	$K_i$	650.0
	<i>Saturation</i>	18.0
DC Input Voltages	$u_a$	240.0
	$u_f$	240.0

The parameters for PI speed controller ( $K_p$ ,  $K_i$ ,  $Saturation$ ) if used, had been determined using trial-and-error process and using previous knowledge of the motor dynamics, to give the best speed response it can achieve:

The simulation is done on FLC and PI control under the same parameters presented in Table 5-1. The FLC controller used is the same as the one described in section 4.4, but with a change in the range of the change in control signal  $\Delta u$  from (-150  $\rightarrow$  150) to (-100  $\rightarrow$  100), and the error  $e$  range from (-2  $\rightarrow$  2) to (-1  $\rightarrow$  1).

## 5.2.2 Simulation results

### 5.2.2.1 Case 1

Figure 5-1 shows reference values used for Speed and Load Torque:

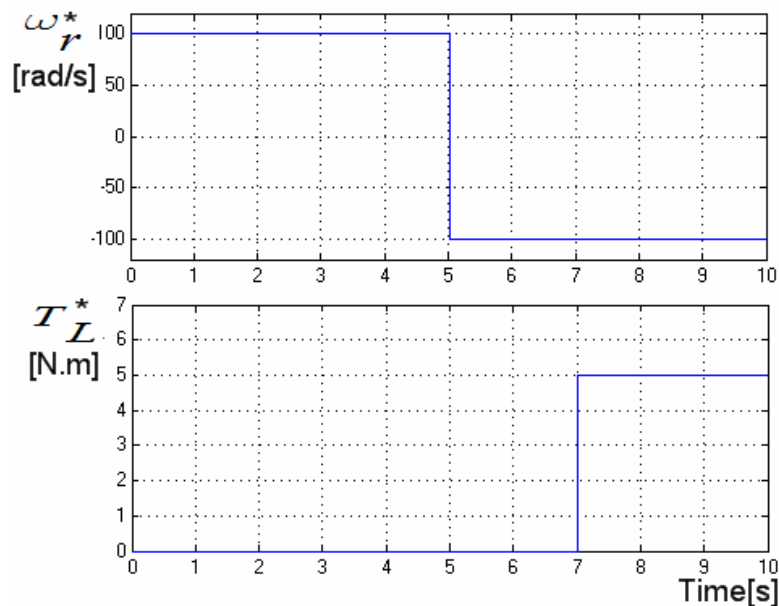


Figure 5-1: Reference values for speed and torque

The motor is initially at standstill and at no load when a step command in speed is applied at time 0 seconds; when steady-state conditions are reached, a reversal

of speed is commanded at time 5 seconds followed by a step load application at time 7 seconds, simulation results is shown in Figure 5-2. Where  $\overline{u_a}$  [V] is the average DC value of the armature voltage:

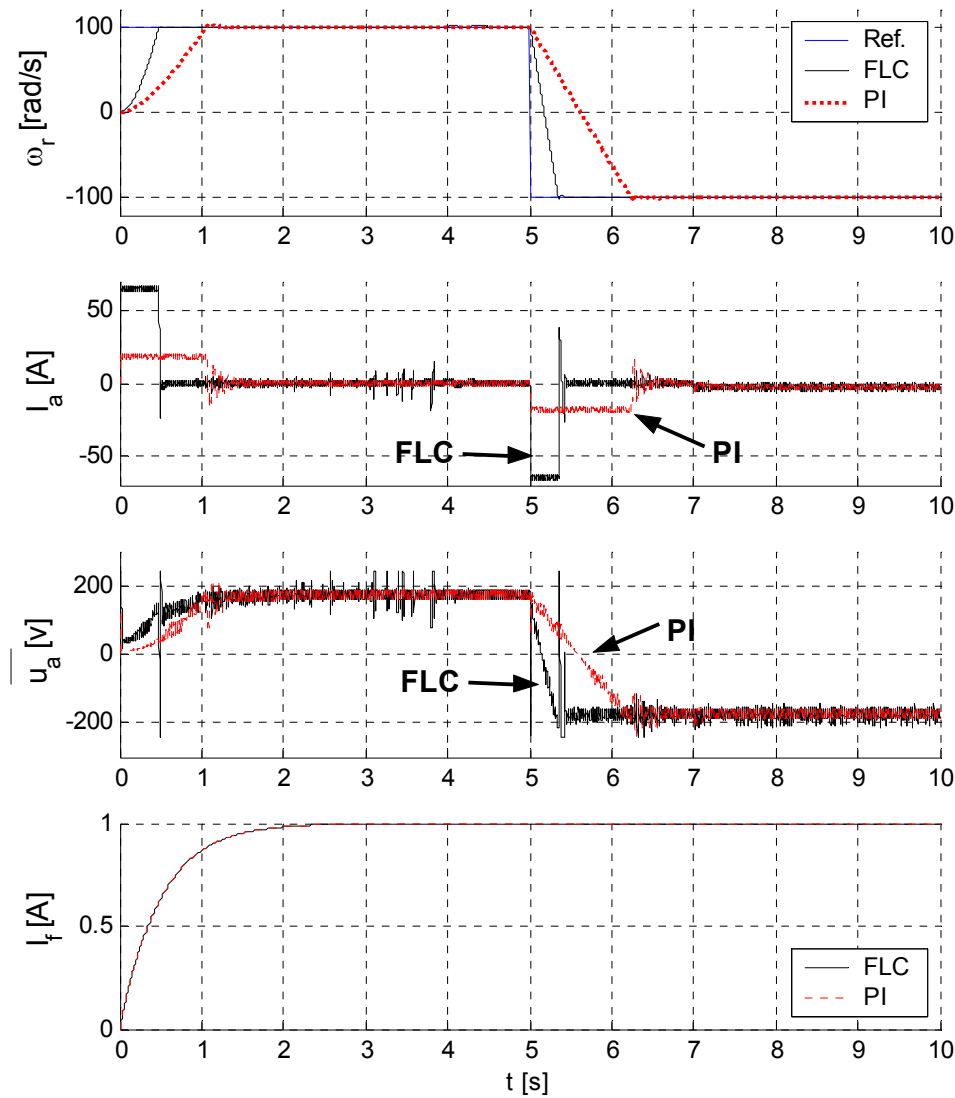


Figure 5-2: DC Simulation results (Case 1)

It can be seen in Figure 5-2 how the control system follows the reference speed in an excellent way, and it can be seen that the response of the FLC controller is faster than the PI one. And also it can be seen that the armature current  $I_a$  shows a big value in the transient state and a small value in the steady state. It can be see

also how the field current  $I_f$  is built at the beginning of the simulation and reaches the value of 1 after that.

### 5.2.2.2 Case 2

The same parameters used in case 1, but with different Ref. Speed, as shown in Figure 5-3, the same response properties can be seen, and FLC also showed better response:

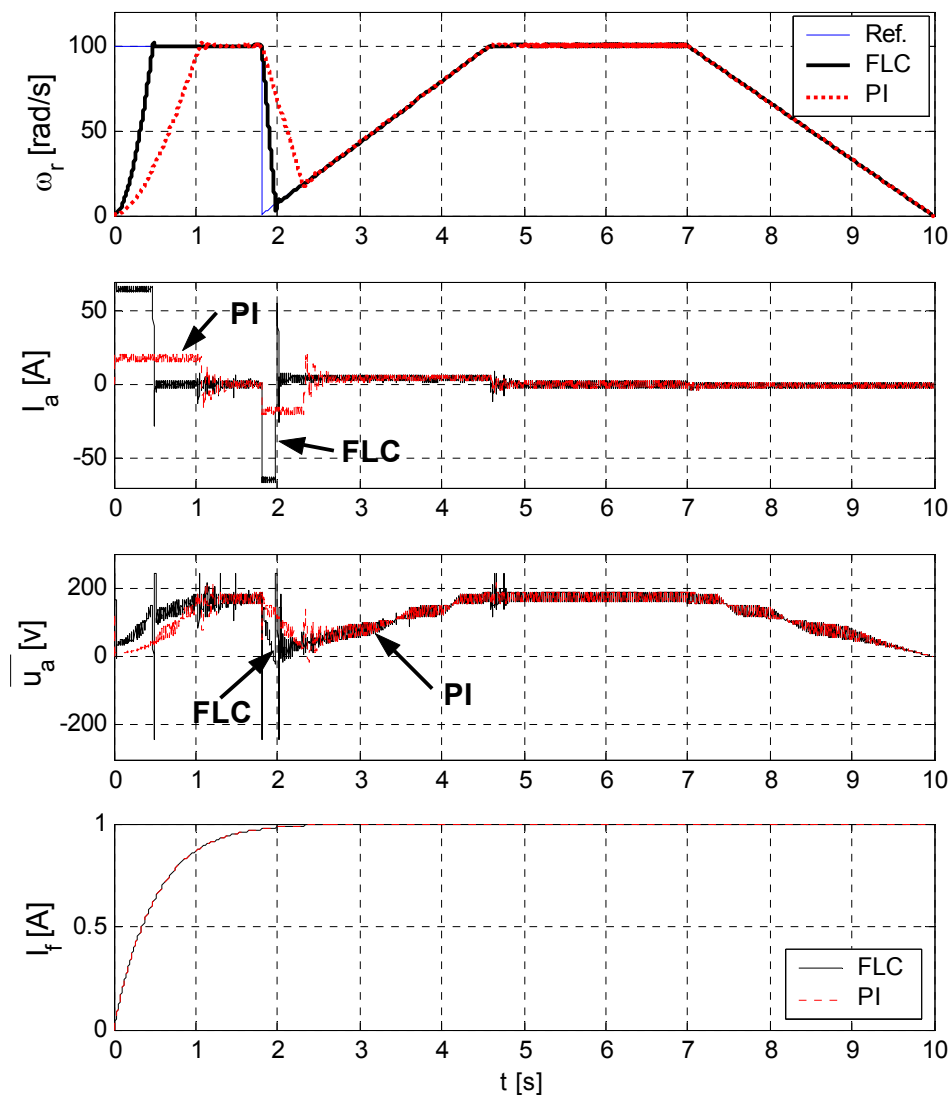


Figure 5-3: DC Simulation results (Case 2)

### 5.3 Speed Sensorless Induction Motor Simulation Results

#### 5.3.1 System specifications

Table 5-2 shows control system simulation parameters for the motor block in per unit (**pu**) values, PI controllers, and speed PI controller if used, where  $K_p$  is the proportional gain, and  $K_i$  is the integral gain. The table shows the limiters used for various variables of the system that need them as discussed at the end of section 3.5, page 40.

Table 5-2: IM Control System Simulation Parameters

Block	System Parameter	Value in [pu]	
Motor Block	$R_r$	0.045	
	$R_s$	0.045	
	$L_r$	1.927	
	$L_s$	1.997	
	$L_m$	1.85	
	$J$	59	
PI controllers	$PI(1)$	$K_p$	30.0
		$K_i$	7.0
	$PI(2)$	$K_p$	30.0
		$K_i$	7.0
	Speed PI controller (If Used)	$K_p$	70.0
		$K_i$	7.0
	$PI(3)$	$K_p$	30.0
		$K_i$	6.5
Limiters	$I_s$	0 → 1.5	
	$z_2$	-40.0 → -0.1 and 0.1 → 40.0	
	$z_3$	-0.8 → -0.1 and 0.1 → 0.8	
	$z_4$	0 → 2.0	

Table 5-3 shows the time constant ( $\tau$ ), used after the output of Reference speed, Speed Controller, and  $\omega_r$  estimated, and also after instantaneous active power ( $p$ ), and reactive power ( $q$ ) to obtain average values ( $P$ ,  $Q$ ) as discussed on section 3.4.2, page 40.

The values for  $K_p$ ,  $K_i$ , limiters ranges, and time constants for the low pass filters in Table 5-2 and Table 5-3 are obtained by trial and error process and by the assessment of the author, in order to give the system the best response it can achieve.

**Table 5-3: Used Low Pass Filters (LPF) Time Constants for Control of IM**

Equation No.	Low Pass Filter Time Constant ( $\tau$ ) after output of				
	Reference speed	Speed Controller	$\omega_r$ estimated	Active power( $p$ )	Reactive power( $q$ )
Sensored case	Not used	Not used	Not used	Not used	Not used
(3.16)	1.5	0.5	0.5	0.0001	Not used
(3.17)	0.1	0.03	4.0	Not used	0.0001
(3.18)	2.0	0.7	2.0	Not used	0.0001
(3.19)	0.5	0.15	2.0	Not used	Not used
(3.20)	1.0	0.3	4.0	Not used	Not used
(3.21)	0.5	0.15	4.0	0.0001	0.0001
(3.22)	2.0	0.6	3.0	Not used	Not used
(3.23)	1.5	0.5	1.0	Not used	0.0001
(3.24)	1.5	0.5	1.0	Not used	0.0001
(3.25)	1.5	0.5	0.5	0.0001	Not used

### 5.3.2 Simulation results

Based on the model shown in Figure 3-3, page 44, the results of the simulations are for step changes of the rotor speed set values and of the load torque as shown in Figure 5-4. Data of a 4-kW-squirrel-cage induction motor have been used in the investigations, system parameters used are found in Table 5-2 and Table 5-3.

The control system had been modeled in MATLAB/SIMULINK. Sensored speed simulation results are shown in Figure 5-5. Simulation results for speed sensorless cases of equations (3.16) to (3.25) are presented in Figure 5-6 to Figure 5-15. The whole simulation results are done for the following two cases, under the same system parameters:

1. Case using FLC for speed.
2. Case Using PI controller for speed.

Simulation Results include estimated and actual measurements of  $\omega_r$  which is rotor speed, and measurements of stator current in  $x$ -direction ( $i_{sx}$ ), and  $y$ -direction ( $i_{sy}$ ), also measurements of stator flux in  $x$ -direction ( $\psi_{sx}$ ), and  $y$ -direction ( $\psi_{sy}$ ).

The following notations are used in the figures:

- Act. : Actual value of rotor speed obtained from the IM block.
- Est.: Estimated value obtained from the Calc. block.
- FLC: Using Fuzzy Logic Controller as the speed controller.
- PI: Using Proportional Integral Controller as the speed controller.

The following reference values had been used:

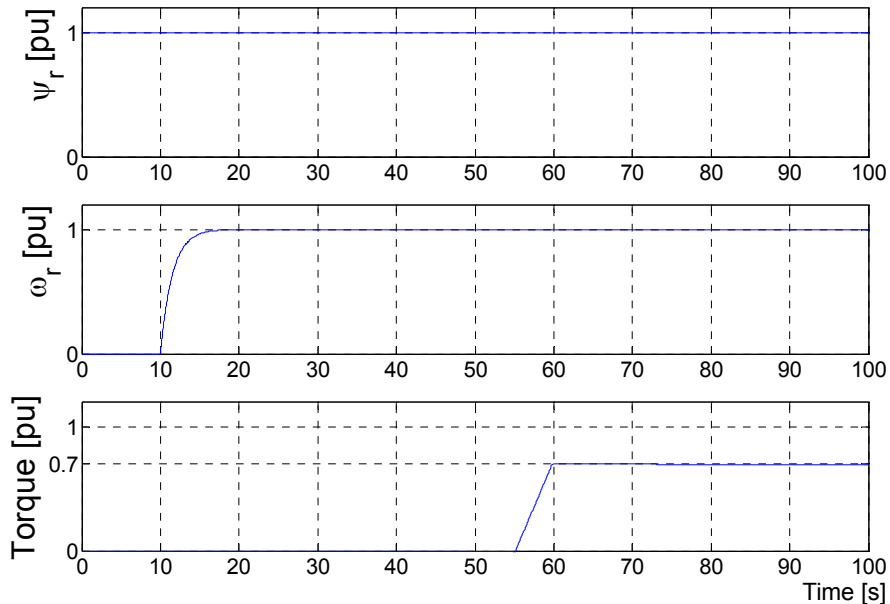


**Figure 5-4: IM Reference command values**



### 5.3.2.1 Sensored case (Without estimation)

Sensored case means that control system is modeled without using the Calculation Block and using  $\omega_r$  directly from the motor model.

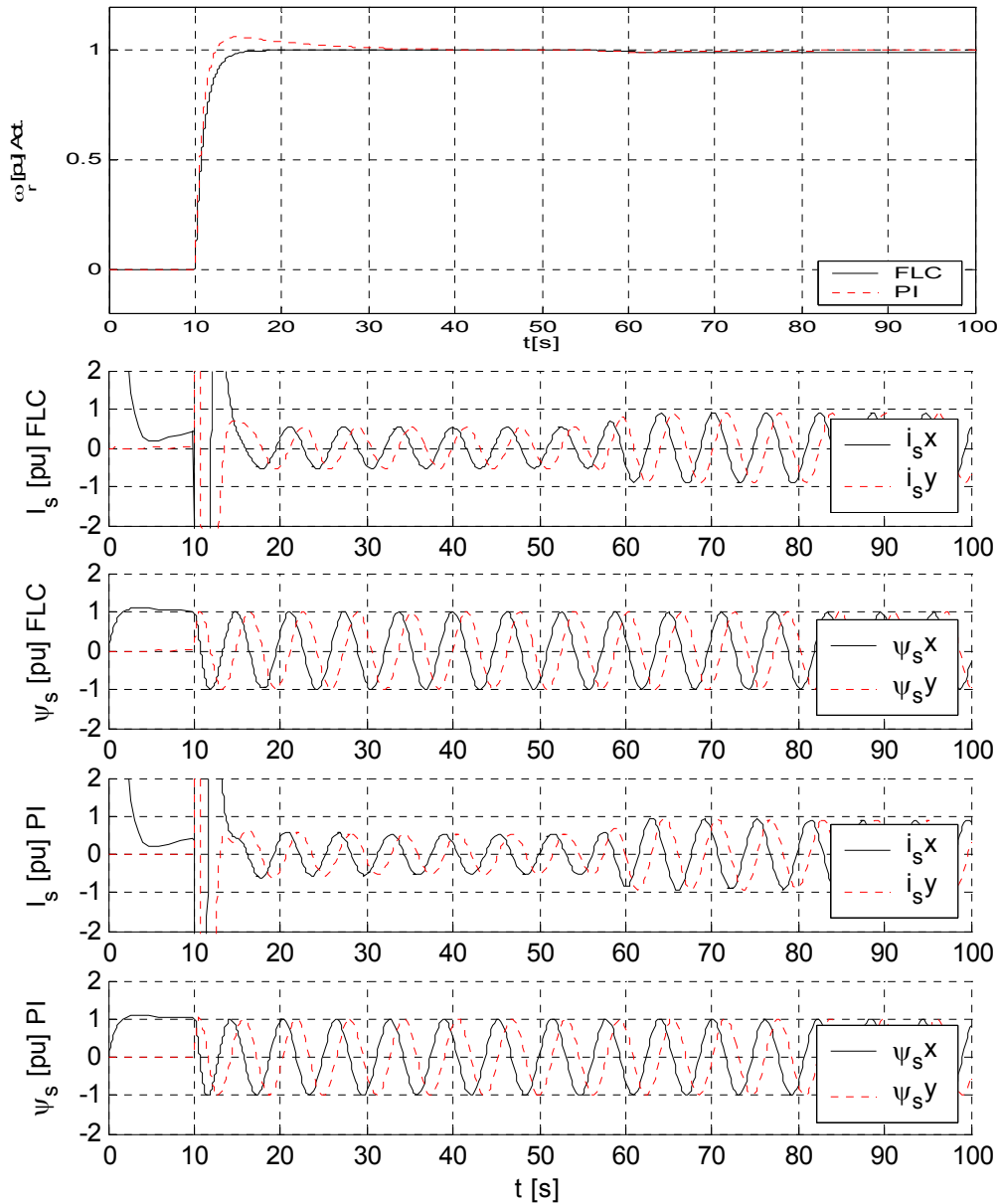


Figure 5-5: Simulation results for Sensored case

In Figure 5-5 the response of the FLC case showed better speed response than the PI case. Note that, when the speed of the motor is close to zero, the frequency of the currents and fluxes decrease and become DC. This range is very

problematic in *induction motor Field oriented control* due to extremely low frequency. The amplitude of the stator currents increases at transient states due to the inertia of the motor and decreases to very low value at steady state.

**5.3.2.2 Simulation results for equation (3.16)**

$$\omega_r = \frac{a_1 I_s^2 + a_2 z_3 + a_4 P}{a_3 z_2} \tag{3.16} \text{ Repeated}$$

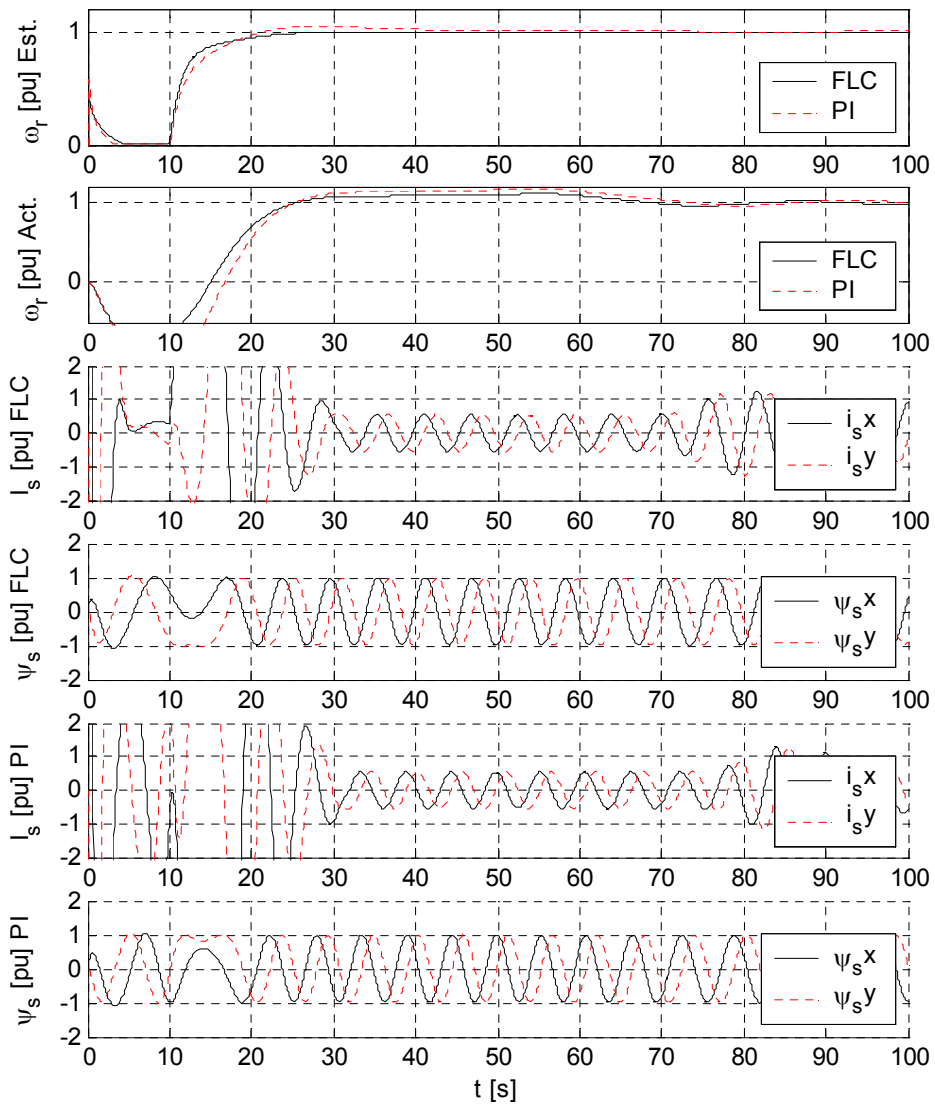


**Figure 5-6: Simulation results for equation (3.16)**

In Figure 5-6 the speed response for both estimated and actual speed is good for full rated speed; there is a delay for speed response due to the First order filters. In

case of zero speed the system shows bad response for speed. In general FLC shows better response than PI.

### 5.3.2.3 Simulation results for equation (3.17)

$$\omega_r = \frac{-a_2 z_2 - \omega_i I_s^2 + a_4 Q}{a_3 z_3} \quad (3.17) \text{ Repeated}$$

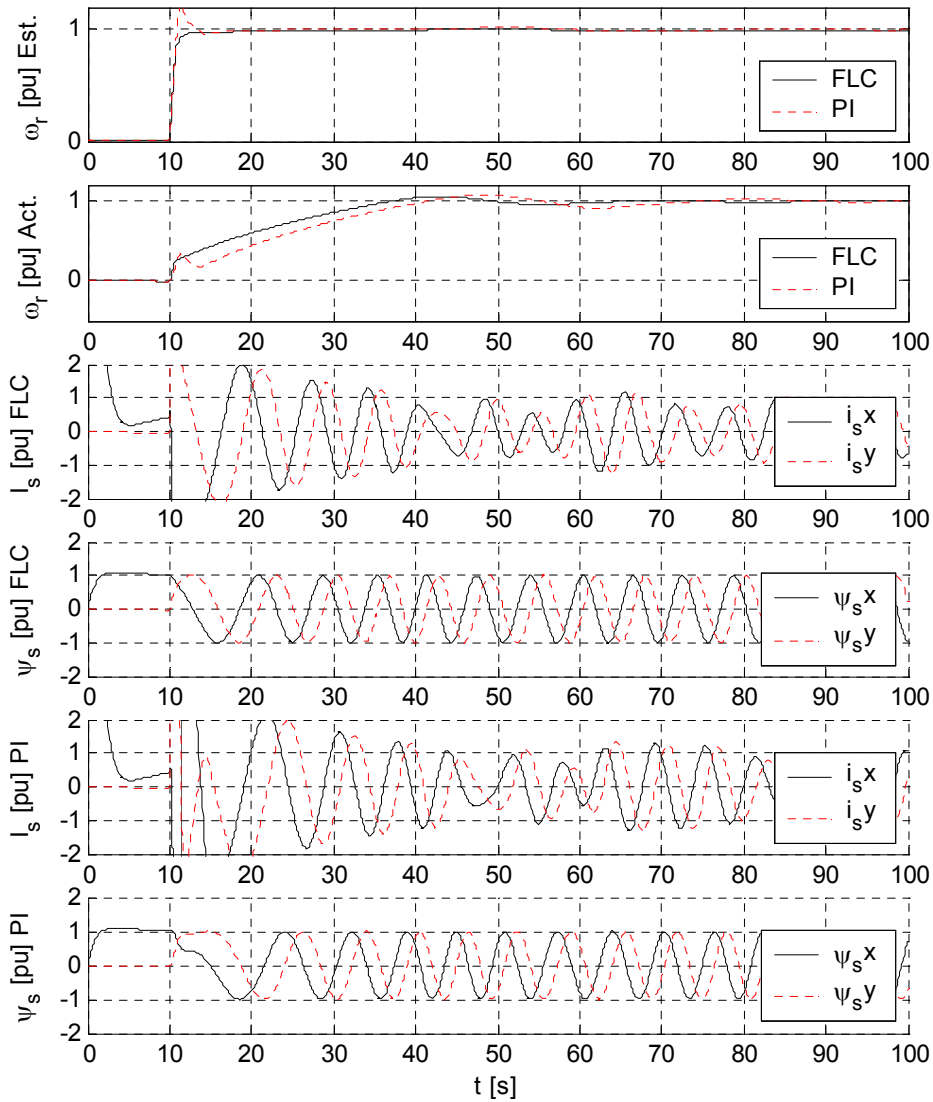
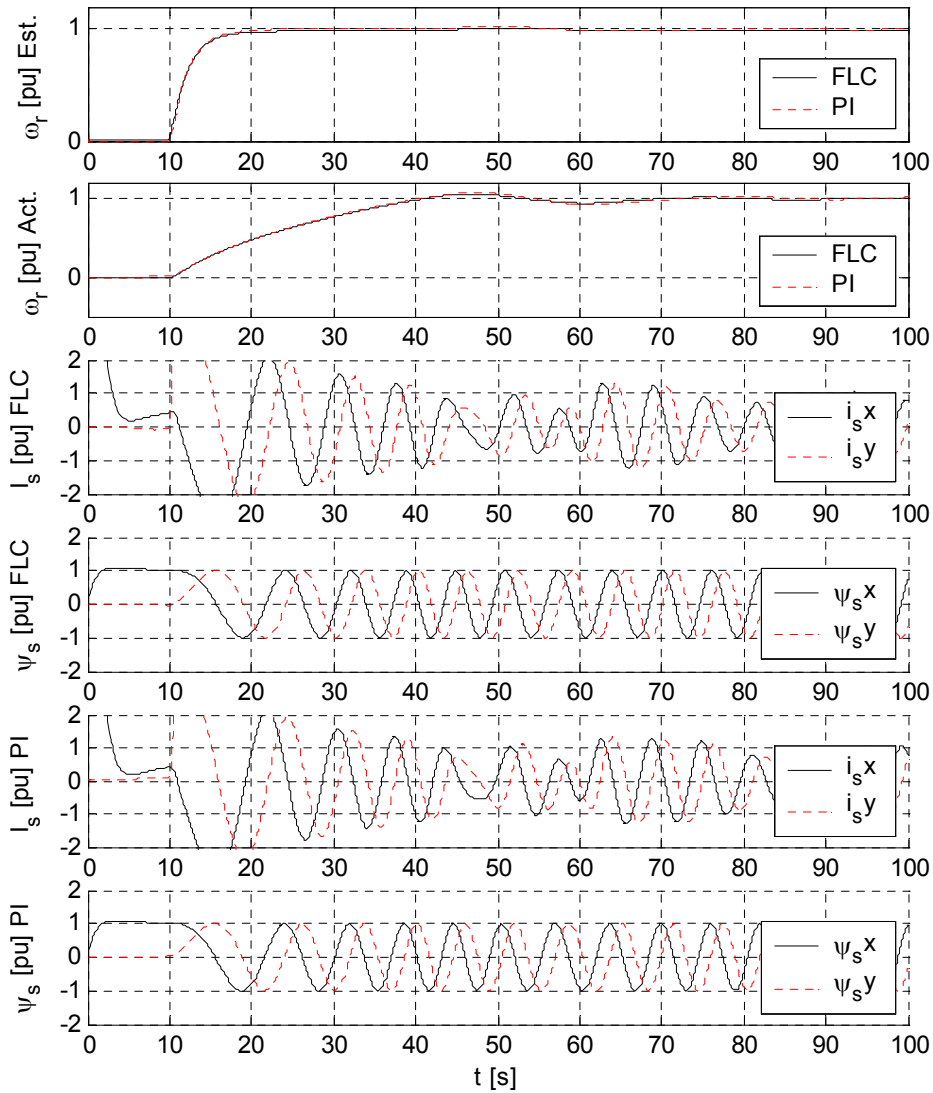


Figure 5-7: Simulation results for equation (3.17)

Here FLC also showed better response than PI, for both estimated and actual rotor speed. But there is a slower response in actual speed. Zero speed response is very good.

### 5.3.2.4 Simulation results for equation (3.18)

$$\omega_r = \frac{-a_2 z_2 - \omega_{si} I_s^2 + a_4 Q}{I_s^2 + a_3 z_3} \quad (3.18) \text{ Repeated}$$



**Figure 5-8: Simulation results for equation (3.18)**

Here FLC showed slightly better response than PI, for both estimated and actual rotor speed. But there is a slower response in actual speed. Zero speed response is also very good.

5.3.2.5 Simulation results for equation (3.19)

$$\omega_r = \omega_i + \frac{R_r}{L_r} \left( \frac{z_3 - L_m I_s^2}{z_2} \right) \tag{3.19} \text{ Repeated}$$

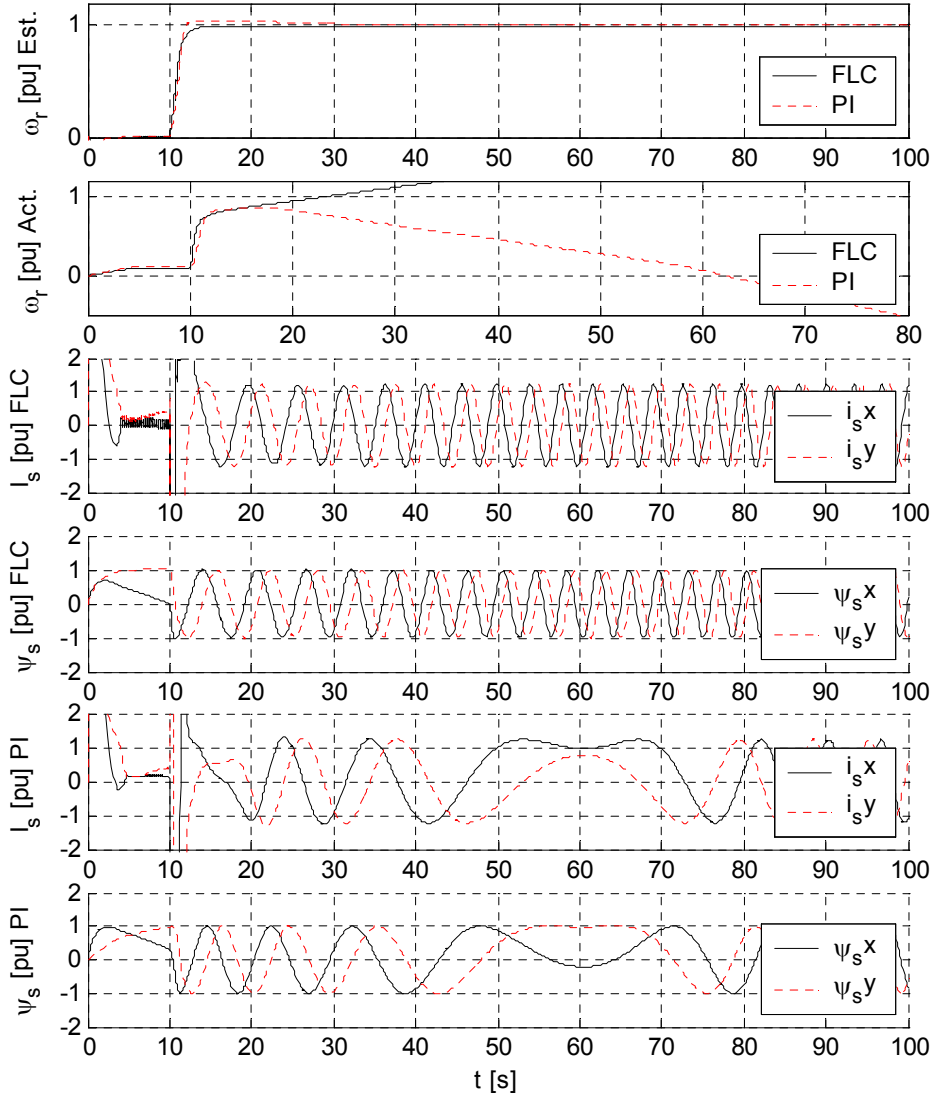


Figure 5-9: Simulation results for equation (3.19)

Here FLC showed better response than PI for estimated rotor speed, while actual speed had shown very bad response. Zero speed response is good.

5.3.2.6 Simulation results for equation (3.20)

$$\omega_r = \omega_i - \frac{R_r}{L_r} \frac{z_2}{z_3} \tag{3.20) Repeated}$$

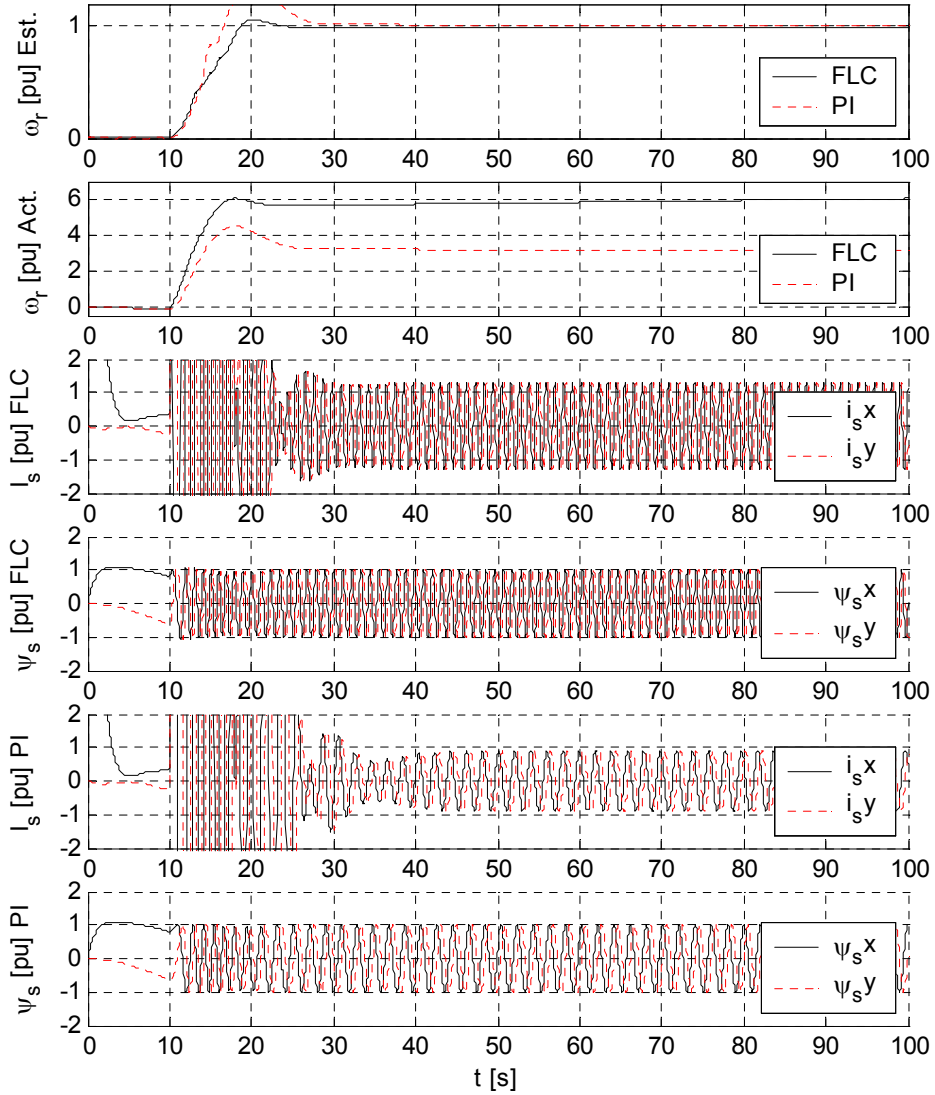
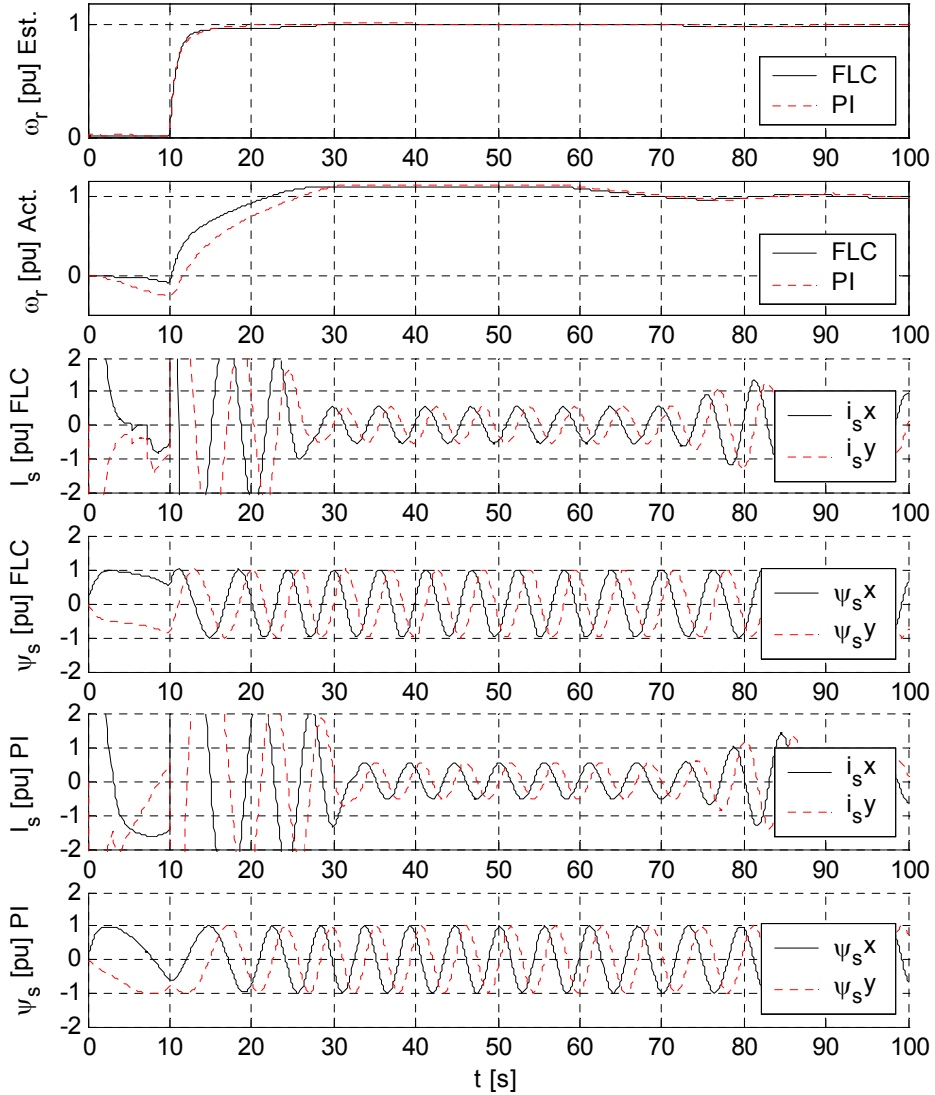


Figure 5-10: Simulation results for equation (3.20)

Here FLC showed better response than PI for estimated rotor speed, while actual speed had shown very bad response. Zero speed response is very good.

**5.3.2.7 Simulation results for equation (3.21)**

$$\omega_r = \frac{I_s^2(a_1 - \omega_{si}) + a_2(z_3 - z_2) + a_4(P + Q)}{I_s^2 + a_3z_3 + a_3z_2} \quad (3.21) \text{ Repeated}$$



**Figure 5-11: Simulation results for equation (3.21)**

Here FLC showed slightly better response than PI, for estimated and actual rotor speed. Zero speed response is good.

**5.3.2.8 Simulation results for equation (3.22)**

$$\omega_r = \frac{\frac{R_r}{L_r} z_3 - \frac{R_r L_m}{L_r} I_s^2}{z_2} + \omega_i \quad (3.22) \text{ Repeated}$$

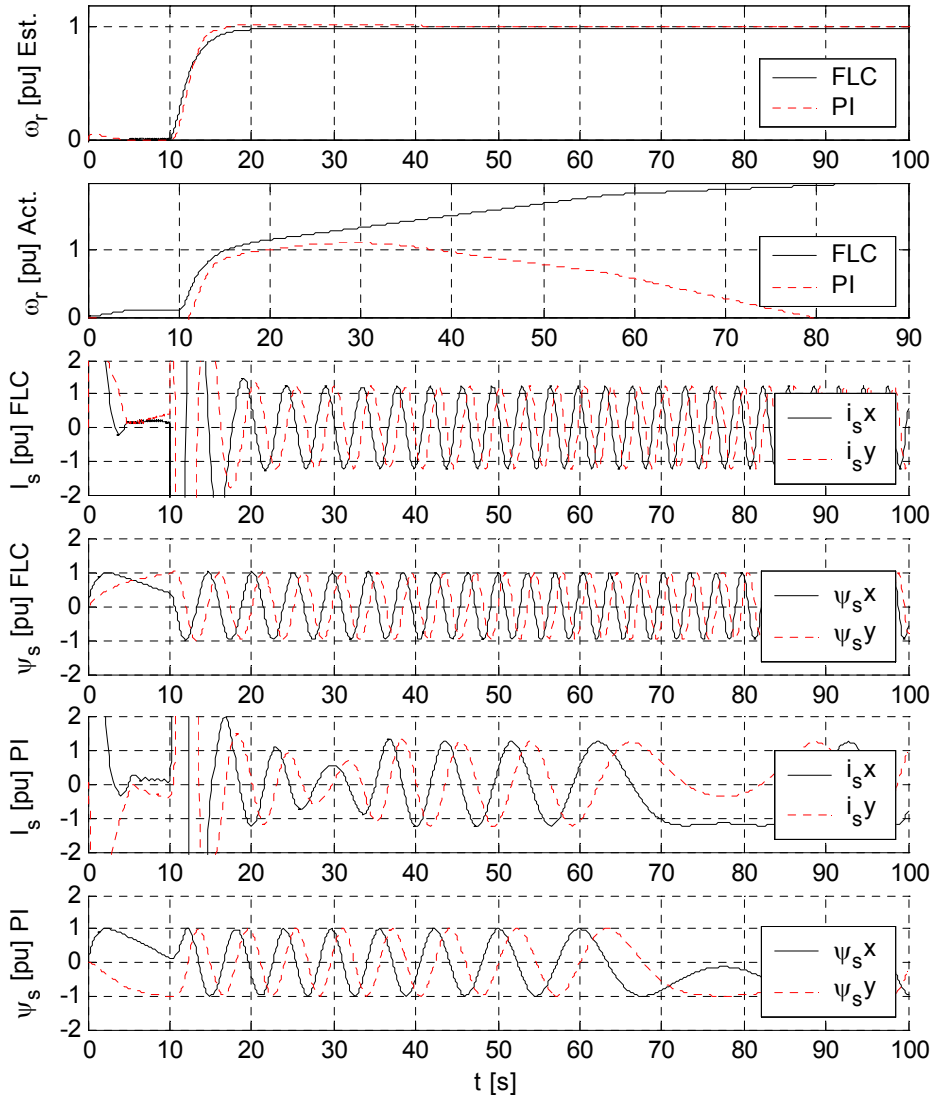


**Figure 5-12: Simulation results for equation (3.22)**

Here FLC also showed better response than PI for estimated rotor speed, while actual speed had shown bad response. Zero speed response is good.



**5.3.2.9 Simulation results for equation (3.23)**

$$\omega_r = \frac{a_4 Q}{a_5 z_3 + I_s^2} - \frac{L_m R_r z_2}{L_r z_4} \tag{3.23) Repeated}$$

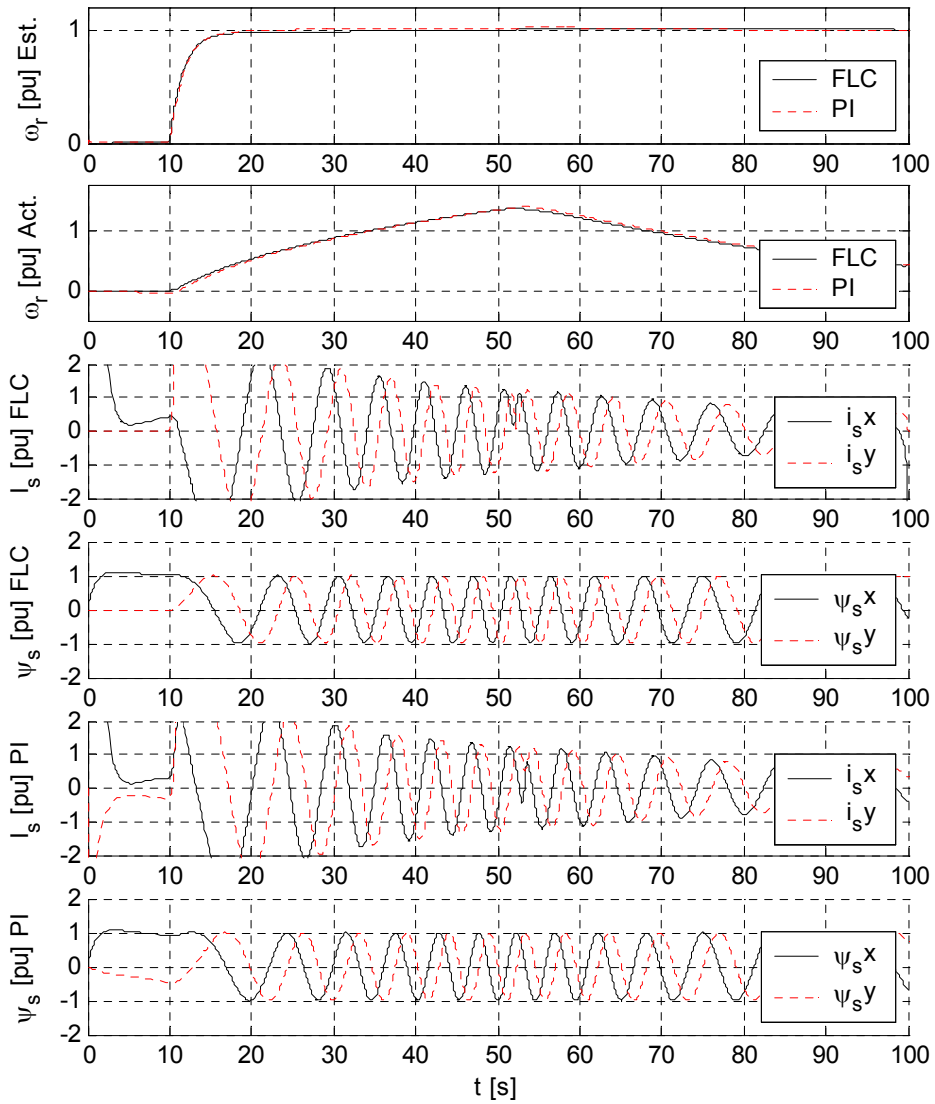


**Figure 5-13: Simulation results for equation (3.23)**

Here FLC showed slighter better response than PI for estimated rotor speed, while actual speed had shown bad response. Zero speed response is very good.

### 5.3.2.10 Simulation results for equation (3.24)

$$\omega_r = \frac{a_4 Q}{a_5 z_3 + I_s^2} - \omega_{si} \quad (3.24) \text{ Repeated}$$

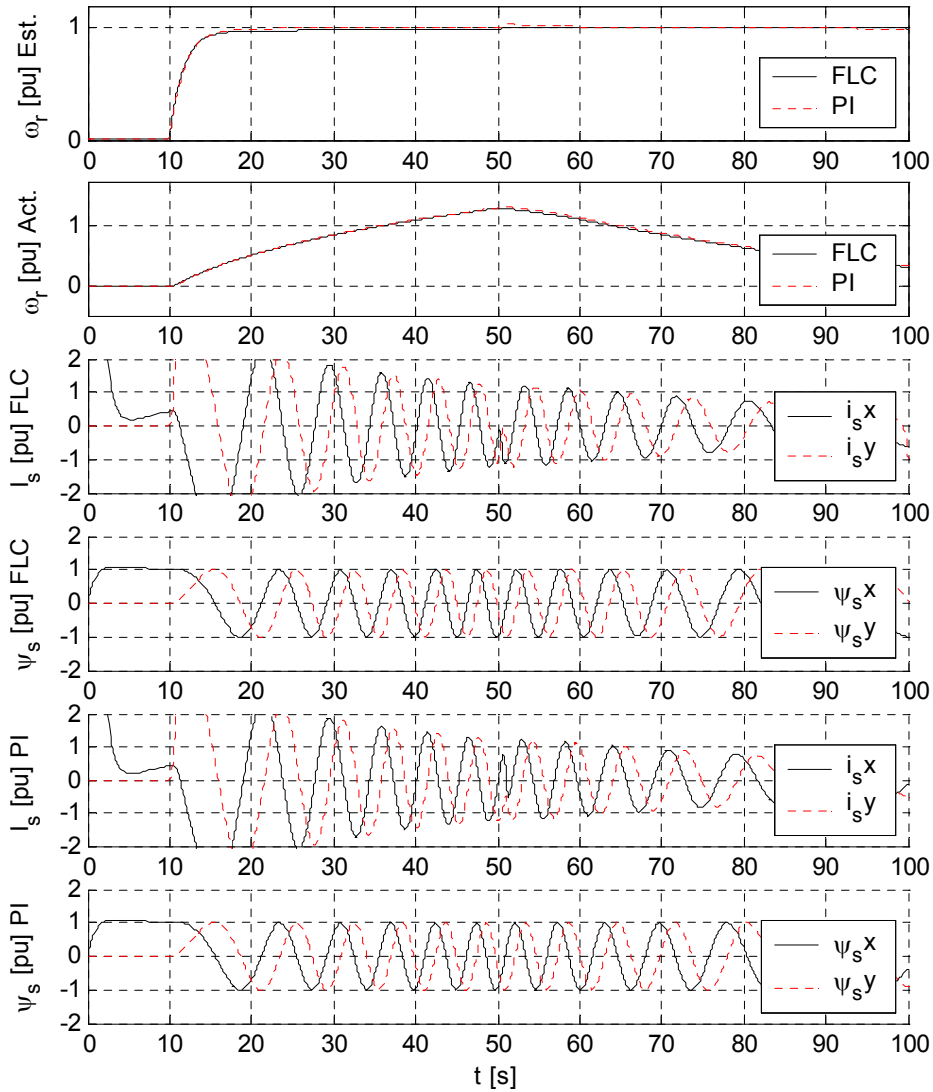


Figure 5-14: Simulation results for equation (3.24)

Here FLC showed slightly better response than PI for estimated rotor speed, actual speed had shown bad response. Zero speed response is very good.

5.3.2.11 Simulation results for equation (3.25)

$$\omega_r = \frac{(L_m + \frac{a_1}{a_2})I_s^2 + \frac{a_4}{a_2}P}{z_2 \frac{L_r}{R_r}} - \frac{R_r L_m z_2}{L_r z_4} \quad (3.25) \text{ Repeated}$$

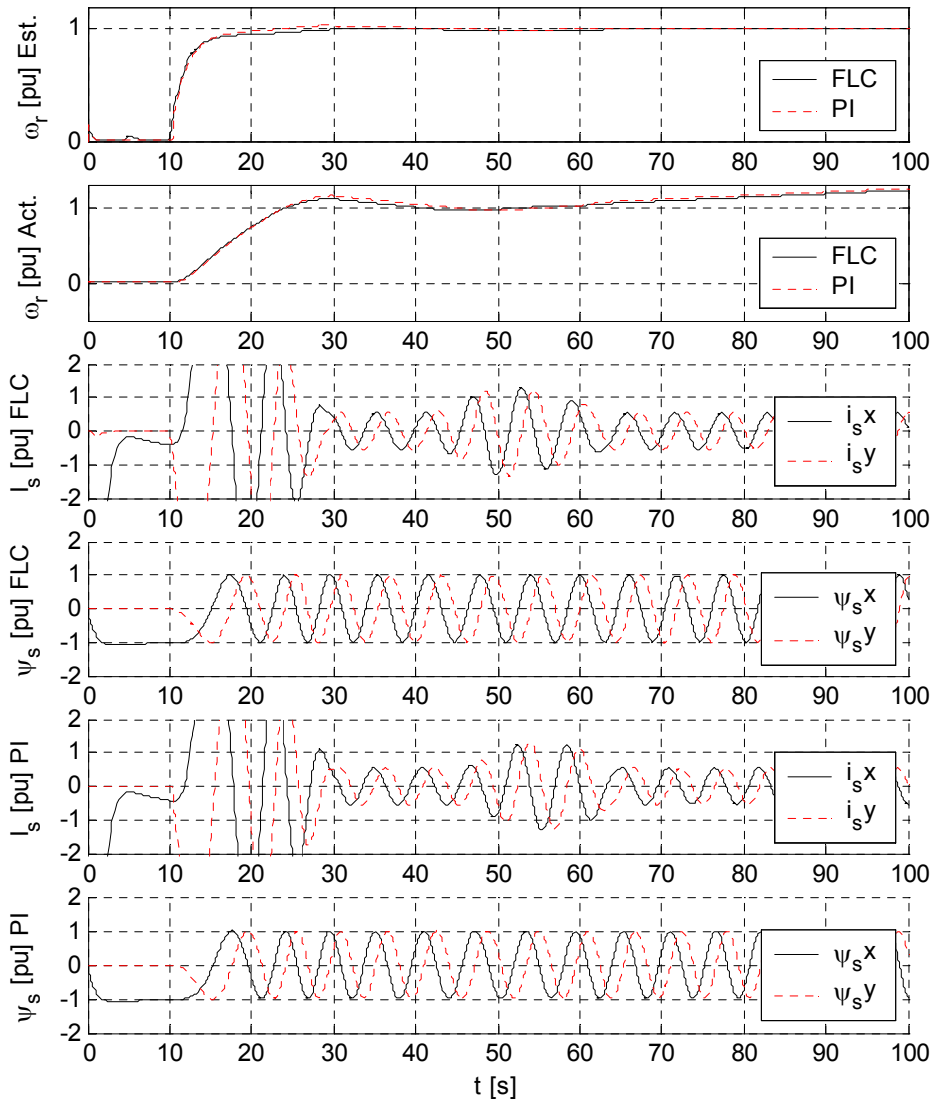


Figure 5-15: Simulation results for equation (3.25)

Here FLC showed slightly better response than PI for estimated and actual rotor speed, Zero speed response is good.

### 5.3.3 Applied load torque effect

In order to study the effect of load torque on the induction motor, a sample study of equation (3.18) , and doing zoom-in around the time when the load torque is applied, as shown in Figure 5-4 the positive torque (against the rotor motion direction) is applied starting at time 55 second. This zoom-in is done in Figure 5-16:

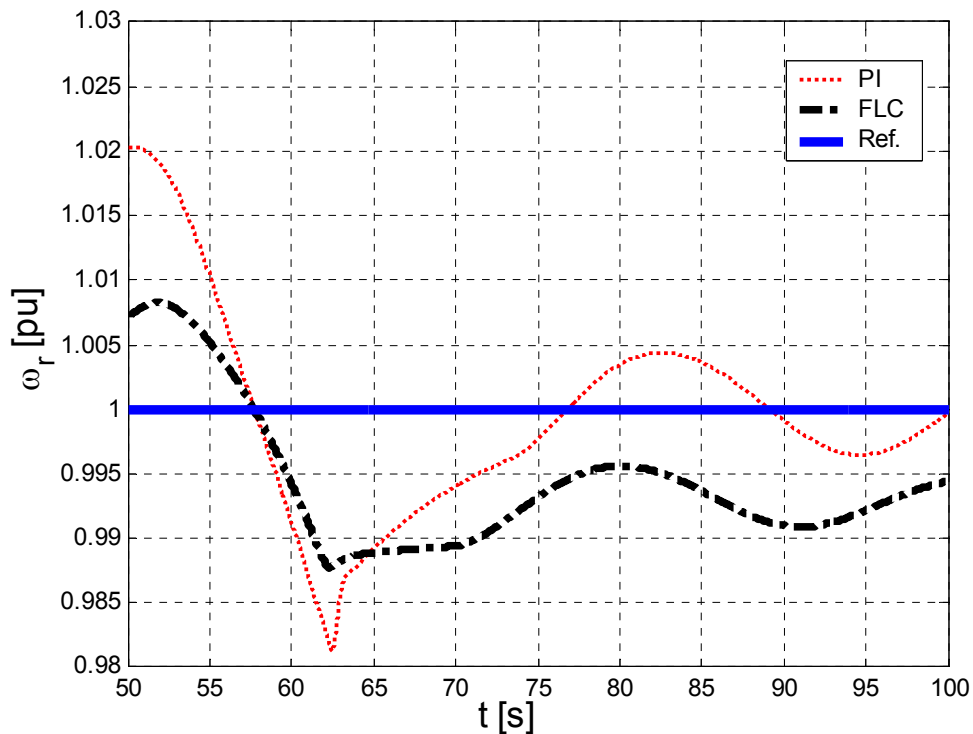


Figure 5-16: Zooming of Figure 5-8, around positive torque application point

Note in Figure 5-16 that after the torque is applied the motor starts to slow down its speed, and then returns back to its steady state, but with larger steady state error in the FLC case. FLC case showed overall better transient response than PI, especially at the time between 60 and 65 second.

That happened when the torque is applied against the rotor motion, but what happens if we apply a *negative load*, i.e. a load that works in the direction of the

rotor motion, thus making the system to work in *generator mode*. This case is shown in Figure 5-17:

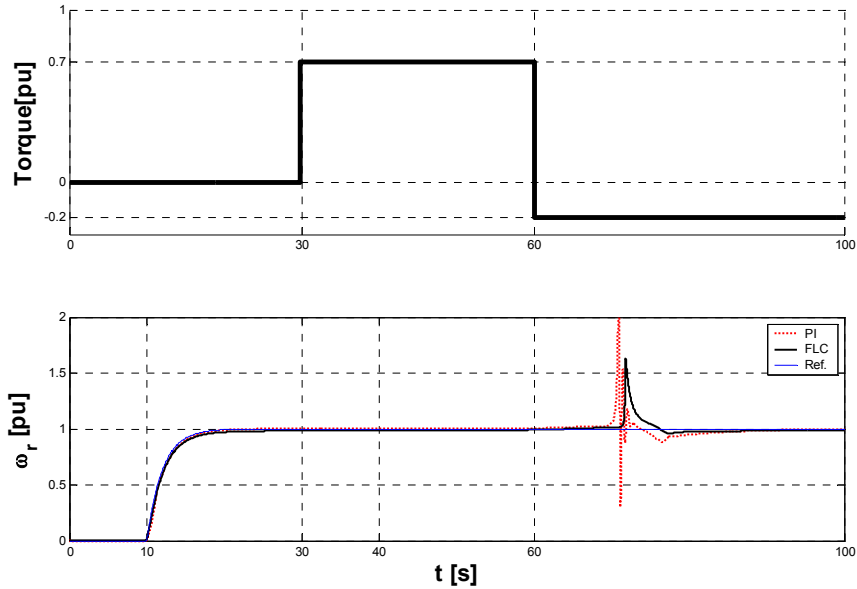


Figure 5-17: Negative load applied to the motor

As it can be seen that at time 30 seconds, a positive load is applied of 0.7 pu, then at time 60 seconds, a negative load is applied of -0.2 pu, a zoomed-in view of the rotor speed response is shown in Figure 5-18.

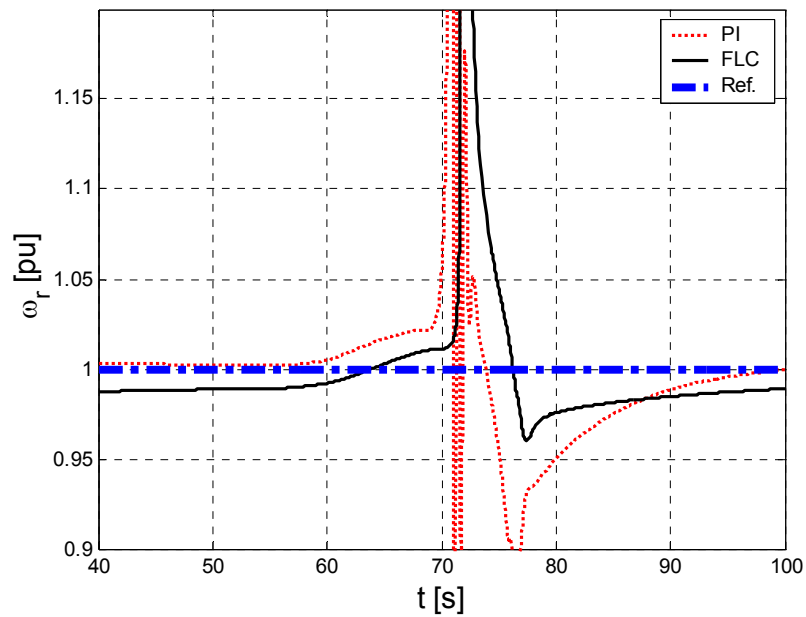


Figure 5-18: Zooming of Figure 5-17, around negative torque application point

Note in Figure 5-18 that after the negative torque is applied the motor starts to speed up its speed, and then returns back to its steady state, as expected, but with larger steady state error in FLC case. FLC case showed better transient response than PI at the time between 60 and 80 seconds.

Other simulation cases were examined, Changing the reference speed showed the same response for equation (3.18), a mixture of step and ramp input is used as shown in Figure 5-19, as it can be seen the FLC case showed better response than PI.

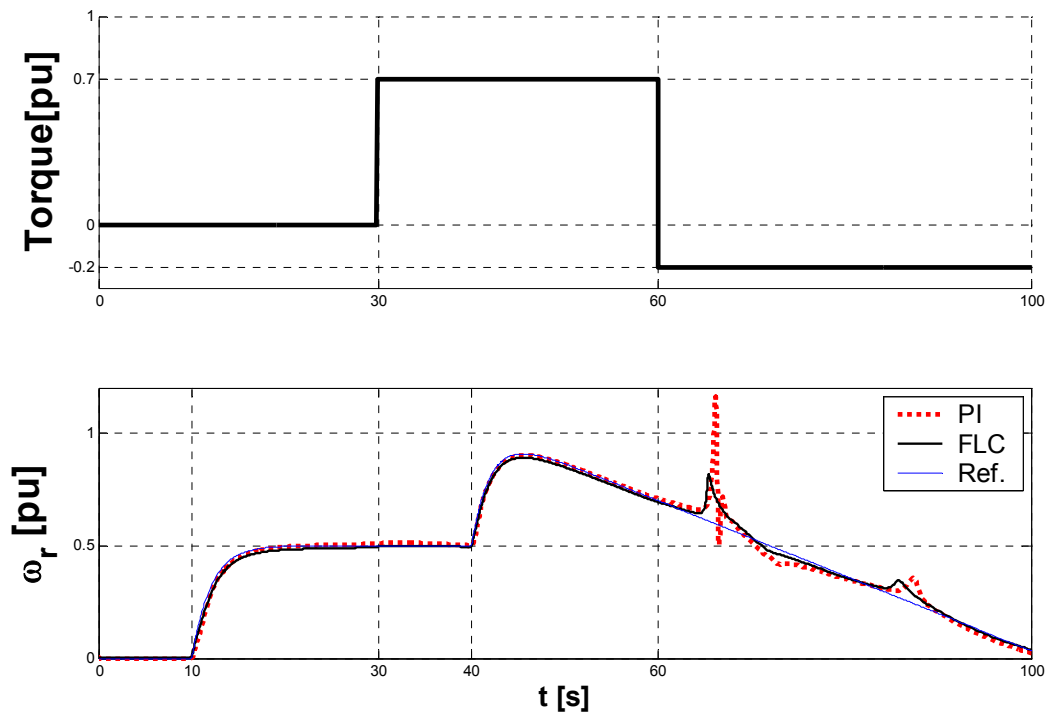


Figure 5-19: A mixture of step and ramp input for rotor speed reference used

## **5.4 Comparison between Fuzzy and PI Sensorless Speed Control of IM**

Comparisons are based on a set of criteria to assign, "figures of merit", which is "Steady-State Error", "Dynamic Behavior", and "Low Speed Operation". According to Ilas and *et al.* [21] this is a convenient and meaning-full way to make such a comparison between the estimating equations of the rotor angular speed  $\omega_r$ , which are equations (3.16) to (3.25). These comparisons are done based on the simulation results shown in Figure 5-5 to Figure 5-19.

### **5.4.1 Steady-State Error (SSE)**

The Steady-State Error is the error between estimated speed and reference values. All equations showed very small SSE (below 2%). Equations (3.16), (3.19), (3.21), (3.22), and (3.25) in FLC case showed the least SSE.

### **5.4.2 Dynamic Behavior (DB)**

Dynamic Behavior deals with the response of the proposed estimating systems, including the rise time, and damping oscillations after introducing a disturbance such as the load torque. Equations (3.17), (3.19), (3.21), and (3.22) in FLC case, also equation (3.21) in PI case showed the best DB.

### **5.4.3 Low Speed Operation (LSO)**

In the proposed sensorless systems, the state variables are calculated using stator flux, this implies frequency limiting near zero. And this had effect on the low speed operation of the estimating equations, as had been discussed at the end of section 3.4.1, page 38. Equations (3.17), (3.18), (3.19), (3.20), (3.21), (3.22), (3.23),

and (3.24) in the FLC case , also equations (3.17), and (3.18) in the PI case showed the best LSO.

Table 5-4 shows a summary comparison between different sensorless speed systems shown in Figure 5-5 to Figure 5-19, using FLC and PI controllers, and actual speed obtained from the motor model by integrating equation (2.12).

"Figures of merit" range is from 0 to 10, where '0' means the poorest behavior and '10' means the best. The rankings for the behavior of the proposed sensorless systems are *noted in accordance to the assessment of the author*.

Nearly in all equations Fuzzy logic controllers (FLC) showed overall better results than PI controllers, as presented in Table 5-4. Best results are obtained using (3.21) shown in Figure 5-11.

**Table 5-4: Comparison between Different Schemes**

Equation No.	FLC				PI			
	SSE	DB	LSO	Actual	SSE	DB	LSO	Actual
Sensored case	---	---	---	10	---	---	---	9
(3.16)	9	7	5	8	8	6	4	7
(3.17)	8	9	9	8	8	7	9	6
(3.18)	8	8	9	8	8	8	9	8
(3.19)	9	9	9	5	8	8	8	4
(3.20)	8	7	9	3	7	6	8	4
(3.21)	9	9	9	9	8	9	8	7
(3.22)	9	9	9	5	8	8	7	4
(3.23)	8	8	9	4	7	8	8	4
(3.24)	8	8	9	4	7	8	8	4
(3.25)	9	8	6	9	8	8	7	8

Figure 5-20 shows a graphical representation of Table 5-4, to present the table in a way that shows that FLC is better than PI control in nearly all equations.



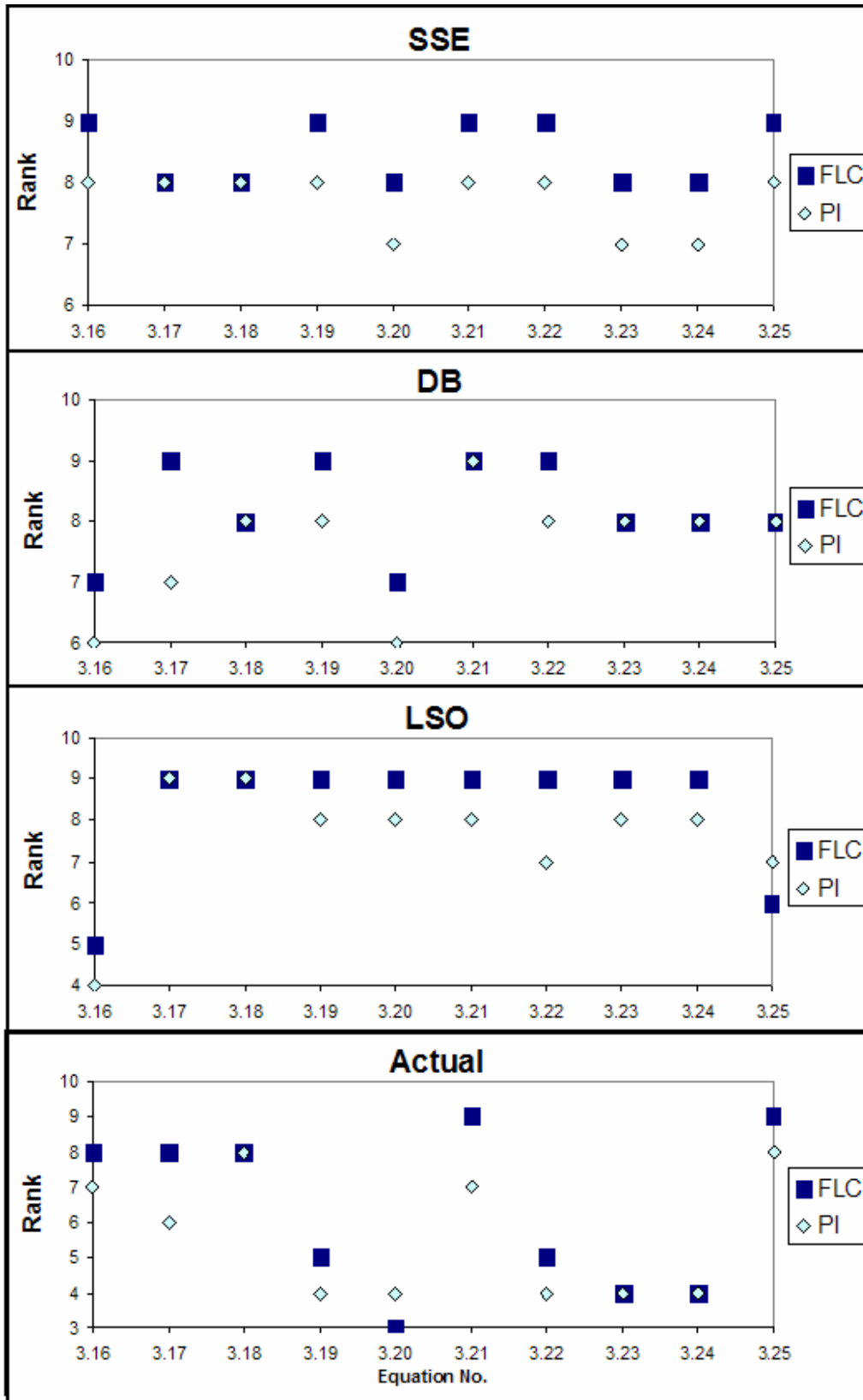


Figure 5-20: Graphical representation of Table 5-4

## 6 CONCLUSIONS AND FUTURE WORK

### 6.1 Conclusions

Separately Excited DC motor theory and control had been presented. Also the equivalent circuit, mathematical model, and MATLAB/SIMULINK model of separately excited DC motor had been investigated. Also Speed control of this Motor, with its modeling in MATLAB/SIMULINK had been worked out.

The construction, equivalent circuit, mathematical model, and MATLAB/SIMULINK model of three-phase Squirrel-Cage Induction Motor had been discussed. Also, theory and basic schema of Field Oriented Control (FOC) of Induction motor were presented.

Speed sensorless Control of an induction motor using power measurements and Multiscalar state variables had been developed. Also advantages of sensorless speed control had been presented, such as eliminating the speed sensor and its disadvantages. The equations used in the Computation and estimation of the rotor angular speed using power measurements had been presented. Finally, MATLAB/SIMULINK model of the sensorless speed control system had been built-up.

Estimating rotor angular speed using the equations (3.16) to (3.25) did not use computationally expensive algorithms and were simple for practical implementation; because there were no matrix conversions or other complex transformations. In comparison with other methods, as in [14]-[21], the proposed systems are simple and may be practically realized with low cost [26].

Theory and history of fuzzy logic control of Induction Motor had been highlighted. Fixed Fuzzy logic controller using heuristic approach had been chosen as a control design approach for speed control. Speed fuzzy logic controller (FLC) used for speed control of both the induction motor and separately excited DC motor had been implemented.

Detailed Simulation results for speed control of separately excited DC motor, and sensorless speed control of squirrel-cage induction motor under FLC, and PI speed controllers had been shown. Through analysis, and comparison between the performance of the FLC and PI had been introduced. In nearly all situations FLC had showed better response than PI control.

As a final point, to conclude with some positive and negative recommendations, the PI controller is implemented much more frequently in industrial applications than FLC; because PI Controllers are naturally much easier to design. But, FLC have come a long way, and the research in this thesis supports its usefulness in applications where robust control is essential for the safe operation of a given nonlinear control system.

## **6.2 Future Work**

The simulation work shows the great promise of the studied methods in this thesis. However, the Fuzzy logic controller performed below its full potential, since static FLC design is used. In static fuzzy control, the structure and parameters of the fuzzy controller are fixed and do not change during real-time operation. On the other hand, in adaptive fuzzy control, the structure and/or

parameters of the fuzzy controller change during real-time operation. One method to do this is using artificial neural networks (**ANN**) [33].

So as a future work, adaptive FLC with ANN and genetic algorithms (**GA**) [42] could be used to automatically fine-tune the weights and ranges for membership functions of the FLC, in order to give better response.

## REFERENCES

- [1] Peter F. Ryff, David Platnick and Joseph A. Karnas, *Electrical Machines and Transformers*, Principles and Applications, Prentice Hall, Inc., 1987.
- [2] N. Mohan, *Electric Drives an Integrative Approach*, MNPETE, Minneapolis, 2<sup>nd</sup> ed., 2001.
- [3] Mats AlaKüla, *Power Electronic Control*, Lund University, 2002.
- [4] P. Krause, *Electromechanical Motion Devices*, McGraw Hill, 1989.
- [5] M. Riaz, *Simulation of Electric Machine & Drive Systems*, Department of Electrical and Computer Engineering, University of Minnesota, <http://www.ece.umn.edu/users/riaz>, 2000.
- [6] MathWorks, *Introduction to MATLAB*. The Math Works, Inc., [http://www.mathworks.com/access/helpdesk/help/techdoc/learn\\_MATLAB/ch1intro.shtml](http://www.mathworks.com/access/helpdesk/help/techdoc/learn_MATLAB/ch1intro.shtml), 2004.
- [7] MathWorks, *What is SIMULINK*, The Math Works, Inc. <http://www.mathworks.com/access/helpdesk/help/toolbox/SIMULINK/SIMULINK.shtml>, 2004.
- [8] Stephen J. Chapman, *Electric Machinery Fundamentals*, McGraw Hill, 2<sup>nd</sup> ed., 1991.
- [9] N. Mohan, *Advanced Electric Drives Analysis, Control, and Modeling using Simulink*, MNPETE, Minneapolis, 2001.
- [10] S. Beierke, "Enhanced Control of an Alternating Current Motor Using Fuzzy Logic and a TMS320 Digital Signal Processor," Texas Instruments, Inc, 1996.
- [11] Texas Instruments Europe, "Field Orientated Control of 3-Phase AC-Motors," Texas Instruments, Inc., 1998.
- [12] B. K. Bose, "Power Electronics and Motion Control – Technology Status and Recent Trends," IEEE Trans. on Industrial Electronics, September/October 1993, vol. 35, No 5, pp. 902-909.

- 
- [13] B. AKIN, *State Estimation Techniques for Speed Sensorless Field Oriented Control of Induction Motors*, Master of science thesis, middle east technical university, August 2003.
- [14] R. Joetten, G. Maeder, "Control Methods for Good Dynamic Performance Induction Motor Drives Based on Current and Voltage as Measured Quantities," *IEEE Trans. on Industrial Application*, 1983, Vol. IA-19, no. 3, pp. 356-363.
- [15] F. Hillenbrand, "A Method for Determining the Speed and Rotor Flux of the Asynchronous Machine by Measuring the Terminal Quantities Only," *IFAC Conference in Power Electronics and Electrical Drives*, Lausanne, Switzerland, 1983, pp. 55-62.
- [16] C. Schauder, "Adaptive Speed Identification for Vector Control of Induction Motors Without Rotational Transducers," *IAS Annual Meeting (San Diego)*, 1989, pp. 493-499.
- [17] M. Boussak, A. G. Capolino, T. V. Phuoc, "Speed Measurement in Vector-Controlled Induction Machine by Adaptive Method," *EPE 4th European Conference on Power Electronics and Application*, Florence, 1991, Vol. 3, pp. 653-658.
- [18] U. Baader, M. Depenbrock, G. Gierse, "Direct Self Control (DSC) of Inverter-Fed Induction Machine - A Basis for Speed Control Without Speed Measurement," *IEEE Trans. on Industry Applications*, May/June 1992, Vol. 28, No. 3, pp. 581-588.
- [19] H. Tajima, Y. Hori, "Speed Sensorless Field Orientation Control of the Induction Machine," *IEEE Trans. on Industrial Application*, 1993, Vol. 29, No. 1, pp. 175-180.
- [20] T. Du, A. M. Brdys, "Shaft Speed, Load Torque and Rotor Flux Estimation of Induction Motor Drive Using an Extended Luenberger Observer," (Sixth International conference on Electrical Machines and Drives), Oxford, UK, 1993, Conf. Pub. No.376, pp. 179-184.

- 
- [21] C. Ilas, A. Bettini, L. Ferraris, G. Griva, F. Profumo, "Comparison of Different Schemes Without Shaft Sensors for Field Oriented Control Drives," IEEE, 1994, pp. 1579-1587.
- [22] H. Abu-Rub, J. Guzinski, Z. Krzeminski, and H. Toliyat, "Speed Observer System for Advanced Sensorless Control of Induction Motor," IEEE Trans. on Energy Conversion, June 2003, vol. 18, No. 2, pp. 219-224.
- [23] J. Guzinski, H. Abu-Rub, and H.A. Toliyat, "An Advanced Low-Cost Sensorless Induction Motor Drive," IEEE Trans. on Industry Applications, November/December 2003, vol. 39, No. 6, pp. 1757-1764.
- [24] H. Abu-Rub, J. Guzinski, Z. Krzeminski, and H. Toliyat, "Advanced Control of Induction Motor Based on Load Angle Estimation," IEEE Trans. on Industrial Electronics, vol. 51, No. 1, pp. 4-14, February 2004.
- [25] Krzeminski Z., "Nonlinear Control of Induction Motor," IFAC 10th World Congress on Automatic Control, Munich, Germany, 1987, pp. 349-354.
- [26] H. Abu-Rub, "Sensorless System Control of Induction Motor with Parameters Estimation," PEMC'98 (Power Electronics and Motion Control), Prague, Czech Republic, 1998, vol. 5, pp.190-194.
- [27] H. Akagi, Y. Kanazawa, A. Nabae, "Generalized Theory of the Instantaneous Reactive Power in Three-Phase Circuits," IPEC'83, Tokyo, Japan, 1983, pp. 1375-1385.
- [28] H. Abu-Rub and W. Hashlamoun, "Comprehensive Analysis and Comparative Study of Several Sensorless Systems Control of Asynchronous Motors," ETEP, June 2001, vol. 11, No. 3, pp.203-210.
- [29] Juhong Nie and Derek A. Linkens, *Fuzzy- Neural Control Principles, algorithms and applications*, New York: Prentice Hall, 1995.
- [30] Constantin Von. Altrock, *Fuzzy logic & NeuroFuzzy Applications Explained*, Englewood Cliffs, N.J: Prentice Hall PTR, 1995.
- [31] Constantin Von. Altrock, *Fuzzy logic & Neuro Fuzzy Applications in Business & Finance*, Englewood Cliffs, N.J: Prentice Hall PTR, 1995.

- [32] Amin Suytno, J. Fujikawa, H Kobayashi, and Yasuhko Dote, "Variable-Structured Robust Controller by Fuzzy Logic for Servomotors," *IEEE Transactions on Industrial Electronics*, February 1993, vol. 40, No 1.
- [33] M. A. Denai, S. A. Attia, "Intelligent Control of an Induction Motor," *Electric Power Components and Systems*, Taylor & Francis, 2002, vol. 30, pp.409–427.
- [34] L. A. Zadeh, "Fuzzy Sets in Information and Control," New York: Academic Press, 1965, vol. 8. pp. 338-353.
- [35] R. E. Bellman and L. A. Zadeh, "Decision-Making in a Fuzzy Environment," *Management Science*, 1970, vol. 17, pp. 141-164.
- [36] E. Cox, *The Fuzzy Systems Handbook*, Academic Press, 1994.
- [37] Wang, L-W, and Mendel, J.M. "Fuzzy Basis Functions, Universal Approximation and Orthogonal Least-Squares Learning," *IEEE Transactions on Neural Networks*, September 92, vol. 3, No.5, pp. 807-814.
- [38] E. Mamdani and S. Assilian. "An Experiment in Linguistic Synthesis with a Fuzzy Logic Controller," *Int. Journal of Man-Machine Studies*, 1975, vol. 7, No.1, pp. 1–13.
- [39] L.-X. Wang, *A Course in Fuzzy Systems and Control*. Prentice-Hall PTR, Upper Saddle River, NJ, 1997.
- [40] B. K. Bose, "Expert System, Fuzzy Logic and Neural Network Application in Power Electronics and Motion Control," *Proc. of the IEEE*, August 1994, vol. 82, No. 8.
- [41] K. Tomsovic and M.Y. Chow, "Tutorial on Fuzzy Logic Applications in Power Systems", Prepared for the IEEE-PES Winter Meeting in Singapore, January 2000.
- [42] Marek Obitko, *Genetic Algorithms*, <http://cs.felk.cvut.cz/~xobitko/ga/>, 1998.



## APPENDICES

## A. MATLAB Fuzzy Editor

This Graphical User Interface (GUI) tool comes with MATLAB Fuzzy Logic Toolbox enables building FLC system with so efficient and friendly way. This Editor consists of the following Basic 5 windows:

### 1) FIS Editor:

The FIS Editor displays general information about a fuzzy inference system. Here the fuzzy operations, fuzzy controller, defuzzification can be set, also the inputs  $e(e)$ ,  $\Delta e$ , and output  $\Delta u$  variables can be determined, as shown in Figure A- 1:

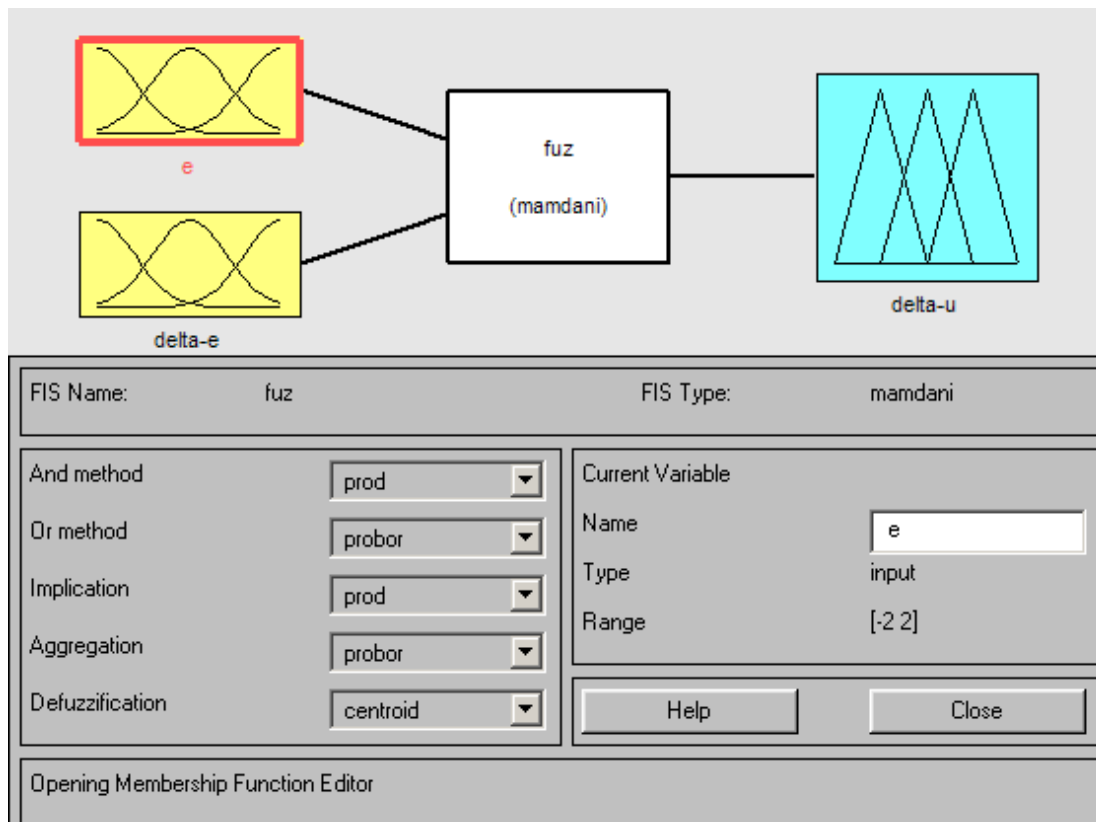


Figure A- 1: FIS editor

### 2) Membership Function Editor :

The Membership Function Editor is the window that enables the displaying and editing of all membership functions associated with all input and output variables for the entire fuzzy inference system, as shown in Figure A- 2:

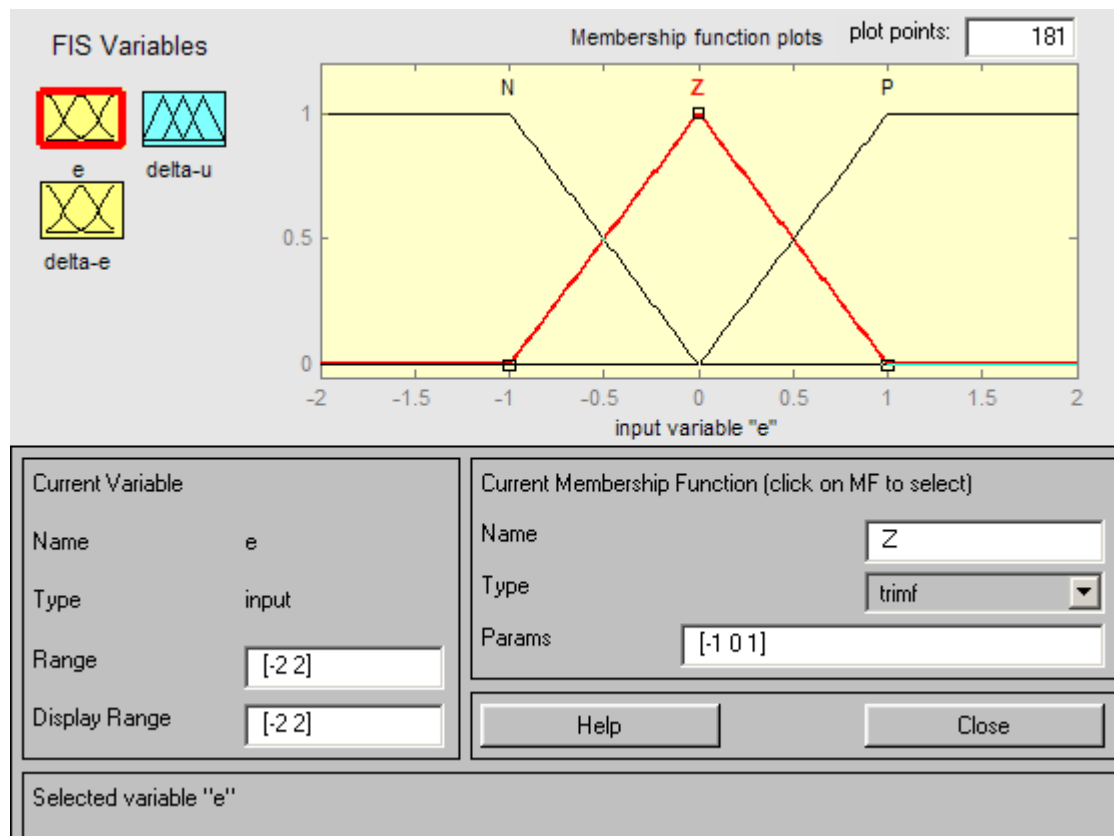


Figure A- 2: Membership functions editor

### 3) Rule Editor :

The Rule Editor allows constructing the rule statements, as shown in Figure A-3.

### 4) Rule Viewer :

The Rule Viewer shows which rules are fired and the contribution of each membership function, as shown in Figure A- 4.

### 5) Surface Viewer:

Surface Viewer shows 3-D surface view of the rules and their relation to output, as shown in Figure A- 5.

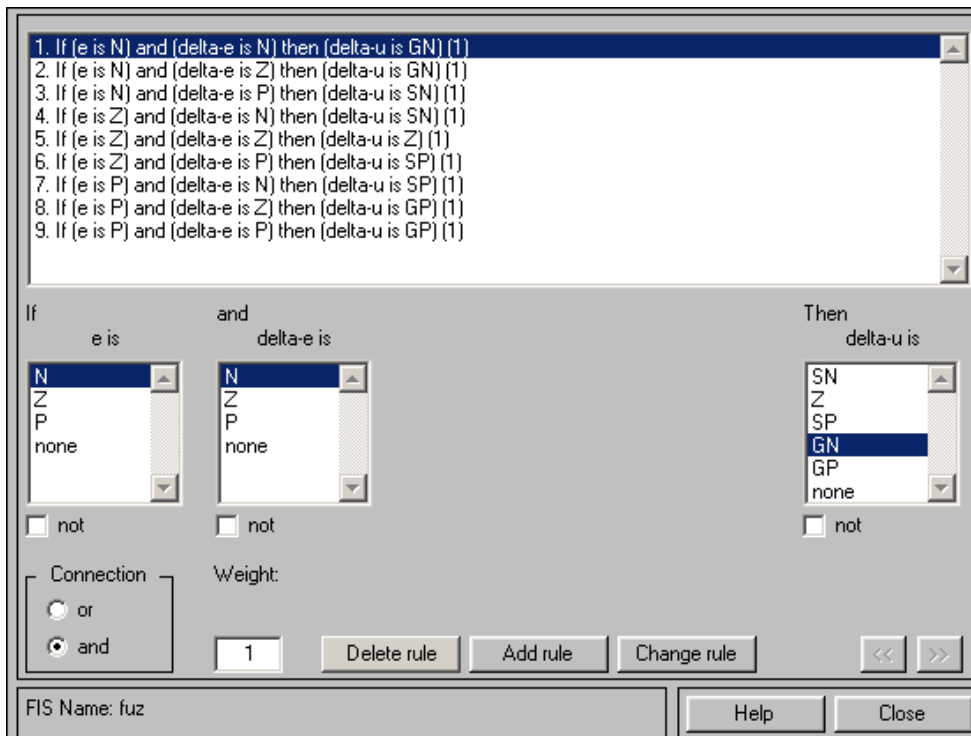


Figure A- 3: Rule editor

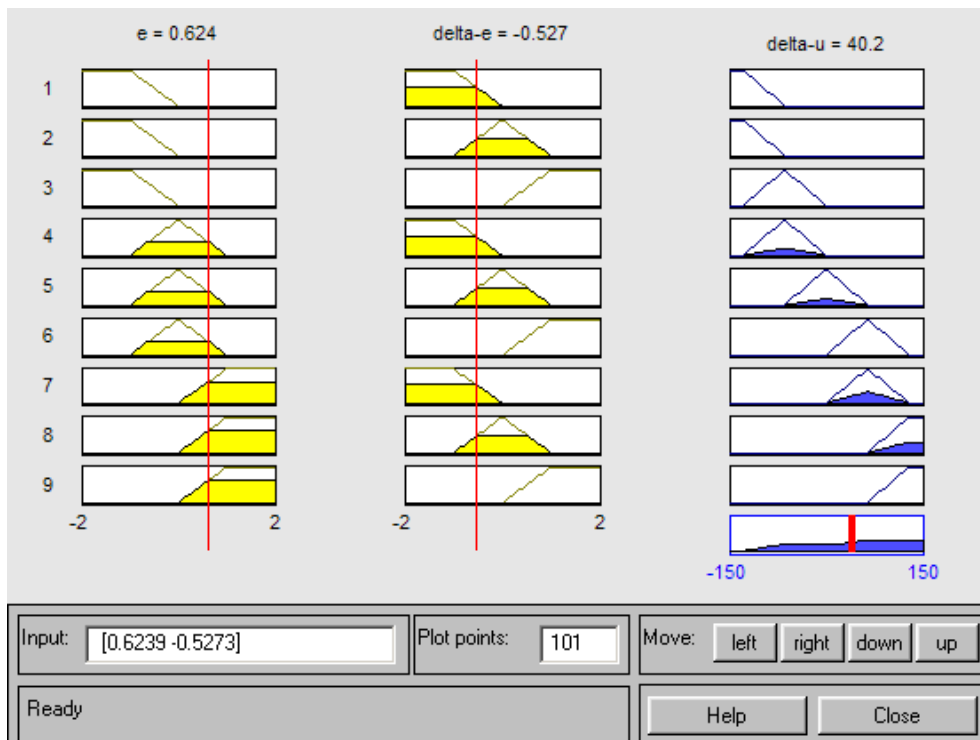


Figure A- 4: Rule viewer

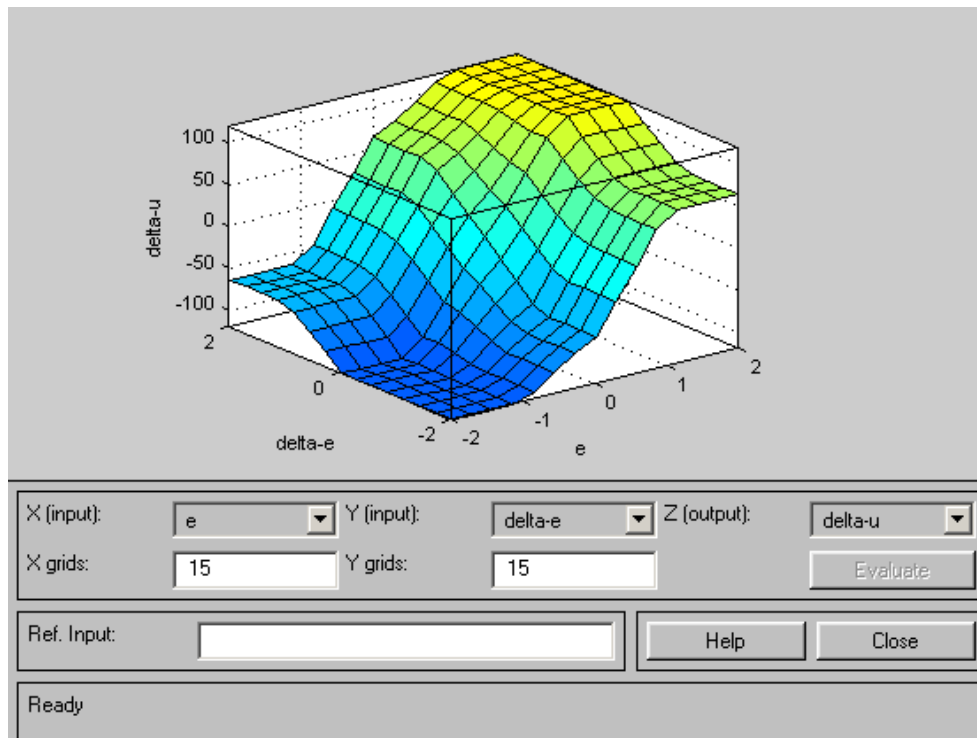


Figure A- 5: Surface viewer

***B. Conference Proceedings Paper***

This paper work had been submitted to “International Electric Machines and Drives Conference”, Sponsored by IEEE, May 15-18, 2005, San Antonio, Texas, USA. Notification of acceptance is expected on January 15, 2005.

# COMPARATIVE ANALYSIS OF FUZZY AND PI SENSORLESS CONTROL SYSTEMS OF INDUCTION MOTOR USING POWER MEASUREMENT

Jafar Titi, Haithem Abu-Rub,

Electrical Engineering Department, Birzeit University, Palestinian Authority, [jafart@scm.birzeit.edu](mailto:jafart@scm.birzeit.edu), [haithem@birzeit.edu](mailto:haithem@birzeit.edu)

**Abstract-** The aim of this work is to present a novel and inexpensive method to develop and assess sensorless control schemes of induction motors. The proposed systems operate without speed sensor; the rotor angular speed is calculated in different ways. The methods are applied to field oriented control principle. Fuzzy logic controller will be used for speed control. A comprehensive analysis and comparative study of several relationships of rotor angular speed is presented.

**Key Words:** vector control, sensorless control, induction motor, fuzzy logic, power measurement.

## I. INTRODUCTION

Multiphase AC Motors working without controlled rotor angular speed consume most of the electrical energy produced [1]. AC motors control drives are used increasingly due to their advantages like robustness, reliability, efficiency.

For the past decade a lot of research effort had been done on the idea of speed sensorless control of induction motor, as in [2] to [12]. The advantages of speed sensorless induction motor drives are reduced hardware complexity, size and cost. Also elimination of the sensor cable, better noise immunity, increased reliability and less maintenance requirements, making it suitable for hostile environments.

In this paper a power measurement for sensorless control of induction motors is used. A favorable solution is applied to field oriented control (FOC) of induction motor without using a sensor of rotor angular speed. All state variables are calculated using only stator variables.

A comprehensive analysis and comparative study between several relationships for rotor angular speed is discussed. Fuzzy logic controller (FLC) will be used and the obtained results will be compared with the obtained when using conventional Proportional-integral controller (PI) one.

## II. INDUCTION MOTOR DESCRIPTION

The squirrel cage type of induction motor as differential equations for the stator current and rotor flux vector components presented in coordinate system XY rotating with arbitrary angular speed is:

$$\frac{di_{sx}}{dt} = a_1 i_{sx} + a_2 \psi_{rx} + \omega_s i_{sy} + a_3 \omega_r \psi_{ry} + a_4 u_{sx} \quad (1)$$

$$\frac{di_{sy}}{dt} = a_1 i_{sy} + a_2 \psi_{ry} - \omega_s i_{sx} - a_3 \omega_r \psi_{rx} + a_4 u_{sy} \quad (2)$$

$$\frac{d\psi_{rx}}{dt} = a_5 \psi_{rx} + (\omega_s - \omega_r) \psi_{ry} + R_r \frac{L_m}{L_r} i_{sx} \quad (3)$$

$$\frac{d\psi_{ry}}{dt} = a_5 \psi_{ry} - (\omega_s - \omega_r) \psi_{rx} + R_r \frac{L_m}{L_r} i_{sy} \quad (4)$$

$$\frac{d\omega_r}{dt} = \frac{L_m}{L_r J} (\psi_{rx} i_{sy} - \psi_{ry} i_{sx}) - \frac{1}{J} m_0 \quad (5)$$

Where  $\psi_{rx}$ ,  $\psi_{ry}$ , and  $i_{rx}$ ,  $i_{ry}$ ,  $u_{sx}$ ,  $u_{sy}$  are the rotor flux and stator current and voltage vectors in coordinate system XY rotating with arbitrary speed,  $\omega_r$ ,  $\omega_s$  is the angular speed of the rotor shaft and coordinate system respectively,  $R_r$ ,  $R_s$ ,  $L_r$ ,  $L_s$  are rotor and stator resistance and inductances respectively,  $L_m$  is a mutual inductance,  $J$  is the inertia,  $m_0$  is the load torque, and:

$$a_1 = -\frac{R_s L_r^2 + R_r L_m^2}{L_r w}; \quad a_2 = \frac{R_r L_m}{L_r w}; \quad a_3 = \frac{L_m}{w};$$

$$a_4 = \frac{L_r}{w}; \quad a_5 = -\frac{R_r}{L_r}; \quad w = \delta L_r L_s; \quad \delta = 1 - \frac{L_m^2}{L_r L_s}$$

Four novel state variables have been used to calculate the rotor angular speed [13]. The new "multiscalar" variables may be interpreted as rotor angular speed, scalar and vector products of the stator current and rotor flux vectors, and the square of the rotor linkage flux, as follows:

$$z_1 = \omega_r \quad (6)$$

$$z_2 = \psi_{rx} i_{sy} - \psi_{ry} i_{sx} \quad (7)$$

$$z_3 = \psi_{rx} i_{sx} + \psi_{ry} i_{sy} \quad (8)$$

$$z_4 = \psi_{rx}^2 + \psi_{ry}^2 \quad (9)$$

The definitions of stator and rotor flux vectors are as follows:

$$\underline{\psi}_s = \int (u_s - R_s i_s) dt \quad (10)$$

$$\underline{\psi}_s = L_s i_s + L_m i_r \quad (11)$$

$$\underline{\psi}_r = L_r i_r + L_m i_s \quad (12)$$

After some manipulation we get the expressions of rotor flux vector components in the stationary coordinate system:





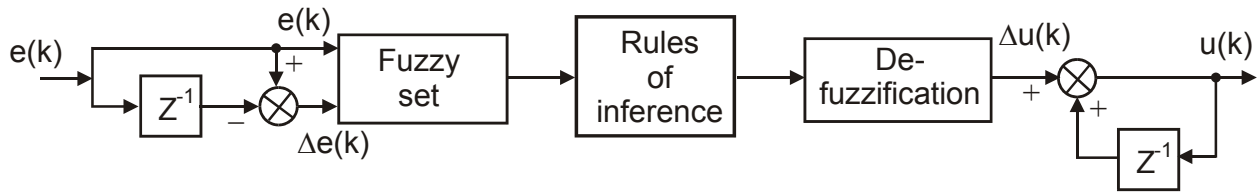


Fig. 2. Mamdani type FLC

because they are sensitive to drive parameter variations and performance may deteriorate if fixed parameter controller are used. Fuzzy logic-based controllers are considered as potential candidates for such application”.

The system shown in Fig. 1 has difficult to describe analytical relationships caused by non-precise variable identification [17], in these situations FLC is right choice for control.

Mamdani type of FLC, presented in Fig. 2, is used for speed control. The input signals for the controller are: control error, ‘e’ and the change of error, ‘Δe’ and the output is the change of control signal, ‘Δu’. The controller consists of three elements: fuzzyfication block, block of rules (rules of inference) and defuzzyfication, which are related by proper relationships.

On the basis of the values, ‘e’ and ‘Δe’, the fuzzy numbers are calculated in the fuzzyfication block using the membership function presented in Fig. 2. Simple membership functions for the three linguistic variables: ‘N’ – negative, ‘Z’ – zero and ‘P’ – positive are used. Symbol ‘G’ means great and symbol ‘S’ means small. The resulting block consists of logic table like, ‘If...Then’ which are described in Table I.

V. SIMULATION RESULTS

The results of the simulations are for step changes of the rotor speed set values and of the load torque as shown in Fig. 3. Data of a 4-kW-squirrel-cage motor have been used in the investigations. The control system had been programmed in MATLAB/Simulink.

Sensored speed simulation results are shown in Fig. 4. Simulation results for speed sensorless cases are presented on Fig. 5.

Sensorless proposed systems provide improved results by adding first order filters in the speed command channel, feedback path, and on the output of the Speed controller, its noticed that the best results are achieved using a time constant for the speed reference three times the time constant of the feedback and output of the speed controller. Furthermore, limiters are used for various variables of the control systems.

TABLE I  
FUZZY LOGIC CONTROLLER RULES OF INFERENCE

		e		
		N	Z	P
Δe	N	GN	SN	SP
	Z	GN	Z	GP
	P	SN	SP	GP
				Δu

VI. COMPARISON BETWEEN SENSORLESS VERSIONS

Table II shows a summary comparison between different sensorless speed systems shown in Fig. 5, using Fuzzy and PI controllers, and actual speed obtained by integrating (5). Comparison based on the following 3 figures of merit [9]:

A. Steady-State Error (SSE)

Is the error between estimated speed and command channel values.

B. Dynamic Behavior (DB)

Concerns about the response of the proposed system, including the rise time, and damping oscillations after introducing a disturbance.

C. Low Speed Operation (LSO)

In the proposed sensorless systems, the state variables are calculated using stator flux, this implies frequency limiting near zero.

Figures of merit range is from 0 to 10, where ‘0’ means poorest behavior and ‘10’ means best one. The rankings for the behavior of the proposed sensorless systems are noted by the assessment of the author.

Nearly in all equations Fuzzy logic controller showed overall better results than PI controllers, as presented in Table II. Best results obtained using (23) shown in Fig. 5(f).

TABLE II  
COMPARISON BETWEEN DIFFERENT SCHEMES

Eq. no.	FLC				PI			
	SSE	DB	LSO	Actual	SSE	DB	LSO	Actual
(15)	9	7	5	8	8	6	4	7
(16)	8	9	9	8	8	7	9	6
(20)	8	8	9	8	8	8	9	8
(21)	9	9	9	5	8	8	8	4
(22)	8	7	9	3	7	6	8	4
(23)	9	9	9	9	8	9	8	7
(24)	9	9	9	5	8	8	7	4
(25)	8	8	9	4	7	8	8	4
(26)	8	8	9	4	7	8	8	4
(27)	9	8	6	9	8	8	7	8

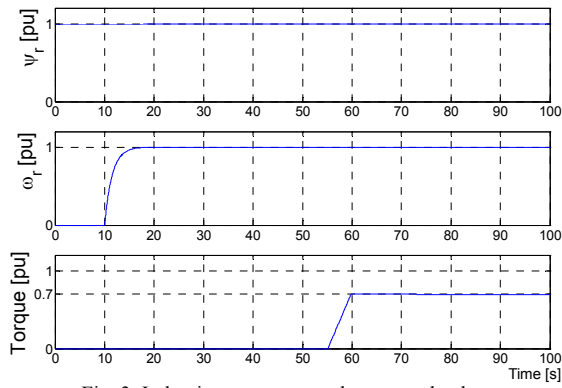


Fig. 3. Induction motor control command values.

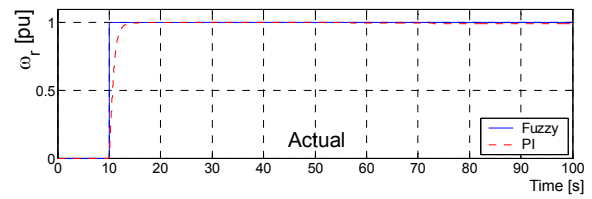
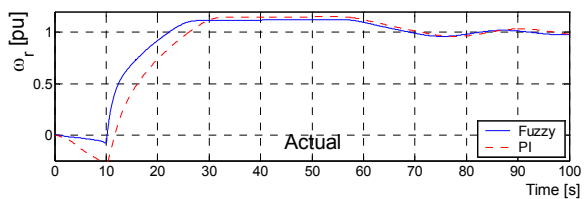
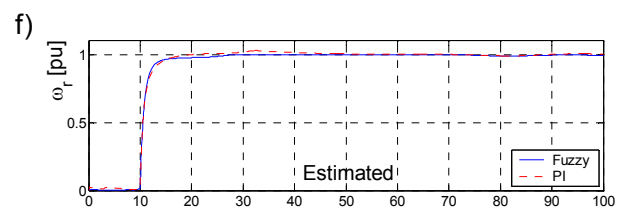
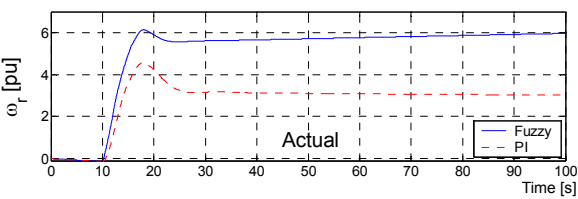
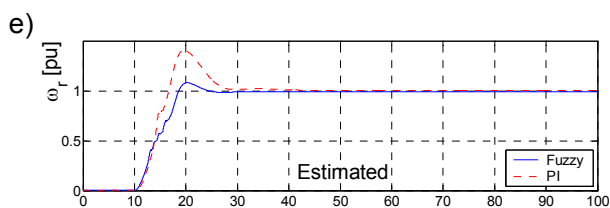
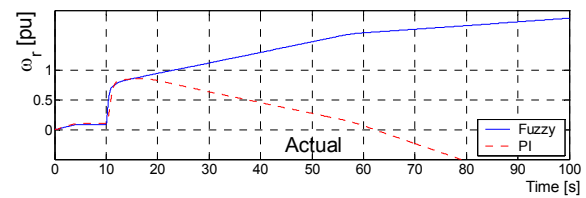
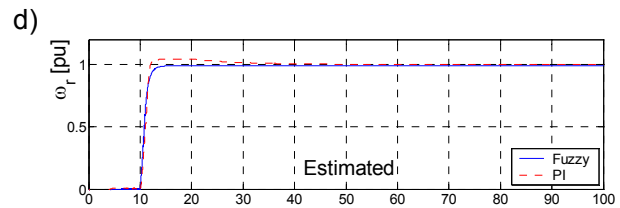
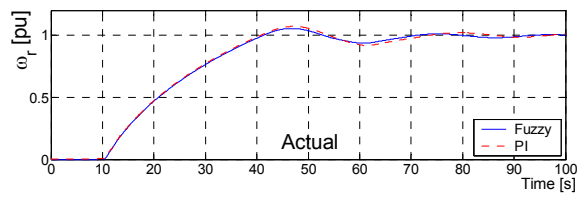
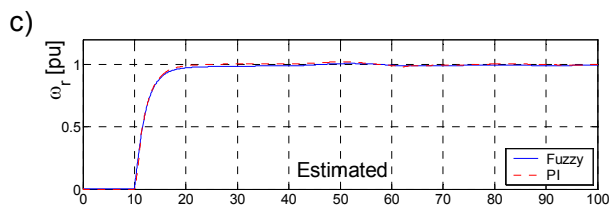
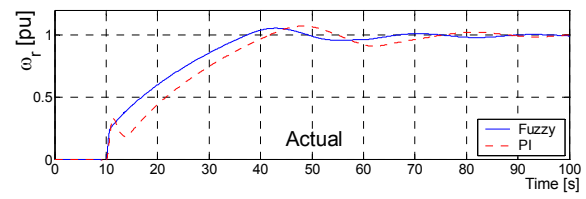
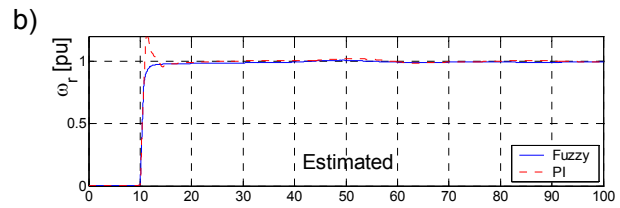
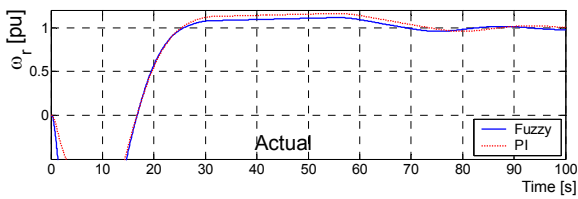
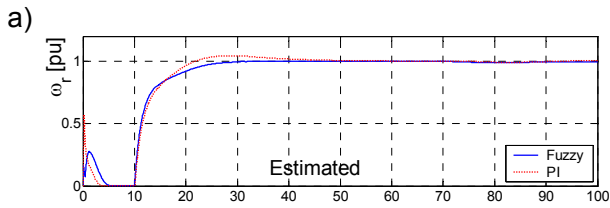


Fig. 4. Without estimation case.



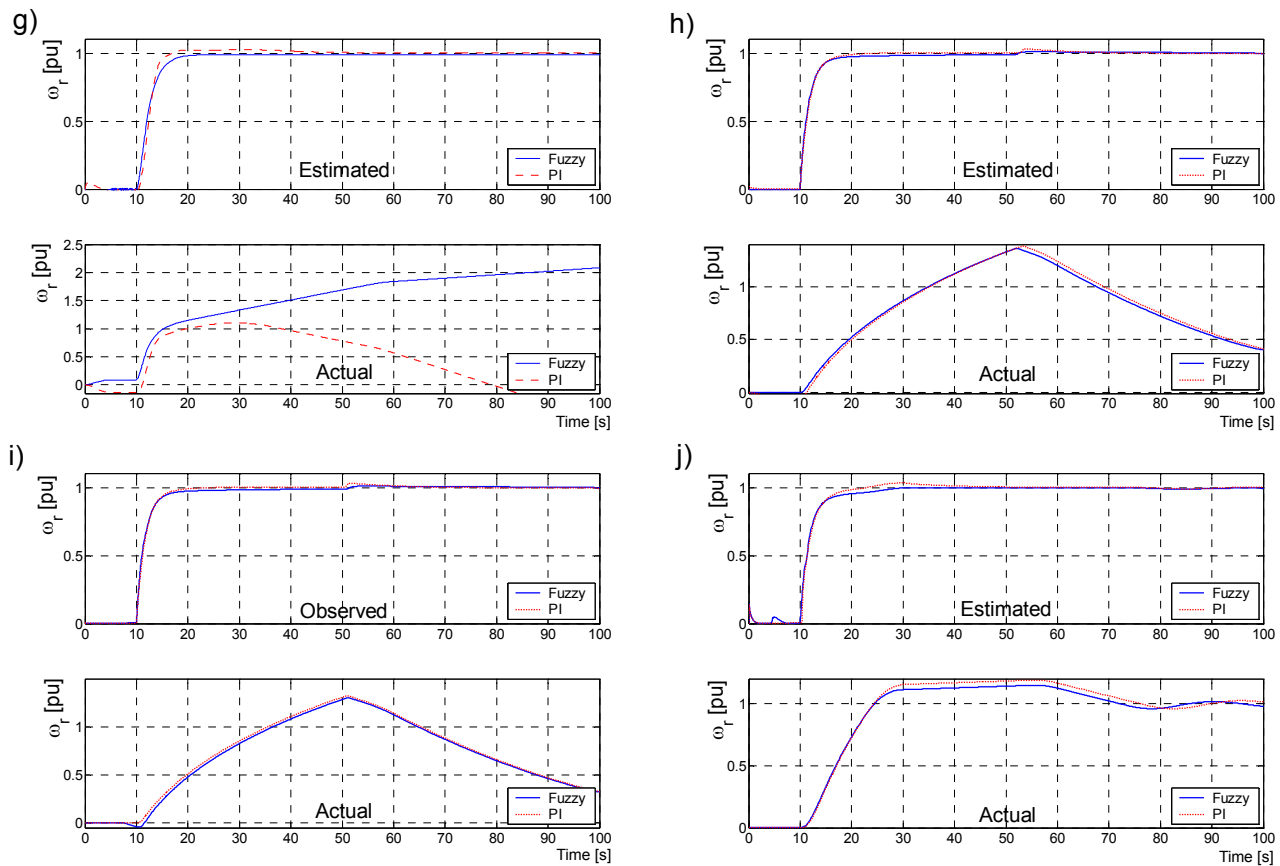


Fig. 5. Behavior of control system under the command values shown in Fig. 3. Plots from a..j represents the behavior of the following equations: a) eq. (15), b) eq. (16), c) eq. (20), d) eq. (21), e) eq. (22), f) eq. (23), g) eq. (24), h) eq. (25), i) eq. (26), j) eq. (27). The upper plot represents the estimated speed; the lower plot represents actual speed.

## REFERENCES

- [1] B. K. Bose, "Power Electronics and Motion Control – Technology Status and recent Trends," *IEEE Trans. on Industrial Electronics*, , vol. 35, No 5, pp. 902-909, September/October 1993.
- [2] R. Joetten, G. Maeder, "Control Methods for Good Dynamic Performance Induction Motor Drives Based on Current and Voltage as Measured Quantities," *IEEE Trans. on Industrial Application*, 1983, Vol. IA-19, no. 3, pp. 356-363.
- [3] F. Hillenbrand, "A Method for Determining the Speed and Rotor Flux of the Asynchronous Machine by Measuring the Terminal Quantities Only". IFAC Conference. in Power Electronics and Electrical Drives, Lausanne, Switzerland, 1983, pp. 55-62.
- [4] C. Schauder, "Adaptive Speed Identification for Vector Control of Induction Motors Without Rotational Transducers", IAS Annual Meeting (San Diego, 1989), pp. 493-499.
- [5] M. Boussak, A. G. Capolino, T. V. Phuoc, "Speed Measurement in Vector-Controlled Induction Machine by Adaptive Method," EPE 4th European Conference on Power Electronics and Application, Florence, 1991, Vol.3, pp. 653-658.
- [6] U. Baader, M. Depenbrock, G. Gierse, "Direct Self Control (DSC) of Inverter-Fed Induction Machine - A Basis for Speed Control Without Speed Measurement," *IEEE Trans. on Industry Applications*, Vol. 28, No. 3, pp. 581-588, May/June 1992.
- [7] H. Tajima, Y. Hori, "Speed Sensorless Field Orientation Control of the Induction Machine," *IEEE Trans. on Industrial Application*, 1993, Vol. 29, No. 1, pp. 175-180.
- [8] T. Du, A. M. Brdys, "Shaft Speed, Load Torque and Rotor Flux Estimation of Induction Motor Drive Using an Extended Luenberger Observer," (Sixth International conference on Electrical Machines and Drives), Oxford, UK, 1993, Conf. Pub. No.376., pp.179-184.
- [9] C. Ilas, A. Bettini, L. Ferraris, G. Griva, F. Profumo, "Comparison of different Schemes without Shaft Sensors for Field Oriented Control Drives," *IEEE*, 1994, pp. 1579-1587.
- [10] H. Abu-Rub, J. Guzinski, Z. Krzeminski, and H. Toliyat, "Speed Observer System for Advanced Sensorless Control of Induction Motor," *IEEE Trans. on Energy Conversion*, Vol. 18, No. 2, pp. 219-224, June 2003.
- [11] J. Guzinski, H. Abu-Rub, and H.A. Toliyat, "An Advanced Low-Cost Sensorless Induction Motor Drive," *IEEE Trans. on Industry Applications*, vol. 39, No. 6, pp. 1757-1764, November/December 2003.
- [12] H. Abu-Rub, J. Guzinski, Z. Krzeminski, and H. Toliyat, "Advanced Control of Induction Motor Based on Load Angle Estimation," *IEEE Trans. on Industrial Electronics*, vol. 51, No. 1, pp. 4-14, February 2004.
- [13] Krzeminski Z., "Nonlinear Control of Induction Motor," IFAC 10th World Congress on Automatic Control, Munich, Germany, 1987, pp. 349-354.
- [14] H. Abu-Rub, "Sensorless System Control of Induction Motor with Parameters Estimation," PEMC'98 (Power Electronics and Motion Control), Prague, Czech Republic, 1998, vol. 5, pp.190-194.
- [15] H. Akagi, Y. Kanazawa, A. Nabae, "Generalized Theory of the Instantaneous Reactive Power in Three-Phase Circuits," IPEC'83, Tokyo, Japan, 1983, pp. 1375-1385.
- [16] M. A. Denai, S. A. Attia, "Intelligent Control of an Induction Motor," *Electric Power Components and Systems*, Taylor & Francis, 2002, vol. 30, pp.409-427.
- [17] B. K. Bose, "Expert system, fuzzy logic and neural network application in power electronics and motion control", Proc. of the IEEE vol. 82 No. 8 August 1994